Identification and characterization of angiopoietin-like 4 (ANGPTL4) interacting proteins in wound repair

Mintu Pal

2010

Mintu, P. (2010). Identification and characterization of angiopoietin-like 4 (ANGPTL4) interacting proteins in wound repair. Doctoral thesis, Nanyang Technological University, Singapore.

https://hdl.handle.net/10356/42403

https://doi.org/10.32657/10356/42403

IDENTIFICATION AND CHARACTERIZATION OF ANGIOPOIETIN-LIKE 4 (ANGPTL4) INTERACTING PROTEINS IN WOUND REPAIR

MINTU PAL

School of Biological Sciences

A thesis submitted to the Nanyang Technological University
in partial fulfillment of the requirement for the degree of
Doctor of Philosophy

2010

ACKNOWLEDGEMENTS

I would like to express my deep and sincere gratitude to my supervisor, Dr. Andrew Tan Nguan Soon, Division of Molecular & Cell Biology, School of Biological Sciences (SBS), Nanyang Technological University (NTU). His wide knowledge and logical way of thinking have been of great value for me. His understanding, encouragement and personal guidance have provided a good basis for the present thesis.

My heartfelt thanks to Prof. Ding Jeak Ling, Department of Biological Sciences, National University of Singapore (NUS); Prof. Ho Bow, Department of Microbiology, NUS; and Prof. Sander Kersten, Division of Human Nutrition, Wageningen University, The Netherlands, for their collaboration in developing the project work based on the proposed framework. Their kind support and guidance have been of great value in this study.

I am grateful to Dr. Li Hoi Yeung, SBS, NTU for his valuable suggestions throughout this work and constructive comments on my research problems.

My sincere thanks to the thesis advisory committee members, Dr. Koh Cheng Gee and Dr. Surajit Bhattacharyya, SBS, NTU for their detailed review, constructive criticism and excellent advice during confirmation of my PhD candidature.

During this work I have collaborated with many colleagues for whom I have great regards, and I wish to extend my warmest thanks to all those who have helped me with my work in our laboratory and department. In addition, I enjoyed the parties and trips with my supervisor and friends. I also enjoyed playing badminton with my bengali group.

I owe my loving thanks to my parents, wife and other members of my family for their infinite love and encouragements during my PhD programme.

Finally, I wish to acknowledge the financial support for this study provided by NTU.

TABLE OF CONTENTS

LIST OF FIGURES

LIST OF TABLES

LIST OF ABBREVIATIONS

Ac5	Actin 5
AE	Anion-exchange
Af	Affinity chromatography
Ang1	Angiopoietin-like protein 1
ANGPTL3	Angiopoietin-like protein 3
ANGPTL4	Angiopoietin-like 4
anti-EGF receptor	Anti-epidermal growth factor receptor
anti-EGFR antibody	Anti-epidermal growth factor receptor antibody
B	Bound fractions
bp	Base pair
BSA	Bovine serum albumin
cANGPTL4	C-terminal ANGPTL4
DNA	Deoxyribonucleic acid
cDNA	Complementary deoxyribonucleic acid
CM	Conditioned medium
CO_2	Carbon dioxide
COL-1	Collagen-1
CRIB	cdc42 and Rac interactive binding
DAPI	4',6-diamidino-2-phenylindole
^oC	Degree celcius
DMEM	Dulbecco's modified eagle's medium
E	Epidermis
E. Coli	Escherichia coli
ECM	Extracellular matrix
EDC	N-ethyl-*N′*-(3-dimethylaminopropyl) carbodiimide hydrochloride
EDTA	Ethylenediaminetetraacetic acid
EGF	Epidermal growth factor
EGFR	Epidermal growth factor receptor
ERK-1	Extracellular signal-regulated kinase-1
FAK	Focal adhesion kinase
FBS	Fetal bovine serum
FIAF	Fasting induced adipose factor
FGF-7	Fibroblast growth factor-7
FN	Fibronectin
GAGs	Glycosaminoglycans
GAPs	GTPase-activating proteins
GDI	Guanine nucleotide dissociation inhibitors
GDP	Guanosine diphosphate
GEFs	Guanine nucleotide exchange factors
GM-CSF	Granulocyte macrophase-colony stimulating factor
GSK-3β	Glycogen synthase kinase-3beta
GST	Glutathione-S-transferase
GST-PAK	GST coupled to Rac1/cdc42 binding domain of p21 activated kinase

GST-Rhotekin	GST coupled to Rho binding domain of Rhotekin
GTP	Guanosine triphosphate
GTPase	Guanosine triphosphatase
h	Hour
HBS-P	Hepes (4-(2-hydroxyethyl)-1-piperazineethanesulfonic acid) buffered saline
HDL	High density lipoprotein
HEK	Human Embryonic Kidney cells
HEPES	(4-(2-hydroxyethyl)-1-piperazineethanesulfonic acid)
hf	Hair follicle
HFARP	Hepatic fibrinogen/angiopoietin-related protein
HRP	Horseradish peroxidase
IEF	Isoelectric focusing
I-EGF	Integrin-epidermal growth factor
IF	Immunofluorescence
IgG	Immunoglobulin G
IL-1	Interleukin-1
ILD	I-like domain
ILK	Integrin-linked kinase
IPTG	Isopropyl β-D-1-thiogalactopyranoside
ISOPrime	Isoelectric preparative membrane electrophoresis
JNK	c-Jun N-terminal kinase
Ka	Association rate constant
$K_{ANGPTL4}$	ANGPTL4-knockdown keratinocytes
K_{CTRL}	Wild type keratinocytes
Kd	Dissociation rate constant
K_D	Equilibrium dissociation constant
kDa	Kilodalton
KGF	Keratinocyte growth factor
K_{off}	Dssociation rate constant
K_{on}	Association rate constant
$K_{TAK1\text{-}A}$	TAK1-A siRNA transduced keratinocytes
$K_{TAK1\text{-}B}$	TAK1-B siRNA transduced keratinocytes
L	Litre
LB	Luria broth
LC-MS/MS	Liquid chromatography-tandem mass spectrometry
LN-5	Laminin-5
M	Molar
mAb	Monoclonal antibody
MALDI	Matrix-assisted laser desorption/ionization
MAPK	Mitogen-activated protein kinase
MAPK activator	MAPK kinase
MAPKK activator	MAPKK kinase
MAPKKK	Mitogen-activated protein kinase kinase kinase
MEK/ERK	Mitogen-activated protein kinase kinase/extracellular regulated kinase

µg	Microgram
mit C	Mitomycin C
µl	Microlitre
µm	Micrometre
µM	Micromolar
mg/L	Miligram per litre
min	Minutes
ml	Millilitre
mM	Millimolar
M-PEK	Proteoextract native membrane protein extraction kit
mRNA	Messenger ribonucleic acid
MS/MS	Mass spectrometry/mass spectrometry
nANGPTL4	N-terminal ANGPTL4
NaCl	Sodium chloride
NF-kB	Nuclear factor kappa-light-chain-enhancer of activated B cells
ng	Nanogram
NHS	N-hydroxy-succinimide
NLS	Nuclear localization signal
nm	Nanometre
OTC	Organotypic co-culture
pAb	Polyclonal antibody
PAI-1	Plasminogen activator inhibitor type-1
PAK	p21-activated kinase
PBD	p21-binding domain
PBS	Phosphate buffered saline
PCR	Polymerase chain reaction
PDGF	Platelet-derived growth factor
PDGF-B	Platelet-derived growth factor-B
PDK-1	Phosphoinositide-dependent kinase-1
pFAK	Phosphorylated FAK
PI3K	Phosphotidylinositol 3-kinase
PKB	Protein kinase B
PKC	Protein kinases C
PKC α	Protein kinases Cα
PMSF	Phenylmethylsulphonyl fluoride
PPAR	Peroxisome-proliferator-activated receptor
PPARα	Peroxisome-proliferator-activated receptor alpha
PPARβ/δ	Peroxisome-proliferator-activated receptor beta/delta
PPARγ	Peroxisome-proliferator-activated receptor gamma
PSI	Plexin semaphoring integrin
PSI-ILD	Plexin semaphoring integrin I-like domain
PVDF	Polyvinylidene Fluoride
pVHL	von hippel-lindau tumor suppressor
qPCR	Quantitative real-time polymerase chain reaction
RBD	Rho-binding domain
RGD motif	Arginine-glycine-aspertic acid motif

ROS	Reactive oxygen species
Rpl27	60S ribosomal protein L27
RTKN	Rhotekin
RU	Response unit
s	Second
S2 cells	Schneider 2 cells
S.D.	Standard deviation
SDS	Sodium dodecyl sulfate
SDS-PAGE	Sodium dodecyl sulfate-polyacrylamid gel electrophoresis
siRNA	Small interfering ribonucleic acid
SPARC	Secreted protein acidic and rich in cysteine
SPR	Surface plasmon resonance
SPR-MS	Surface plasmon resonance-mass spectroscopy
TAK1	Transforming growth factor activated kinase-1
TAK1-KO	TAK1-knockout
TBS	Tris-buffered saline
TBST	Tris-buffered saline with Tween-20
TGF	Transforming growth factor
TGF-β	Transforming growth factor-beta
Tie-1	Tyrosine kinase-1
Tie-2	Tyrosine kinase-2
TNF-α	Tumor necrosis factor-alpha
TSP	Thrombospondin
TUNEL	Terminal deoxynucleotidyl transferase dUTP nick end labeling
U	Unbound fractions
UI	Uninduced
VN	Vitronectin

SUMMARY

Cutaneous wound healing is a complex and highly coordinated process of proliferation and migration of keratinocytes at the wound edge through interactions of different signaling molecules. Growth factors, transmembrane protein integrins and extracellular matrix play an important role in epidermal wound healing process, although the interplay among these proteins is poorly understood. Angiopoietin-like 4 (ANGPTL4), which is a secreted protein, exemplifies the first known non-inflammatory factor that is produced by the keratinocytes and adipocytes, and thus represents a novel connection threading wound repair, diabetes and obesity. We show here that the interacting partners of ANGPTL4 are vitronectin and fibronectin present in wound site. We also identify integrins β_1 and β_5 as binding partners of ANGPTL4, which form a functional ternary complex when present with its cognate matrix protein. This ternary complex modulates cell-matrix communication and enhances the keratinocyte migration through the formation of extended lamellipodia in human keratinocytes during wound healing process.

CHAPTER 1

ROLE OF ANGIOPOIETIN-LIKE 4 (ANGPTL4) DURING WOUND REPAIR

Publications:

1. Goh YY*, **Pal M***, Chong HC, Zhu P, Tan MJ, Punugu L, Tan CK, Roystan H, Sze SK, Tang MBY, Ding JL, Kersten S, Tan NS. Angiopoietin-like 4 interacts with matrix proteins to modulate wound healing (Manuscript in revision, *Authors contributed equally).
2. Goh YY*, **Pal M***, Chong HC, Zhu P, Tan MJ, Punugu L, Yau YH, Tan CK, Roystan H, Tan SM, Tang MBY, Ding JL, Kersten S, Tan NS. Angiopoietin-like 4 interacts with integrins β1 and β5 to modulate keratinocyte migration (Manuscript in review, *Authors contributed equally).
3. Zhu P, Tan MJ, Roystan H, Tan CK, Chong HC, **Pal M**, Lam CRI, Boukamp P, Pan JY, Tan SH, Kersten S, Li HY, Ding JL, Tan NS. Angiopoietin-like 4 modulates superoxide level to regress tumor by apoptosis (Manuscript in preparation).
4. Roystan H, Teo Z, Chong HC, **Pal M**, Goh YY, Tan MJ, Zhu P, Tan CK, Tan SM, Li HY, Ding JL, Tan NS. Tumor-derived angiopoietin-like 4 disrupts endothelial integrity through a bimodal association with integrin α5β1, VE-cadherin and claudin-5 (Manuscript in preparation).

1.1 ABSTRACT

Wound repair is one of the most complex biological processes, involving a series of events such as epidermal cell proliferation and migration through interactions of different signaling molecules. Growth factors, transmembrane protein integrins and extracellular matrix are known to play key roles in epidermal wound healing, although the interplay among these proteins is not fully understood. Studies have shown that PPARβ/δ plays a critical role in the keratinocytes response to epidermal injury. Our recent finding showed that PPARβ/δ stimulates the expression of Angiopoietin-like 4 (ANGPTL4) in epidermis. ANGPTL4, which is a secreted protein, exemplifies the first known non-inflammatory factor that is produced by the keratinocytes and adipocytes, and thus represents a novel connection threading wound repair, diabetes and obesity.

As a circulating protein, various forms of ANGPTL4 are likely to interact with their specific plasma cofactors and exert their actions via membrane bound receptor(s). However, these cofactors and their cognate receptor(s) remain to be elucidated. To this end, we produced the various forms of recombinant ANGPTL4 and used them as baits to isolate their interacting protein partners using surface plasmon resonance technology. We showed that ANGPTL4 and activation of its receptors integrin β_1 and β_5 in keratinocytes induced FAK, Rho GTPases and 14-3-3σ-mediated signaling pathways. Interestingly, we found that ANGPTL4 could form a functional ternary complex with integrin receptors as well as extracellular matrix proteins; vitronectin/fibronectin and ANGPTL4 were involved in the formation of extended lamellipodia regulating migratory mechanism of normal human keratinocytes. Based on these results, we propose a mechanism involving a ternary complex that might be critically concerned in human epidermal wound healing.

1.2 INTRODUCTION

1.2.1 Human skin

The skin is the largest organ in the human body. Although it has multiple functions, its primary role is to serve as a barrier against the external environment. The skin provides a barrier against attacks from outside organisms and protects underlying tissues from injuries. Its pigments guard the body from the dangerous ultraviolet rays of sunlight. It also waterproofs the body, preventing excessive loss or gain of bodily moisture. Other functions of the skin include thermoregulation, immune surveillance and sensory detection. In all cases, the injury to the skin triggers a response aimed at restoring the integrity and function of the skin. The skin contains two main layers of cells-a thin outer layer called epidermis and a thicker inner layer called dermis (Fig. 1.1). The epidermis

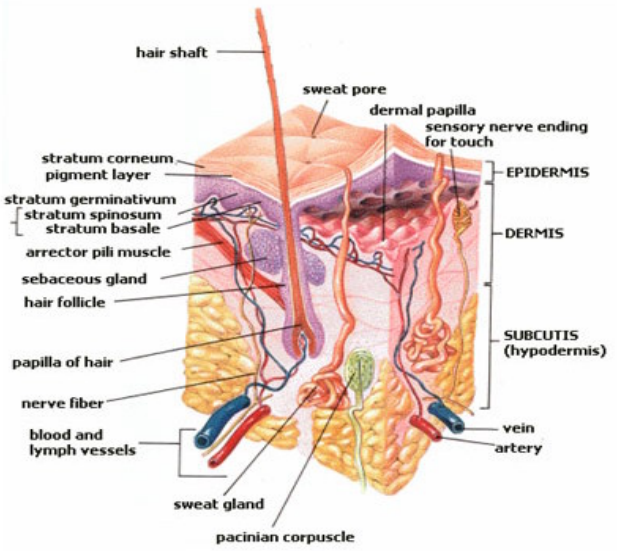

Figure 1.1 Different layers of human skin. Skin is composed of two main layers namely epidermis and dermis. The outermost epidermis layer consists of stratified squamous epithelium. The epidermis can be further subdivided into the following *strata* (beginning with the outermost layer): corneum, granulosum, spinosum and basale. The dermis lies below the epidermis and contains a number of structures including blood vessels, nerves, hair follicles, smooth muscle, glands and lymphatic tissues. The hypodermis layer lies below the dermis layer, helps to attach the skin to underlying bone and muscle as well as supplying it with blood vessels and nerves (taken from www.wikipedia.org/wiki/Skin).

layer is composed of many sheets of flattened, epithelial cells known as keratinocytes. At the base of the epidermis, keratinocytes undergo rapid proliferation. Since younger cells continuously multiply, they drive the older cells towards the surface of the skin. The outermost layer is mostly composed of terminally differentiated cells. The dermis layer, whose major cell type is the fibroblasts, regulates the proliferation and terminal differentiation of epidermal keratinocytes. Such communications between these two repeat layers occur via a double-paracrine mechanism (Mass-Szabowski et al., 1999) i.e. epithelial-mesenchymal interactions.

1.2.2 Wound repair

Acute and chronic cutaneous wounds are very common. Each year there are more than 8 million traumatic lacerations (Singer et al., 2002) and 1 million burns treated in the United States alone (Tustin, 2001). In addition, up to 90 million surgically induced incisions are created each year (Brigham et al., 1996). Chronic wounds, such as diabetic ulcers are also quite common with more than 6 million ulcers reported annually (Irvine, 1997). Chronic ulcers are especially problematic because they tend to affect the most vulnerable populations, such as the elderly, the diabetic, and the physically debilitated.

Injury that results from the exposure of the skin to external factors triggers a cascade of events that aims to repair the damaged tissue. Wound healing is a complex and dynamic process that may be broadly divided into 3 major phases, namely inflammation, re-epithelialization and matrix/tissue remodeling. It also involves a coordinated series of events including chemotaxis, phagocytosis, neocollagenesis, collagen degradation, and collagen remodeling within these 3 broad phases. In addition, angiogenesis and the

production of new glycosaminoglycans (GAGs) and proteoglycans are vital to the wound healing in milieu. The culmination of these biological processes results in the replacement of normal skin structures with fibroblastic mediated scar tissue. Failure to re-epithelialize the wound surface affects many biological processes. It contributes to pathologies including chronic inflammatory disease, tumor formation and metastasis (Prud'homme, 2007). Indeed, the barrier integrity of epithelial cells is restored after migrating cells have covered the denuded wounded area. Understanding the precise molecular mechanisms of wound repair regulation *in vivo* is important in developing effective therapeutic strategies for controlling disease progression.

1.2.3 Cell migration

Different *in vivo* and *in vitro* models of wound repair have shown that the proliferation and migration of neighboring epithelial cells at the wound margin are the pivotal events in the wound repair process (Herard et al., 1996). Re-epithelialization of the wound involves the proliferation and migration of keratinocytes from the wound edge, followed by their stratification and re-differentiation to form an intact epithelium. Cell migration is a multistep process involving changes in cytoskeleton, cell-substrate adhesion. There are two main theories to how the cell stretches forward in the front edge, namely (A) the cytoskeletal and (B) membrane flow model (Fig. 1.2). In cytoskeletal model, the soluble actin monomers undergo rapid polymerisation to form filaments in the leading edge of the cells to produce the main motile force for advancing the cells. In membrane flow model, studies have shown that the membrane in the front side of cell is returned to the cell surface from internal membrane pools at the end of the endocytic cycle. This has led

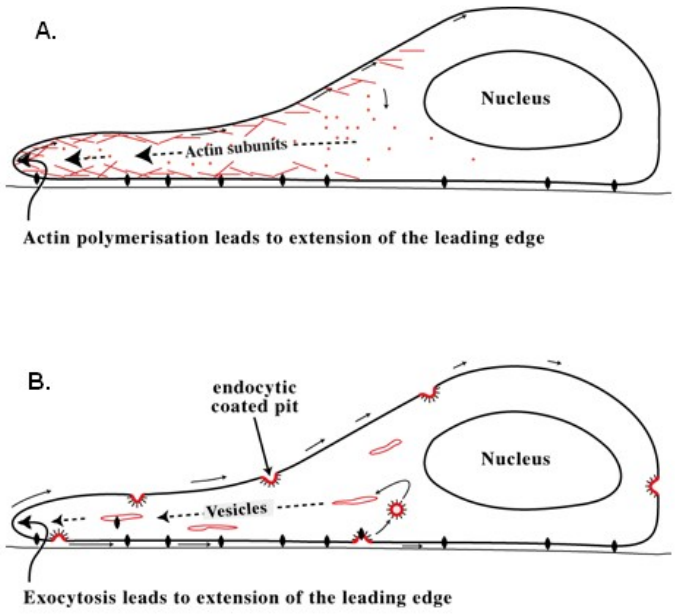

Figure 1.2 Two different models for cell migration. (A) Cytoskeletal and **(B)** Membrane flow model.

to the view that extension of the leading edge occurs due to exocytosis. The actin filaments which form at the front might stabilize the extended membrane so that a structured extension, or lamella, is formed rather than the cell directing membrane vesicles towards its anterior edge.

1.2.4 Integrin-matrix interaction

After wounding, the keratinocytes at the wound edge come into contact with dermal collagens I, III and fibrin clot constituents fibrin, fibronectin, and vitronectin. Simultaneously, the expression profile of integrins on wound margin keratinocytes changes, characterized by the induction of specific integrins that bind proteins of the dermal matrix and specific components of the fibrin clot that act as a provisional matrix during wound repair (Grinnell, 1992). Keratinocytes migrate over the wound bed via an interaction between integrin and its cognate extracellular matrix (ECM).

Integrins are transmembrane receptors which promote both cell-cell and cell-extracellular matrix adhesion. These heterodimers of non-covalently-bound α and β subunits show a wide tissue distribution and play key roles in developmental, physiological and pathological processes. The ligand specificity relies on the combination of both α/β subunits (18 different α integrins and 8 different β integrins). Ligand binding to the receptor extracellular domain induces a conformational change that is propagated to the cytoplasmic domain and initiates downstream signaling events related to cytoskeletal rearrangements. The major integrins in the epidermis are $\alpha_2\beta_1$, $\alpha_3\beta_1$, $\alpha_5\beta_1$ and $\alpha_v\beta_5$ (Kirfel et al. 2004). Intracellular communication with the external environment can be triggered by such receptor/ligand interaction. Receptor activation in response to ligand binding leads to changes in target gene expression that ultimately modulate cellular processes. Such cellular processes can also be influenced by intracellular signaling facilitated via various signaling networks. As a result, integrins are involved in many fundamental cellular functions, including proliferation, adhesion, motility, differentiation, survival, and apoptosis (Hynes, 2002).

1.2.5 Rho family GTPases

Cell proliferation and migration are modulated by growth factors which are soluble polypeptides that act in a paracrine or autocrine fashion (Deuel, 1989). Growth factors exert their influence on cells by binding to their cognate transmembrane receptors on the cell surface which convey signals via tyrosine kinases and other second-messenger systems such as cyclic AMP-dependent kinase and protein kinase C. A key event in stimulating motility is the activation of the small guanosine triphosphatase (GTPase) Rac,

which mediates the actin polymerisation-driven lamellipodia extension and the assembly of focal adhesion complexes (Felsenfeld et al. 1999).

The Rho family GTPases regulates serum-dependent and growth-factor-dependent changes in actin polymerization, leading to the formation of stress fibers, filopodia or lamellipodia, and ruffles (Mackay et al., 1998). During cell migration, new integrin –matrix adhesions are formed at the tips of lamellipodia, whereas adhesion sites at the cell rear must be disrupted for a cell to move. It can be concluded that this dynamic behaviour of integrins is important in governing cell migration. Such morphological changes appear to be important in growth-factor and integrin-dependent signaling. It is reported that Rho is required for the formation of large focal adhesions from which actin stress fibers radiate, as well as for the phosphorylation of focal adhesion kinase (FAK) and paxillin (Clark et al., 1998). Fibronectin adhesion-stimulated membrane ruffling, however, is dependent on both cdc42 and Rac. cdc42 was also shown to regulate integrin-dependent activation of mitogen-activated protein kinase (MAPK) and stimulation of protein kinase B (PKB) (Clark et al., 1998).

1.2.6 Secreted factors affecting cell proliferation and migration during wound repair

1.2.6.1 Growth factors and cytokines

The multitude of complex biological processes, which occur during the different stages of wound repair, is regulated spatio-temporally by the concerted actions of numerous growth factors and cytokines. Cell proliferation and migration are indispensable during re-epithelialization for the rapid reconstitution of a cohesive epithelial structure. There is

a tremendous diversity in how these processes occur and the mediators involved. The variety of these signals and their effects on wound repair has been well studied (Werner and Grose, 2003). It is clear that epithelial-mesenchymal communication is essential for the proper production of these cytokines. One of the most well-established double paracrine signaling essential for wound repair involves interleukin-1 (IL-1) and keratinocyte growth factor (KGF). Keratinocyte-derived IL-1 stimulates fibroblasts to produce growth factor KGF/fibroblast growth factor-7 (FGF-7), which in turn stimulates keratinocytes proliferation (Werner et al., 2007). In addition, keratinocytes also produce a variety of growth factors like TGF (transforming growth factor) α and β that are relevant to wound healing. While most of the growth factors operate in synergy, it is also well recognized that some of these factors exert opposing effects in cell proliferation and migration. For example, KGF potentiates keratinocyte growth while TGFβ exerts a potent growth inhibitory action on epithelial cells. Recent studies showed that crosstalk among different signaling cascades where dominance of certain pathways culminates to appropriate cell responses (Tan et al., 2004).

Certain growth factors such as platelet-derived growth factors (PDGFs) and granulocyte-macrophage colony stimulating factor (GM-CSF) can also stimulate cell migration of different cell types and are accordingly called motogenic growth factors or motogens (Nickoloff et al. 1988). Motogens can either induce chemokinesis, i.e., migratory reactions with random orientation, or chemotaxis, i.e., directional migrations following a gradient of growth factor concentrations. Motogens exert their influence on cells by binding to transmembraneous protein receptors on the cell surface.

1.2.6.2 Extracellular matrix

The extracellular matrix (ECM) is a complex and dynamic structural network that serves as a stabilizing element of all multicellular organisms to ensure their functional integrity and to mediate mechanical forces. The ECM is composed of structural proteins, proteoglycans, latent and active growth factors and matricellular proteins. The structural and functional diversity of different ECM proteins are predicted by site-specific biosynthesis of their structural components such as vitronectin, fibronectin, collagen, laminin and elastin. During the entire wound repair process, the changes in the ECM composition, amongst other, would have a direct effect on cell-matrix communication and consequently the behavior of the epithelial cells. Vitronectin is a glycoprotein with diverse distribution and functions. In the plasma, vitronectin has been found complexed with members of the complement as well as the coagulation cascade (Preissner, 1991). In the tissues, vitronectin is found in the ECM associated with angiogenesis (Brooks et al., 1994) and tumor progression (Gladson et al., 1990), suggesting its role in directed cell migration. Fibronectin is a dimeric glycoprotein that interacts strongly with other components of the ECM and is involved in a number of biological processes, such as cellular adhesion, motility, differentiation and homeostasis (Yamada, 1991). It has also been shown to play an important role in wound healing because it appears to be the stimulus for migration of epidermal cells (Donaldson et al., 1983; Takashima et al., 1986). Overall, the distribution and role of different ECM proteins in wound healing have been extensively studied, but the exact mechanism in wound healing is poorly known.

1.2.6.3 Matricellular proteins

Matricellular proteins, such as secreted protein acidic and rich in cysteine (SPARC), thrombospondin (TSP), tenascin and osteopontin, belong to a group of matrix-associated factors that modulate cell-matrix communications (Bornstein and Sage, 2002). Matricellular proteins do not subserve a primary structural role, in the sense that most collagens, laminins, and elastin are structural proteins. Rather, the complex nature of their functions derives from their ability to interact with multiple cell-surface receptors, cytokines, growth factors, proteases, and structural proteins. The contextual nature of their function thus reflects the composition of the matrix, the availability of cytokines and proteases, and the expression of integrins and other receptors in a given cellular environment. They are expressed when tissues undergo events that require tissue renewal, tissue remodeling or embryonic development. In spite of their importance during wound repair, there is a lack of information about their roles and mechanism of action when compared to growth factors and extracellular matrix proteins (Werner and Grose, 2003; Midwood et al., 2004). The interaction of integrin receptors with specific matricellular proteins appears to initiate a signal transduction pathway that involves the activation of intracellular protein Rho family of GTPase. The activation of Rho GTPases including cdc42, Rac1 and RhoA dramatically affects on cell migration through cytoskeleton reorganization events.

1.2.6.4 Adipocytokines

Adipose tissue not only serves as a passive reservoir for energy storage, it also produces and secretes in copious level a variety of bioactive molecules called adipocytokines,

including leptin, tumor necrosis factor, resistin and plasminogen activator inhibitor type-1 (PAI-1) (Shimomura et al., 1996), that have both systemic and local effects on wound repair. The dysregulated production of adipocytokines is associated with the pathophysiology of obesity-related metabolic diseases (Hotamisligil et al., 1993). Emerging works showed that some of these adipocytokines have a profound impact on wound healing. Leptin is a hypoxia-inducible pleiotropic adipocytokine known to participate in multiple cellular and physiological processes. Leptin is predominantly produced by white adipocytes and secreted into the bloodstream (Zhang et al., 1994). It is structurally related to cytokines and acts on receptors that have considerable homology to class I cytokine receptors (Tartaglia et al., 1995). The main effect of leptin in human body lies in the regulation of energy homeostasis especially under the conditions of restricted energy availability. Circulating leptin is also involved in glucose and lipid metabolism, angiogenesis, blood pressure regulation, bone mass formation and wound healing process. Leptin acts as potent angiogenic and mitogenic stimulus to keratinocytes during skin repair (Frank et al., 2000). Leptin is acutely up-regulated in the injured skin and was proposed that this local production of leptin serves a critical functional role as an autocrine/paracrine regulator of normal wound healing process (Murad et al., 2003). Interestingly, the systemic and topical application of leptin has been demonstrated to accelerate the wound healing process in wild type mice, suggesting a fundamental role during wound repair (Stallmeyer et al., 2001). However, its importance during wound healing under physiological circumstances and its mechanism of action remains unclear.

1.2.7 Angiopoietin-like 4 (ANGPTL4)–a novel adipocytokine: Implication for wound healing process

ANGPTL4 also known as peroxisome proliferator-activated receptor (PPAR), angiopoietin-related, fasting induced adipose factor (FIAF) and hepatic fibrinogen/angiopoietin-related protein (HFARP), is a circulating protein primarily expressed in adipose tissue and liver. ANGPTL4 is a glycosylated secretory protein with a predicted molecular weight of approximately 46 kDa. It is characterized by the presence of a signal peptide, an N-terminal coiled-coil domain and a C-terminal angiopoietin/fibrinogen-like domain. The ANGPTL4 protein exists as an oligomer containing intermolecular disulfide bonds. Oligomerized ANGPTL4 undergoes proteolytic processing to release its carboxyl fibrinogen-like domain which circulates as a monomer. The N-terminal coiled-coil domain of ANGPTL4 mediates its oligomerization which by itself is sufficient to form higher order oligomeric structure. The cleavage of full-length ANGPTL4 into the two fragments is serum dependent (Mandard et al., 2004). Further analysis show that the cleavage occurs at amino acids 164-165 as a major and 167-168 as a minor cleavage site (Chomel et al., 2009; Yang et al., 2008). Adenovirus-mediated overexpression of ANGPTL4 in HEK 293T cells shows that the conversion of full-length, oligomerized ANGPTL4 is mediated by a cell-associated protease activity induced by serum. These findings demonstrate a novel property of angiopoietin-like proteins and suggest that oligomerization and proteolytic processing of ANGPTL4 may regulate its biological activities *in vivo* (Ge et al., 2004). Apart from these physiological regulatory roles of ANGPTL4, the mechanisms which initiate the intra- or intercellular signaling events still remain largely unknown. This raises the question if there is a cell

surface ‘receptor’ for ANGPTL4.

ANGPTL4 was first identified as a target gene of the nuclear hormone receptor PPAR, which directs lipid metabolism in liver and white adipose tissue, respectively. The expression of ANGPTL4 is stimulated by hypolipidemic fibrate drugs and insulin-sensitizing thiazolidinediones. Studies have shown that human liver produces the truncated form of ANGPTL4; whereas human adipose tissues only produce the full-length form (Mandard et al., 2004). It is detected in various tissues and in blood plasma. Its abundance is increased by fasting conditions and decreased by chronic high-fat feeding which suggests that it has a novel endocrine signal involved in the regulation of metabolism, especially under fasting conditions (Kersten et al., 2000). Now it is known as an extremely powerful regulator of lipid metabolism and adiposity (Mandard et al., 2006). ANGPTL4 over-expression increases plasma levels of triglycerides, free fatty acids, glycerol, total cholesterol and high density lipoprotein (HDL)-cholesterol by inhibiting lipoprotein lipase activity. In addition, its overexpression severely impairs plasma triglyceride clearance but had no effect on very low density lipoprotein production. In human both full length and truncated ANGPTL4 were associated with HDL (Mandard et al., 2006). An earlier study reported the distinct effect on glucose metabolism and that its beneficial effect on glucose homeostasis might be useful for the treatment of diabetes (Xu et al., 2005). Recently it is reported that the down-regulation of ANGPTL4 expression in the intestine is essential for the increase in adipose mass induced by intestinal microbiota (Backhed et al., 2004). In addition, ANGPTL4 has also been associated with angiogenesis. It is also suggested that it acts as an apoptosis survival factor for vascular endothelial cells (Kim et al., 2000). Recent data also showed that

ANGPTL4 may be involved in the functional partitioning of postnatal intestinal lymphatic and blood vessels (Backhed et al., 2007).

Despite the well-established role of ANGPTL4 in lipid and glucose homeostasis, no studies have been undertaken to elucidate the effect of ANGPTL4 on keratinocyte migration during wound healing. Findings from our lab showed that the expression of adipocytokine ANGPTL4 was also stimulated in the wound epithelia during wound repair (Goh et al., in submission). As a secretory protein, the various forms of ANGPTL4 are likely to interact with specific membrane-bound receptors which initiate intracellular cascades leading to appropriate cellular responses including cell migration. Thus the goal of our present study is to identify and characterize the binding partners of ANGPTL4. We hypothesized that the identification of downstream interacting partners or receptors of ANGPTL4, which will provide important insights into its mechanism during wound healing process.

Herein, we decipher the molecular mechanism by which ANGPLT4 exerts its effects on keratinocyte survival, differentiation and migration. We identified and characterized the binding partners of ANGPLT4 using surface plasmon resonance (SPR) technology. Our current findings revealed a novel role of ANGPTL4 as a matricellular protein that interacts with matrix proteins such as vitronectin and fibronectin. This interaction enhances integrin-mediated intracellular signaling cascades to affect keratinocyte migration, differentiation and survival. Consistent with the critical role of ANGPTL4 during wound healing, we showed that topical application of anti-ANGPTL4 antibodies onto the skin excisional wounds severely delayed wound healing.

1.3 MATERIALS AND METHODS

1.3.1 Reagents

Glutathione sepharose 4B beads were purchased from Amersham Biosciences; rat tail collagen type I (BD Biosciences); purified vitronectin (Calbiochem); M106 medium with low serum growth supplement (Cascade Biologics); Pfu polymerase, transfection reagent, ExGen 500 and RevertAid H minus M-MuLV reverse transcriptase (Fermentas); Amine coupling kit, Immobiline pK buffers, Ni-NTA resin, Sensor chip (CM5) and Superdex 200 prep grade (GE Healthcare); pAc5.1/V5-His A plasmid, 4', 6-diamidino-2-phenylindole dihydrochloride (DAPI), Platinum quantitative PCR superMix-UDG, transfection reagent, Cellfectin and *Drosophila* medium for Schneider 2 (S2) insect cells (Invitrogen Life Technologies); Immobilin western chemiluminescent HRP substrate and PVDF membrane (Millipore); Seize X Protein G immunoprecipitation kit (Pierce Biotechnology); DNA purification, gel and PCR clean up kits (Promega); Collagen type 1 (Santa Cruz Biotechnology); 10 kDa cut-off membrane (Sartorius); purified fibronectin and laminin (Sigma-Aldrich). Unless otherwise stated chemicals were obtained from Sigma-Aldrich.

1.3.2 Antibodies

Polyclonal antibody against C-terminal region of human (186-406 amino acid) ANGPTL4 were produced by Biogenes. Antibodies against EGF receptor (Cell signaling); vitronectin, cdc42, integrin β_1, β_3 and β_5 (Chemicon); RhoA and Rac1 (Cytoskeleton); V5, Alexa Fluor 488 goat anti-rabbit IgG, Alexa Fluor 594 goat anti-rabbit IgG and Alexa Fluor 488 goat anti-mouse IgG (Invitrogen Life Technologies); Ki67 (NovoCastra).

Polyclonal antibody against C-terminal region of mouse (190-410 amino acids) ANGPTL4 produced by ProSci. Antibodies against fibronectin, goat anti-rabbit IgG HRP and goat anti-mouse IgG HRP were obtained from Santa Cruz Biotechnology.

1.3.3 Cloning of ANGPTL4

Human ANGPTL4 cDNA was subcloned into the actin 5 (Ac5) promoter-driven Drosophila cell expression vector pAc5.1/V5-His A. The full length ANGPTL4 cDNA was released by KpnI and XbaI restriction enzyme digestion from pcDNA3.1 and subcloned into similar sites in the pAc5.1 plasmid. The construct designated pAc5.1-ANGPTL4 contained the entire coding sequence of ANGPTL4 tagged to V5 epitope and Histidine at the carboxy terminus. The cDNA encoding the truncated N-terminal ANGPTL4 protein (nANGPTL4), amino acid 25 to 229 was amplified by Pfu polymerase and subcloned into the KpnI and Xba-I site of pAc5.1/V5-His A plasmid. The forward and reverse primers for polymerase chain reaction (PCR) were 5'-GATCGGTACCATGAGCGGTGCTCCGACGGCCGGG-3' and 5'-GATCTCTAGAC AGCCGGTGCAGGCGGCTGACATT-3', respectively. Cycle parameters were 95 °C for 2 min, followed by 30 cycles of 95 °C for 45 s, 56 °C for 45 s, 72 °C for 1 min 45 s and a final extension at 72 °C for 6 min. The DNA sequence encoding for the C-terminal ANGPTL4 fragment (cANGPTL4; amino acids 185 to 406) lacks the secretory sequence. To allow for its secretion, the corresponding DNA sequence were amplified and subcloned into a proprietary secretion vector, pAc5.1-SS (Tan et al., 2002) at the Eco47III and XbaI restriction enzyme sites. All ligated products were transformed into competent *E. coli* Top10 bacteria and selected on Luria broth (LB) agar plates containing

80 µg/ml ampicillin. Positive clones were verified by enzymatic digestions and finally confirmed by DNA sequencing. Positive constructs were used for transfection into S2 Drosophila cells as described in section *1.3.6.*

1.3.4 Cloning of ANGPTL4 siRNA template into pFIV-H1/U6 vector

The sense and antisense siRNA sequences targeting ANGPTL4 and control oligomers were synthesized (1st Base, Singapore) (Table 1.1). The corresponding sense and antisense oligomers were annealed, phosphorylated and ligated to linearised pFIV-H1/U6 provided by manufacturer (System Biosciences). The ligated product was transformed into *E. coli* Top 10 competent bacteria and selected for ampicillin resistance. Positive clones were identified by PCR using H1 and U6 primers and subsequently confirmed by sequencing (1st Base, Singapore). Positive constructs were used to make pseudoviral particles as described in section *1.3.7.*

1.3.5 Cell Cultures

Human embryonic kidney (HEK) cell line 293T cells and human keratinocytes were cultured in Dulbecco's modified Eagle's medium (DMEM) supplemented with 10 % fetal bovine serum (FBS) at 37 ^{o}C in a 5 % CO_2 humidified incubator. Human fibroblast cells were cultured in M106 medium with low serum growth supplement. Schneider 2 (S2) cells were cultured in suspension flask with Drosophila Medium at 25-27 ^{o}C in a humidified box. Both HEK 293T and keratinocytes were routinely subcultured using 0.2 % trypsin and 1 mM EDTA, while 0.05 % trypsin was used to subculture human fibroblasts. S2 cells grew in suspension and these cells were subcultured at a seeding

density of 5 x 10^5 viable cells/ml in growth medium, once the culture density reached more than 1 x 10^7 viable cells/ml.

Table 1.1 Primer sequences for polymerase chain reaction

siRNA		
ANGPTL4 siRNA	sense	5'- AAAGCTGCAAGATGACCTCAGATGGAGGCTG – 3'
	anti-sense	5'- AAAAGGCTTAAGAAGGGAATCTTCTGGAAGAC -3'
Control siRNA	sense	5'- AAAGCTGTCTTCAAGATTGATATCGAAGACTA -3'
	anti-sense	5'- AAAATAGTCTTCGATATCAAGCTTGAAGACA -3'
Real-time qPCR[1]		
Human ANGPTL4	Forward	5'- CTCCCGTTAGCCCCTGAGAG -3'
	Reverse	5'-AGGTGCTGCTTCTCCAGGTG -3'
	Taqman probe	5'- (6-FAM) ACCCTGAGGTCCTTCACAGCCTGC (TAMRA) -3'
Mouse ANGPTL4	Forward	5'- GCTTTGCATCCTGGGACGAG -3'
	Reverse	5'- CCCTGACAAGCGTTACCACAG -3'
	Taqman probe	5'- (6-FAM) ACTTGCTGGCTCACGGGCTGCTAC (TAMRA) -3'
Rpl27	Forward	5'- CTGGTGGCTGGAATTGACCGCTA -3'
	Reverse	5'- CAAGGGGATATCCACAGAGTACCTTG -3'
	Taqman probe	5'- (HEX) CTGCCATGGGCAAGAAGAAGATCGCC (BHQI) -3'

[1]Melting curve analysis was performed to assure that only one PCR product was formed. Primers were designed to generate a PCR amplification product of 100 to 250 bp. Only primer pairs yielding unique amplification products without primer dimer formation were subsequently used for real-time PCR assays.

1.3.6 Transfection of ANGPTL4 into S2 cells

Human ANGPTL4 cDNA constructs were introduced into S2 cells using Cellfectin. Stable S2 cells expressing the various forms of ANGPTL4 were selected using

hygromycin (300 µg/ml). For protein expression, stably transfected S2 cells were seeded into 400 ml of *Drosophila* serum-free medium at a density of 5 x 10^5 cells/ml in a 1L spinner flask and maintained at 25 °C with propeller speed at 115 rpm for 9 days to reach the culture density more than 1x 10^7 viable cells/ml.

1.3.7 Lentivirus expressing ANGPTL4 siRNA

The pFIV/siRNA and packaging plasmids were transfected into HEK 293T cells using ExGen 500. HEK 293T cells (2 x 10^5) were seeded per well of 6-well multi plate prior to the day of transfection. One µg each of expression and packaging vectors were diluted in 200 µl of 150 mM NaCl. It was briefly mixed and centrifuged. ExGen 500 (9.87 µl) was added immediately to the mixture and incubated at room temperature for 10 min. The volume of DNA/ExGen 500 mixture represents 1/10^{th} of the total volume of medium in the well. The cells were incubated at 37 ºC in 5 % CO_2 humidified incubator. The transfection reagent had minimal toxicity to the cell; therefore no change of medium was required after transfection. Supernatants containing pseudoviruses were collected 24 h and 36 h post transfection in 12 % polyethylene glycol 8000. They were incubated overnight in ice. After centrifugation, supernatants were discarded and the viral pellets were pooled together to transduce keratinocyte cells in the presence of polybrene (10 µg/ml). The tranduced cells were enriched by puromycin selection with 350 ng/ml concentration. Transfection efficency was assessed by quantitative real-time polymerase chain reaction (qPCR) and immunoblot analysis.

Gene constructs of human integrin β_1, β_3 and β_5 subcloned into pcDNA3.1 were introduced into HEK 293T cells for transient overexpression using ExGen 500 according

to the manufacturer's instructions.

1.3.8 Purification of recombinant human ANGPTL4

Culture medium of recombinant human full-length ANGPTL4 (ANGPTL4) and N-terminal ANGPTL4 (nANGPTL4) proteins were purified using a combination of affinity nickel-Sepharose and anion exchange chromatographies, as well as gel filtration in Tris buffer saline (TBS) on the Fast Performance Liquid Chromatography (FPLC) (AKTA). All steps were carried out at 4 °C. The supernatant of ANGPTL4 proteins were injected into the chamber fitted with Source 15Q anion-exchanger column (Amersham Biosciences) at a flow rate of 1 ml/min containing a buffer with 50 mM Tris pH 8, 50 mM NaCl. The protein was eluted with increasing concentration of 1 M NaCl. Five ml fractions were collected each over 2 column volumes. Analysis of eluent was done using UV absorption at 280 nm wavelength. Coomassie blue staining and western blot using anti-nANGPTL4 primary antibody was performed to determine which eluted fractions contained the desired proteins. Purified ANGPTL4 proteins were dialyzed overnight against TBS buffer at 4 ºC and were concentrated using 10 kDa cut-off polyethersulfone membrane Vivaspin tubes. Purified proteins were stored at −80 °C until further analysis.

To purify C-terminal ANGPTL4 (cANGPTL4) protein on a preparative scale, we used PI 8 IsoPrime Multi-chambered Electrofocussing unit (Amersham Biosciences). Isoelectric Preparative Membrane Electrophoresis (ISOPrime) protein purification technology was capable of separating proteins which differ in isoelectric point (Righetti et al., 1990). The culture medium was partially purified and desalted using diafiltration. The samples were subjected to preparative isoelectric focusing in 20 % glycerol.

Fractions were analyzed using coomassie blue staining of SDS-PAGE as well as immunoblot (see section *1.3.11*) with anti-histidine antibody.

1.3.9 Membrane protein extraction

We used two different kits to isolate the integral and membrane-associated proteins from mammalian frozen cell pellets. The ProteoExtract Native Membrane Protein Extraction Kit (M-PEK) of Calbiochem (method 1) was used for the isolation of native membrane proteins from mammalian cells. Mem-PER Eukaryotic Membrane Protein Extraction Reagent Kit of Pierce (method 2) was used to separate the hydrophobic proteins from the hydrophilic proteins through phase partitioning at 37 °C from cultured mammalian cells.

1.3.10 Quantitative real-time polymerase chain reaction (qPCR)

Total RNA was isolated from cells using Qiagen extraction kit. Real Time PCR was used to quantify the level of ANGPTL4 mRNA. Two µg of total RNA was used to synthesize cDNA using RevertAid H minus M-MuLV reverse transcriptase according to manufacturer's instructions. Real Time PCR was performed using Platinum Quantitative PCR SuperMix-UDG (Invitrogen). After a 10 min denaturation step of the template at 95 ºC, the PCR mix was subjected to 20 s denaturation at 95 ºC, 45 s annealing at 60 ºC and 20 s extension at 70 ºC for 40 cycles. At the end of each cycle, the melting curve was plotted with the readings at every ºC for 5 s between 50 ºC and 95 ºC. Housekeeping gene, 60S ribosomal protein L27 (Rpl27) was used for normalization. All oligonucleotides and Taqman probes were synthesized by Sigma-Proligo and their sequences provided in Table 1.1.

1.3.11 Immunoblots

Proteins were precipitated by a chloroform/methanol solvent method (Wessel and Flugge, 1984) prior to being resolved on 12 % SDS-PAGE. The proteins were electrotransferred onto a PVDF membrane using transfer buffer containing 25 mM Tris base pH 8.3, 150 mM glycine and 20 % methanol. For proteins of higher than 100 kDa, the transfer buffer contained 0.005 % SDS and reduced to 10 % methanol. The membranes were blocked with 5 % skim milk in TBS (0.25 M Tris/HCl pH 7.6, 0.15 M NaCl) containing 0.05 % Tween-20. The membrane was incubated with polyclonal primary antibody overnight at 4 ^{o}C and goat anti-rabbit IgG-HRP secondary antibody (1:10000) for 1 h at room temperature.

Rho GTPase proteins including cdc42, Rac1 and RhoA were separated by 12 % SDS-PAGE followed by transferred onto PVDF membranes. The membranes were blocked 1 h with 1 % BSA and 1 % skim milk in TBS containing 0.01 % Tween 20 (TBST). Membranes were washed three times for 5 min each in TBST. The PVDF membranes were incubated overnight at 4 °C with primary antibodies diluted 1:500 in TBST. Membranes were washed three times for 5 min each in TBST, prior to incubation for 1 h at room temperature with horseradish peroxidase-conjugated goat anti-rabbit for cdc42; goat anti-mouse for Rac1 and RhoA secondary antibodies diluted 1:5000 in TBST.

The extraction efficiency of membrane proteins extraction were assessed by SDS-PAGE and western blot analysis using anti-ERK-1 (1:1000 dilution) for cytosolic fraction and anti-EGF Receptor (1:1000 dilution) for membrane fraction.

1.3.12 Surface plasmon resonance (SPR)

The BIAcore 3000 (BIAcore, Uppsala, Sweden) was used to evaluate specific protein-protein interactions by Surface Plasmon Resonance (SPR) technology. In order to investigate the interactions between biomolecules at the surface of a sensor chip, optimization steps were performed in three major steps of SPR assay, namely immobilization, interaction analysis and regeneration. The carboxylated dextran matrix of a gold chip CM5 (research grade CM5, BIAcore, Uppsala, Sweden) was activated by mixing equal volumes of 0.2 M N-ethyl-*N*'-(3-dimethylaminopropyl) carbodiimide hydrochloride (EDC) and 0.05 M *N*-hydroxysuccinimide (NHS) (amine coupling kit, BIAcore, Uppsala, Sweden). The mixture was injected onto the sensor surface for 7 min at a flow rate of 10 µl/min. The experimental protein samples were immobilised individually on the chip at the concentration of 40 ng/µl in 10 mM acetate buffer pH 4.5 for EGF receptor antibody and cANGPTL4 at 10 mM acetate buffer pH 4.0 for ECM proteins such as vitronectin, fibronectin, collagen-1 and laminin-5, after performing immobilization pH scouting to determine the appropriate immobilization conditions. The immobilisation injection flow rate was 10 µl/min with a total volume of 110 µl for each sample at 25 °C. The procedure was completed by injection of 1 M ethanolamine hydrochloride (75 µl) to block any remaining ester groups. Hepes-buffered saline (HBS-P) buffer [10mM (4-(2-hydroxyethyl)-1-piperazineethane- sulfonic acid) pH 7.4, 0.15 M NaCl, 0.005 % Tween 20] was used as the running buffer. After immobilization, the indicated analytes (35 µl) were injected at a flow rate of 30 µl/min into the appropriate immobilized sensor surface chip at 40 ng/µl concentration. The binding interactions were monitored in real time. Following each interaction and prior to the next sample being

tested, the sensor chip was regenerated with 10 mM glycine-HCl pH 3.5 at a flow rate of 30 µl/min followed by washing with running buffer. No loss of binding capacity was observed under these conditions. Thus the same surface was used for subsequent experiments. All the plots of response against time (sensorgram) were processed by using automatic correction for nonspecific bulk refractive index effects.

The association and dissociation were monitored by injection of different analyte samples as indicated in figures into the immobilized flow cell at a flow rate of 30 µl/min. In all kinetic studies, protein samples were injected over the test and control chip surfaces at a flow rate of 30 µl/min. The apparent equilibrium dissociation constant, K_D was determined from the ratio of dissociation rate constant (K_{off}) and association rate constant (K_{on}). The binding kinetic parameters were analyzed by using BIAevaluation version 3.1 software (BIAcore).

1.3.13 SPR coupled to liquid chromatography-tandem mass spectrometry (LC-MS/MS)

To identify the binding partners of ANGPTL4, acute wound plasma exudates buffered with 50 mM Tris at pH 8.0 was introduced into the cANGPTL4 conjugated CM5 chip at a flow rate of 5 µl/min for 10 min with running buffer (50 mM Tris pH 8.0, 100 mM NaCl). After incubation for 45 s, the chamber was washed with same buffer, and the bound molecules were subsequently eluted using 10 mM glycine pH 6.0 and collected in a recovery vial. The CM5 chip was reused to pool more samples after washing with running buffer for 10 min at 20 µl/min. The recovered cANGPTL4-binding proteins were tryptic digested, reduced, alkylated and then analyzed with a Finnigan Surveyor HPLC

system coupled online to a LTQ-Orbitrap mass spectrometer (Thermo Electron) equipped with a nano-spray source. Mascot search was performed for protein identification.

1.3.14 Affinity Co-precipitation (Co-IP) assay

Purified recombinant His-tagged ANGPTL4, nANGPTL4 or cANGPTL4 was immobilized onto the Ni-NTA resin. The resin was washed with wash buffer (50 mM Tris pH 7.5, 150 mM NaCl, 0.1 % TritonX-100) to remove excess ANGPTL4. Equal amount of ANGPTL4-bound resin was dispensed and incubated with 500 ng of purified matrix protein in PBS at 25 °C for 30 min. The resin was next thoroughly washed with wash buffer. The unbound fractions (U) were pooled and the bound (B) fractions were released by SDS-PAGE loading dye. Both fractions were analyzed by immunoblotting with their indicated antibodies. As control, resin treated with PBS was used.

1.3.15 Sucrose gradient sedimentation assay

Linear 25-40 % sucrose gradients in buffer containing 50 mM Tris pH 8.0, 100 mM NaCl were prepared by layering successive decreasing sucrose density solutions upon one another in 5 ml polyallomer ultracentrifuge tubes (Beckman). In order to make continuous sucrose density gradient, tubes were kept into 4 °C for 6 h. One μg of indicated proteins were allowed to interact in 150 μl of tris buffer containing 50 mM Tris pH 8.0, 100 mM NaCl, for 2 h at 4 °C. The protein mixture was layered on top of the gradient and size-fractionated by ultracentrifugation at 132000 x g for 16 h at 18 °C. Fractions of 300 μl were collected from the top of the tubes, chloroform/ethanol precipitated and detected for the various proteins by immunoblotting using their respective antibodies (see section *1.3.11*).

1.3.16 Organotypic co-culture (OTC)

Primary human keratinocyte cells (10^6 cells/insert) were seeded onto rat tail collagen type I gels containing 10^5/ml human fibroblasts cast in 24-mm diameter Transwell cell culture filter inserts (pore size 3.0 μm, BD Biosciences) and cultured in serum-free OTC medium overnight as described in detail previously (Chong et al., 2009). The serum-free OTC contains basal medium, 3:1 (vol/vol) DME (low glucose), Ham's F-12 nutrient mixture, basal supplements 5 μg/ml insulin, 1 ng/ml epidermal growth factor, 0.4 μ g/ml hydrocortisone, 100 nM adenine, 10 μM serine, 100 nM cholera toxin, 10 μM carnitine, 1 mg/ml fatty acid-free albumin, lipid supplements 0.05 mM ethanolamine, 1 μM isoproterenol, 1 μM α-tocopherol, and 50 μg/ml ascorbic acid. The cultures were raised to the air-liquid interface by lowering the upper medium level to the lower part of the collagen gel. Medium was replaced every 3 days for 2-weeks. Cultures were embedded in Tissue Tec OCT Compound and frozen in liquid nitrogen for cryosectioning.

1.3.17 Cryofreezing and cryosectioning

For histological analysis and immunofluorescence studies, OTCs were fixed in 4 % paraformaldehyde for 2 h at room temperature. After washing in PBS for 10 min, they were embedded in Tissue-Tek OCT freezing medium and incubated for 1 h at room temperature. They were kept in 4 °C overnight before freezing at -80 °C. The frozen blocks were cryosectioned at 5 μm using LEICA CM 3050S and air dried on charged slides (SuperFrost Plus). The slides were stored at -20 ºC for further analysis.

1.3.18 Haematoxilin and eosin staining

The sections were fixed in 4 % paraformaldehyde for 10 min and stained with haematoxylin for 5 min. The sections were then rinsed for 2 s in 0.1 % HCl and allowed to develop in running water for 3 min. The sections were counterstained with 0.5 % eosin aqueous solution for 27 s. The sections were rinsed for 10 s in water. Mounting was done with 90 % glycerol/10 % 10X PBS. The sections were viewed using Nikon ECLIPSE 90i, Plan Fluor 10X/0.3 objective, and QCapture pro version 5.0.1.26 software with constant exposure and gain.

1.3.19 Immunofluorescence

The frozen sections were allowed to equilibrate to room temperature. They were then fixed, blocked and probed with antibodies suitable for immunofluroscence as described in Table 1.2.

Table 1.2 Conditions for the various immunofluorescence

Marker	Fixing conditions	Blocking conditions	Primary antibody conditions
Ki67	4 % paraformaldehyde 10 min Room temperature	3 % normal goat serum 1 h Room temperature	1: 100 in 3 % normal goat serum 1 h Room temperature
cANGPTL4	4 % paraformaldehyde 10 min Room temperature	3 % normal goat serum 1 h Room temperature	1: 100 in 3 % normal goat serum 1 h Room temperature

Proliferation marker Ki67, being a nuclear protein, needs antigen retrieval for detection. Sodium citrate buffer (10 mM) at pH 6.0 was used for antigen retrieval. Following fixation in 100 % acetone at -20 °C for 5 min, the slides were rinsed in 1X PBS for 5 min. The slides were boiled for 10 min in the sodium citrate buffer and allowed to cool to room temperature for 30 min. The sections were rinsed in 1X PBS before blocking as described in Table 1.2.

Paraffin sections (3 μm thickness) of wound tissue were used to examine the localization of ANGPTL4 in skin. Deparafinization and rehydration of sections were done by immersing the sections sequentially in xylene (twice) for 5 min, 100 % ethanol (twice) for 5 min, 90 % ethanol for 3 min, 80 % ethanol for 3 min and 70 % ethanol for 3 min at room temperature. The slides were rinsed in 1X PBS for 5 min before antigen retrieval procedure as described above.

Cryosections of OTC for integrins β_3 and β_5 were fixed with 4 % paraformaldehyde in PBS for 15 min at room temperature. The sections were permeabilized with 0.5 % Triton X-100 for 1 min, washed and blocked with 5 % bovine serum albumin (BSA) in PBS. The permeabilized sections were incubated with either anti-β_3 (monoclonal) or anti-β_5 (polyclonal) integrin antibodies at room temperature for 1 h. The sections were washed with PBS thrice for 5 min and subsequently incubated with either Alexa Fluor 488 goat anti-mouse IgG or Alexa Fluor 488 goat anti-rabbit IgG at room temperature for 1 h. After washing, sections were mounted with medium containing molecular antifade probes 4', 6-diamidino-2-phenylindole dihydrochloride (DAPI) and viewed using Nikon inverted microscope ECLIPSE TE2000-U with a Plan-NeoFluor 20X/0.45 objective, and Image-Pro® Plus software with constant exposure and gain.

1.3.20 TUNEL (Terminal deoxynucleotidyl transferase dUTP nick end labeling) assay

TUNEL assays were performed on frozen sections for assessment of apoptotic cells. The sections were fixed in 4 % paraformaldehyde for 15 min. After rinsing for 5 min in 1X PBS, the sections were permeabilised with 0.1 % TritonX-100, 1 % BSA in 1X PBS into humid chamber at 37 ºC for 8 min. Section to be used as positive control was incubated with DNase I (3 U/µl in 50 mM Tris-HCl, pH 7.5, 1 mg/ml BSA) for 10 min at room temperature to induce DNA strand breaks. The sections were then treated with labeling solution and enzymatic solution at 9:1 ratio and incubated at 37 ºC for 1 h at room temperature in the dark. For negative control, section was incubated only with labeling solution. All the sections were rinsed thrice in 1X PBS, before mounting with DAPI.

1.3.21 In vitro scratch wound assay

In vitro scratch wound assays were performed using wild type (K_{CTRL}) and ANGPTL4 knockdown ($K_{ANGPTL4}$) human keratinocytes as previously described (Michalik et al. 2001). Live cell images at 2 min intervals over 6 h were captured using a temperature-controlled, 5 % CO_2-chambered Axiovert 200M inverted microscope, Plan-Neofluor 10X/0.3 objective with a 1.0X magnification, Ph1 phase contrast and 40X/0.6 objective with a 1.6X magnification, Ph2 phase contrast, and MetaMorph version 6.3r1 software with constant exposure and gain (Zeiss). Similar experiments were performed using wounded K_{CTRL} culture in the presence of either pre-immune IgG or anti-cANGPTL4 antibody at 2 µg/ml.

1.3.22 Rho GTPases pull-down assay

GST-Rhotekin and GST-PAK constructs were transformed into *E. coli* BL21 cells and grown at 37 ºC until the optical density (OD) at 600 nm reached 0.6-0.7. Bacterial cells were then induced with 1 mM Isopropyl β-D-1-thiogalactopyranoside (IPTG) for 3 h at 30 ºC for the expression of target proteins and cells were harvested by centrifugation at 5000 x g for 10 min. Bacterial pellets were resuspended in ice-cold NP-40 lysis buffer (PBS containing 0.2 % NP-40 and 1 mM PMSF), sonicated and centrifuged at 14,000 x g for 10 min at 4 ºC. Supernatant was collected and incubated with 20 µg of glutathione-S-transferase (GST) beads for 1 h at 4 ºC with gentle rocking and finally beads were washed twice in NP-40 lysis buffer and twice in PBS buffer. The Rho binding domain (RBD) of Rho effector Rhotekin and PAK were purified as GST fusion proteins and verified by commassie blue staining of 12 % SDS PAGE.

Activation of Rho family small GTP binding proteins were investigated and quantified in cell extracts using pull-down assay by precipitation with GST protein coupled to the Rho binding domain of rhotekin (GST-Rhotekin) and Rac1/cdc42 binding domain of PAK (GST-PAK). Cells around 60-70 % confluent into tissue culture dish (Ø 100 X 20 mm) were incubated for 3 h with serum free DMEM medium and stimulated with complete DMEM medium having 10 % serum for the different time periods. Cells were lysed into 500 µl of lysis buffer containing 20 mM HEPES ((4-(2-hydroxyethyl)-1-piperazineethanesulfonic acid) pH 7.4, 100 mM NaCl, 0.5 % NP-40, 5 mM $MgCl_2$, 1 mM sodium orthovanadate, 1 mm PMSF and 1 % glycerol at 4 ºC for 5 min. Supernatant was collected after centrifugation at 14,000 x g for 10 min. At indicated time, 1 mg of cell lysates were incubated with either GST-Rho binding domain of PAK for cdc42 and

Rac1, or with GST-Rho binding domain of Rhotekin for RhoA, coupled to GST beads for 1 h at 4 ºC. Collected beads were washed twice in wash buffer (20 mM HEPES pH 7.4, 100 mM NaCl, 0.1 % NP-40, 5 mM $MgCl_2$, 1 mM sodium orthovanadate, 1 mM PMSF and 1 % glycerol) and bound active proteins were denatured in SDS sample buffer and separated on 12 % SDS PAGE followed by immunoblotting using antibodies against cdc42, Rac1 and RhoA. Total cdc42, Rac1, RhoA and β-tubulin were detected using cell lysate.

1.3.23 Skin wounding experiments in vivo

Under anaesthesia, a full thickness wound (0.5 cm^2 surface, square shaped), were made in the backs of C57BL/6 mice (6-weeks old) 2 weeks after shaving, corresponding to the telogen phase of hair follicle cycle. In each animal, one such wound was made on each side of dorsal midline separated from each other by at least two centimeters. The wounds were kept moist with occlusive dressing (Tegaderm). Wounds were topically treated daily with 50 µg of either pre-immune IgG or anti-cANGPTL4 antibodies. Treatments were rotated to avoid site bias. At indicated days post-injury, animals were anaesthetized, and biopsies were taken from all wound sites at once. Each biopsy included the entire wounded area and some adjacent unwounded tissue. Wound biopsies were fixed in 4 % paraformaldehyde and processed for paraffin sectioning. Sections of 5 µm thick were cut and stained with haematoxilin and eosin (see section *1.3.18*).

1.4 RESULTS

1.4.1 Expression of ANGPTL4 is up-regulated during wound healing

Earlier studies have shown that the expression of ANGPTL4 is up-regulated by nuclear hormone receptor PPARα in the liver and PPARγ in the adipose tissue (Kersten et al., 2000). However, the expression of ANGPTL4 during skin wound repair, when PPARδ is elevated, had not been investigated (Michalik et al., 2001; Tan et al., 2001). Herein, using quantitative PCR (qPCR) and immunoblot analysis, we examined the mRNA and protein expression profiles of ANGPTL4 during the healing of mouse skin full-thickness excisional wound. The expression profile of ANGPTL4 mRNA was similar to PPARδ, peaking at Days 3 to 5 post-injury (Fig. 1.3A, left panel). Using polyclonal antibodies that recognized either the N- or C-terminal region of ANGPTL4, we showed that only the full-length ANGPTL4 and cANGPTL4 were detected in wound biopsies (Fig. 1.3A, right panel). Information regarding the site of ANGPTL4 protein expression in tissues can provide valuable insights and may reveal novel functions of ANGPTL4. To this end, we performed dual immunofluorescence staining using antibodies against cANGPTL4 and proliferation marker Ki67 on mice skin wound biopsies. The staining revealed that the expression of ANGPTL4 increased progressively and reached its maximum at Day 5 post-wounding, coincidental with an increase in the number of Ki67-positive proliferating keratinocytes at Day 7. In addition to the wound epithelia, ANGPTL4 was also detected in the wound bed (Fig. 1.3B). Low level of ANGPTL4 was detected in unwounded skin (Fig. 1.4A, right panel). Immunofluorescence performed using pre-immune serum did not display any staining (Fig. 1.4A, left panel). The anti-nANGPTL4

A.

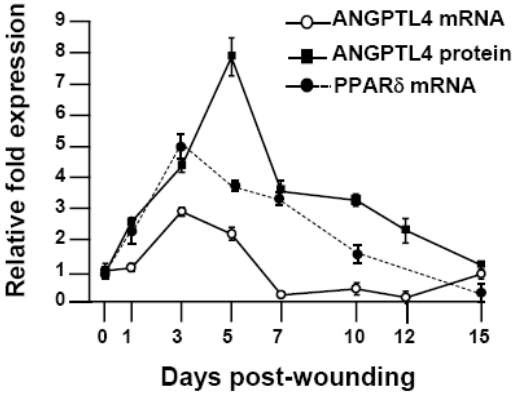

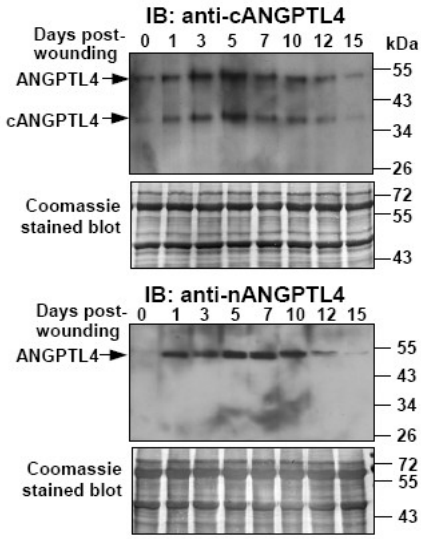

B.

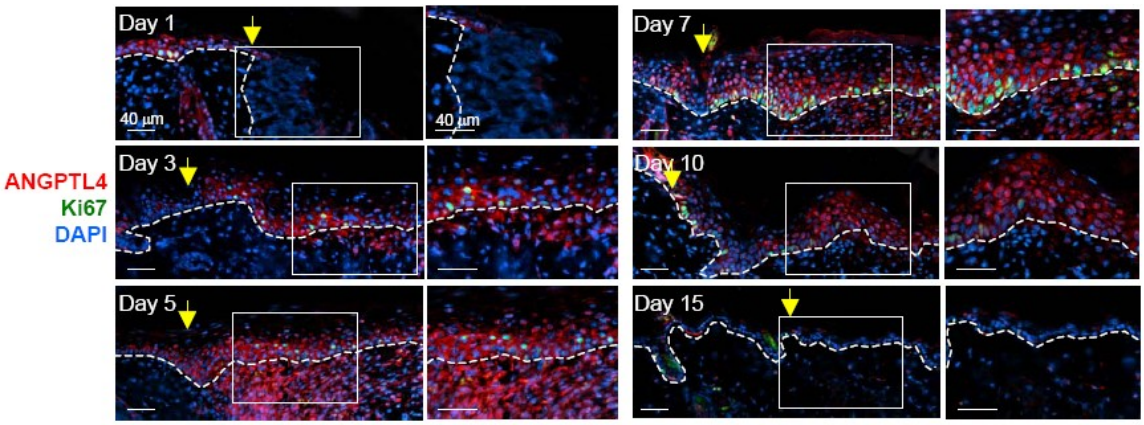

C.

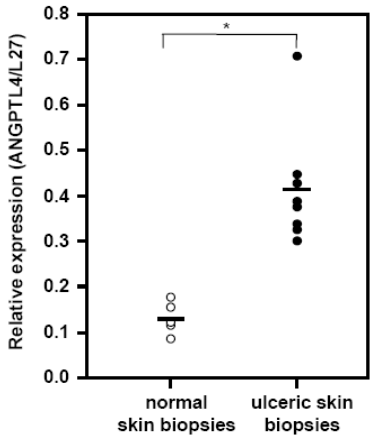

Figure 1.3 ANGPTL4 expression is induced during skin wounding. (A) ANGPTL4 mRNA and protein expression profiles during wound healing determined using qPCR and immunoblotting. Polyclonal antibodies that recognized the N- (anti-nANGPTL4) and C-terminal (anti-cANGPTL4) of ANGPTL4 were used. Coomassie-stained blot showed equal loading and transfer. **(B)** Immunofluorescence staining of ANGPTL4 in skin wound biopsies. Mice skin wound biopsies at indicated days of post-wounding were cryosectioned and stained with antibodies against cANGPTL4 (red) and Ki67 (green), and counterstained with DAPI (blue). Representative pictures from wound edge and the adjacent wound bed were shown. The basal layer of keratinocytes and the underlying extracellular matrix are highlighted in the smaller windows next to the main figures. Yellow arrow represents wound edge at Day 0. Dotted white line represents epidermal-dermal junction. Higher magnifications are shown in boxes. Scale bars 40 μm. **(C)** Relative expression level of ANGPTL4 mRNA in normal human skin and chronically inflamed ulcer skin biopsies as determined by qPCR. Ribosomal protein Rpl27 was used as a normalizing housekeeping gene in **A** and C. (* denotes p=0.0016; two-tailed Mann-Whitney test). Values are mean ± SEM of three independent experiments (n=3).

antibody was not suitable for immunohistochemistry (data not shown).

To investigate whether the up-regulation of ANGPTL4 was similarly observed in human, we performed a retrospective examination of human wounds. Consistently, human chronic ulcer showed a higher ANGPTL4 expression when compared to normal human skin (Fig. 1.4B). We compared the level of ANGPTL4 mRNA in human ulceric skin biopsies to normal human skin by qPCR. Consistent with the immunofluorescence staining results, the ANGPTL4 mRNA level was also up-regulated (see Fig. 1.3C). These observations underscore an important role of ANGPTL4 during re-epithelialization of rodents and human skin wound.

1.4.2 Study of ANGPTL4 binding target proteins

To gain mechanistic insight into the molecular action of ANGPTL4 in wound repair, we sought to identify ANGPTL4-binding proteins using SPR coupled to mass spectroscopy

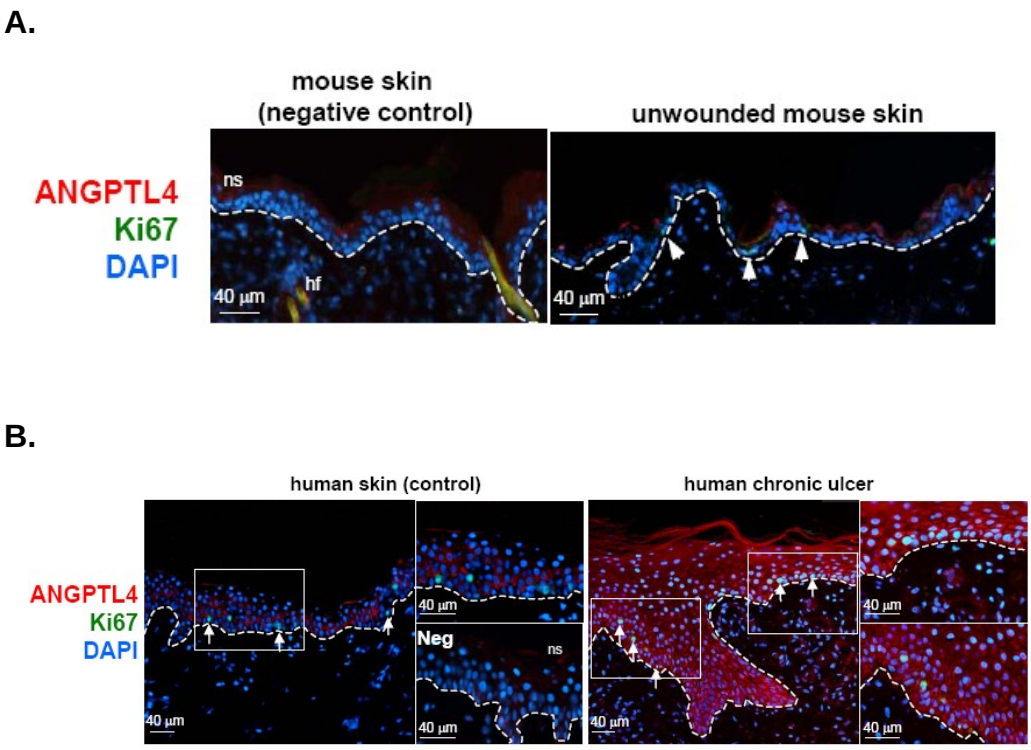

Figure 1.4 Immunofluorescence staining of ANGPTL4 in unwounded mouse skin and human skin ulcer biopsy. ANGPTL4 is expressed in **(A)** unwounded mouse skin and **(B)** unwounded human skin and ulcer. Higher magnifications are shown in boxes. Polyclonal antibodies against mouse and human cANGPTL4 were used. The anti-nANGPTL4 antibodies were not suitable for immunofluorescence staining. Negative controls without primary antibody. White arrows indicate proliferating Ki67-positive keratinocytes. Scale bars 40 μm. Representative pictures of immunostained sections were shown. Immunostaining were performed on five mice skin and eight paraffin-embedded human ulcer biopsies.

(SPR-MS), which enables us to recover interacting proteins and to deposit the proteins directly to MALDI for analysis by MS. Purified ANGPTL4 was immobilized onto the CM5 sensor chip via amine coupling.

1.4.2.1 Expression of recombinant ANGPTL4 proteins into Schneider 2 (S2) insect cells

Our earlier work and that of others have shown that ANGPTL4 protein is expressed as an insoluble protein in both bacteria and yeast expression systems. Thus far, the mammalian system was used to produce small amount of soluble and functional ANGPTL4 protein. To produce sufficient amount of ANGPTL4 protein to be used as bait for interacting proteins, we used a proprietary *Drosophila* secretory expression system (Tan et al., 2002). The cDNA sequences encoding full length, N-terminal and C-terminal ANGPTL4s were subcloned into *Drosophila* expression vector pAc5.1 and the resulting constructs (Fig. 1.5A) were named as pAc5.1 ANGPTL4, pAc5.1 nANGPTL4 and pAc5.1 cANGPTL4, respectively. Recombinant plasmids were verified by restriction enzyme digestion (Fig. 1.5B) and finally confirmed by DNA sequencing.

Drosophila S2 insect cells in suspension were transfected with the various recombinant plasmids. Transfection of S2 cells with pAc5.1 ANGPTL4, nANGPTL4 or cANGPTL4 resulted in ~50 % transformants and stable recombinant cell lines were obtained by hygromycin selection. To examine the expression of the various recombinant ANGPTL4 proteins, we performed western blot analysis using anti-V5 antibody. Western blot revealed proteins of apparent molecular weight of ~50 kDa, 23.5 kDa and 32 kDa, corresponding to ANGPTL4, nANGPTL4 and cANGPTL4 respectively in the S2 culture

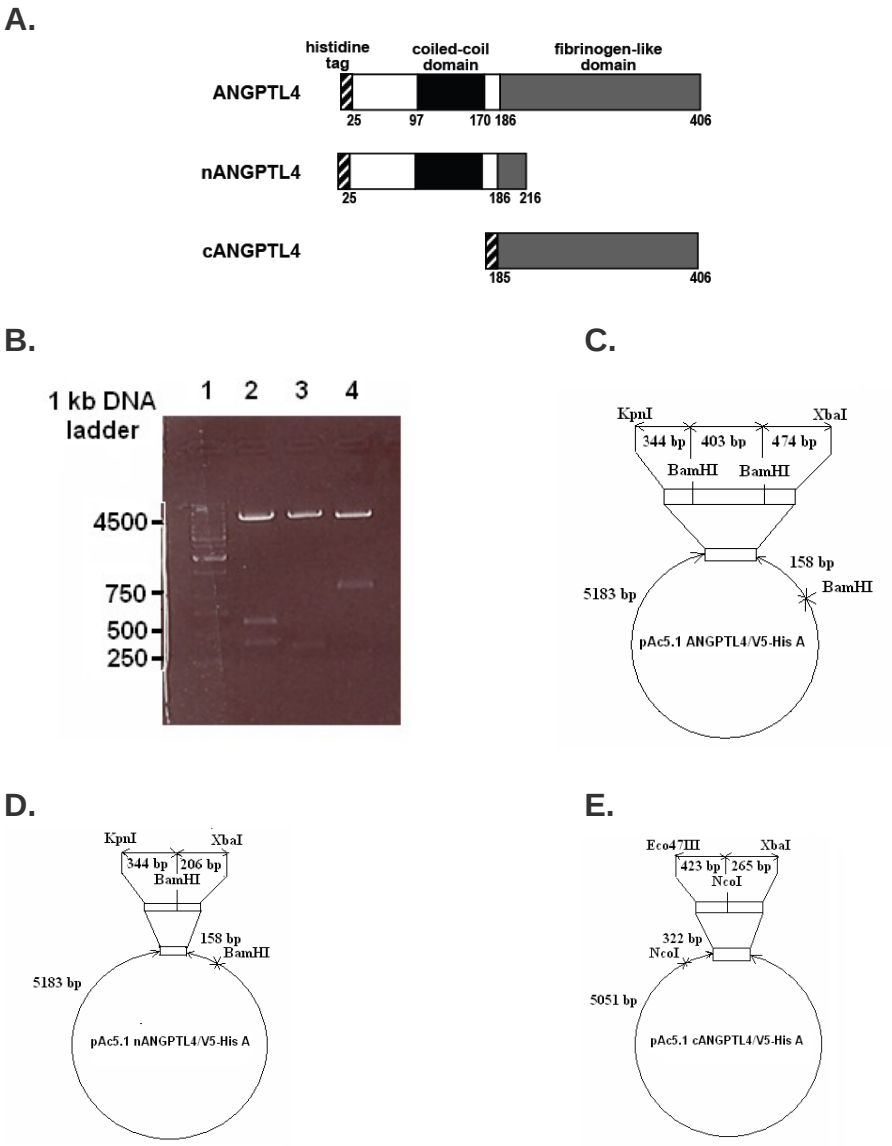

Figure 1.5 Expression of ANGPTL4 recombinant proteins. **(A)** Schematic representation of different forms of ANGPTL4 orientation and its His tag in the expected protein products from constructed vectors pAc5.1 ANGPTL4/V5-His A, pAc5.1 nANGPTL4/V5-His A and pAc5.1 cANGPTL4/V5-His A in which human mature full length ANGPTL4 (ANGPTL4), truncated N-terminal ANGPTL4 (nANGPTL4) and truncated C-terminal ANGPTL4 (cANGPTL4), respectively, are present without the ANGPTL4 signal sequence. **(B)** Recombinant Drosophila expression constructs containing the cDNA of various ANGPTL4 proteins. Restriction enzyme digestion of ANGPTL4 expression constructs. Lane 1: Marker; Lane 2: pAc5.1 ANGPTL4/V5-His A digested with BamHI; Lane 3: pAc5.1 nANGPTL4/V5-His A digested with BamHI and Lane 4: pAc5.1 cANGPTL4/V5-His A digested with NcoI restriction enzyme. Restriction map of **(C)** pAc5.1 ANGPTL4/V5-His A, **(D)** pAc5.1 nANGPTL4/V5-His A and **(E)** pAc5.1 cANGPTL4/V5-His A used in this work. The relative positions in base pairs of selected restriction sites are as shown.

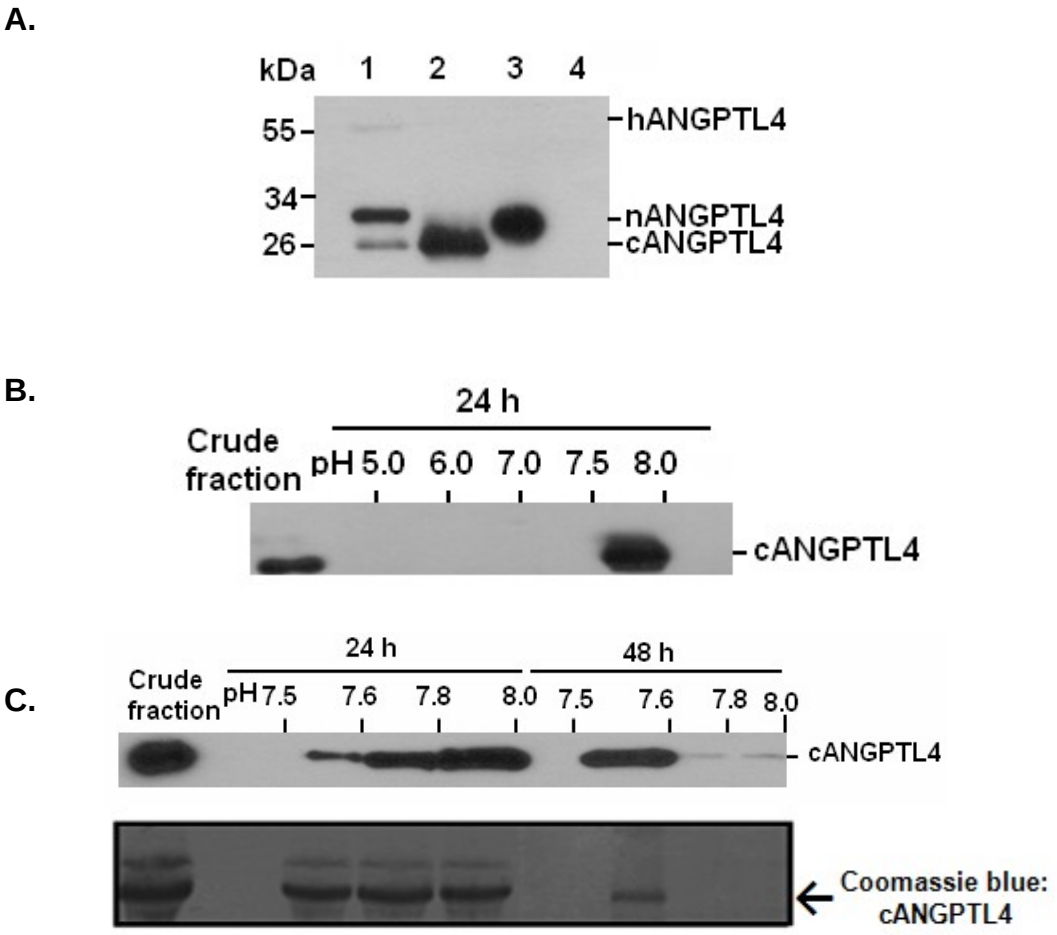

Figure 1.6 Purification of cANGPTL4 recombinant proteins using Isoprime multi-chambered electrofocusing unit. (A) Immunoblot analysis of recombinant ANGPTL4 proteins from medium of transfected S2 cell. Lane 1: ANGPTL4; Lane 2: nANGPTL4; Lane 3: cANGPTL4 and Lane 4: control medium. Culture medium were resolved in a 12 % SDS–PAGE gel, transferred into PVDF membrane, and probed with an anti-V5 polyclonal Ab. Recombinant ANGPTL4 proteins of the expected molecular weight were detected in the culture medium. Two smaller protein bands were detected in the medium of S2 cells expressing the full length ANGPTL4 protein, due to proteolytic cleavage during harvesting of medium. **(B)** Immunoblot analysis of cANGPTL4 protein using IsoPrime multi-chambered IEF purification unit. Immunoblot analysis revealed that all cANGPTL4 proteins focused into the chamber delimited by membranes of pH 7.5 and 8.0 after 24 h. **(C)** Immunoblot and coomassie blue stain analysis shown that 24 h focusing is not sufficient for purification of cANGPTL4 protein. Another 24 h is needed for purification of cANGPTL4 protein which is enriched in between membranes pH 7.5 and 7.6.

medium (Fig. 1.6A). The secretion of ANGPTL4, nANGPTL4 and cANGPTL4 represented more than 90 % of the total recombinant protein expression.

1.4.2.2 Purification and verification of recombinant ANGPTL4 proteins

Next, we investigated the optimal growth conditions for the expression of ANGPTL4 proteins. Stable recombinant *Drosophila* cells secreting cANGPTL4 was grown in serum-free medium in a 500 ml-Bellco spinner flask. The 500 ml medium was inoculated with final concentration of 5 x 10^5 cells/ml. The cell density was enumerated over a period of 9 days. The cell density increased to more than 1 x 10^7 viable cells/ml, thereafter the number of viable cell decrease. Hence, the medium was harvested and kept at -20 ºC temperature for future experiments.

The medium was initially concentrated and desalted via three rounds of ultrafiltration using a 10 kDa cutoff membrane in an Amicon stirred cell. This ultrafiltered medium was subjected to two rounds of preparative isoelectric membrane electrophoresis. In the first round of purification, a set of five membranes of pH 5.0, 6.0, 7.0, 7.5 and 8.0 were used. The ultrafiltered medium was introduced into all the chambers and subjected to 24 h of electrophoresis. The cANGPTL4 protein was localized in chamber delimited by pH 7.5 and 8.0 (see Fig. 1.6B). This partially purified cANGPTL4 protein was then subjected to another round of isoelectric membrane electrophoresis, using membranes of pH 7.5, 7.6, 7.8 and 8.0. The cANGPTL4 protein was subsequently purified to homogeneity (see Fig. 1.6C). A typical yield of 4.3 mg of cANGPTL4/L medium was obtained.

Several problems were encountered during the purification of the full length

(ANGPTL4) and N-terminal ANGPTL4 (nANGPTL4) proteins. As shown in Fig. 1.7A, nANGPTL4 was subjected into isoelectrophoretic chamber 6.0 to 6.5 but was not able to be subsequently purified to homogeneity.

Both proteins tend to form higher molecular weight oligomer at higher concentrations which interfered with their movements through the membranes during isoelectric electrophoresis. With respect to ANGPTL4, the protein has the tendency to undergo proteolysis generating the N-terminal and C-terminal truncated ANGPTL4. Both phenomena were similarly observed in human and mouse. To circumvent these problems, we used anion-exchange chromatography for initial partial purification of the proteins. Our results from the anion-exchange and affinity chromatography showed that the ANGPTL4 and nANGPTL4 proteins were eluted in an increasing salt step-gradient elution profile (Fig. 1.7B). The relative NaCl concentration of 92.5 mM reduced the extent of oligomerized protein. When stable cell lines were established in serum-free medium without hygromycin for a week, a typical yield of 1.34 mg/L for ANGPTL4 and 1.5 mg/L for nANGPTL4 were obtained.

1.4.2.3 Immobilization of cANGPTL4 in sodium acetate buffer

One of the major requirements for the characterization of biomolecular interactions including binding specificity, kinetics and drug discovery using fully automated, high quality biosensor SPR system is the optimal condition necessary for immobilization of the target protein onto the CM5 chip. In repeated experiments for each ligand molecules, concentration and coupling time were varied to give a range of immobilized molecules coupled to the sensor chip, to check for possible mass transport effects, which are

expected to be most pronounced at high immobilization levels and high binding affinities (Schuck, 1996). We used high immobilized CM5 sensor chip for several reasons. First, these sensor chips were used for SPR-MS where maximal recovery of bound analyte is desired. Second, the concentration, size and stability of the potential ANGPTL4 interacting partner(s) in wound fluid are unclear. We used low immobilized CM5 sensor chip for kinetic analysis to minimize the mass transfer limitation. As expected, the electrostatic attraction of the cANGPTL4 protein to the dextran matrix on the CM5 sensor chip was heavily dependent on the pH and the ionic strength of the buffer.

To identify the optimal immobilization condition, we examined the effect of pH on immobilization of cANGPTL4 protein which was diluted in sodium acetate buffer of different pH, ranging from 4.0 to 5.5. Our results showed that the optimum pH was 4.5 for maximum cANGPTL4 protein binding onto the CM5 chip surface (Fig. 1.8A). Consequently, cANGPTL4 protein was covalently immobilized onto CM5 via amine coupling at pH 4.5 (Fig. 1.8B). For further confirmation of the immobilization of cANGPTL4 protein, anti-cANGPTL4 antibody was injected on the surface of immobilized cANGPTL4. As expected, the sensorgram reported a significant specific binding of antibody to the cANGPTL4 as indicated by 575.74 RU value (Fig. 1.8C), suggesting that the immobilized protein retained its proper structure and that the antibody binding site is available. The anti-cANGPTL4 antibody was also injected over the control surface i.e. not immobilized with cANGPTL4; which did not observe any binding. In contrast, we were not able to immobilize ANGPTL4 nor nANGPTL4 on biosensor chip due to their propensity to form oligomers.

A.

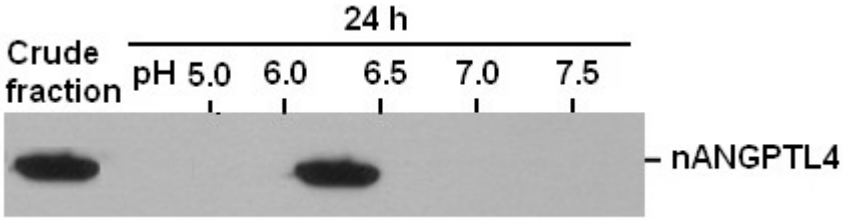

B.

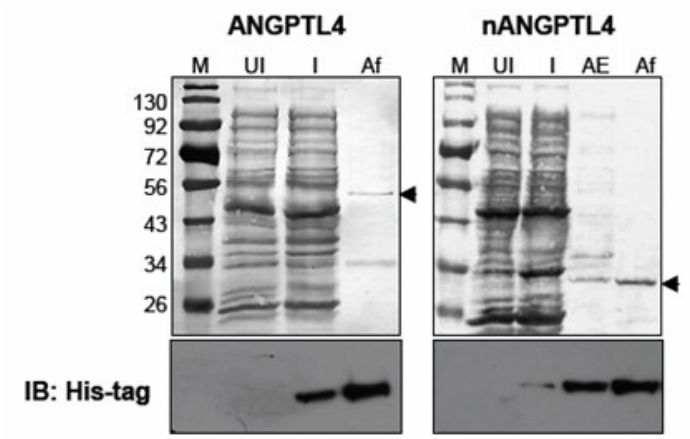

Figure 1.7 Purification of ANGPTL4 and nANGPTL4 recombinant proteins. (A) Immunoblot analysis of nANGPTL4 protein using IsoPrime multi-chambered IEF purification unit. Results shown that all nANGPTL4 proteins focused into the chamber enclosed by membranes of pH 6.0 and 6.5. Coomassie blue staining of the membrane shown that the presence of higher molecular weight bands. Furthermore, this result suggested the higher oligomer of nANGPTL4 protein. **(B)** Purification of mammalian expressed His-tagged ANGPTL4 and nANGPTL4 proteins using FPLC. M: molecular weight marker; UI and I denotes: uninduced and IPTG-induced bacterial lysates; Af: nickel-sepharose affinity chromatography; AE: anion-exchange. Coomassie blue stain and western blot analysis of fractions eluted at different step(s) during purification of proteins.

A.

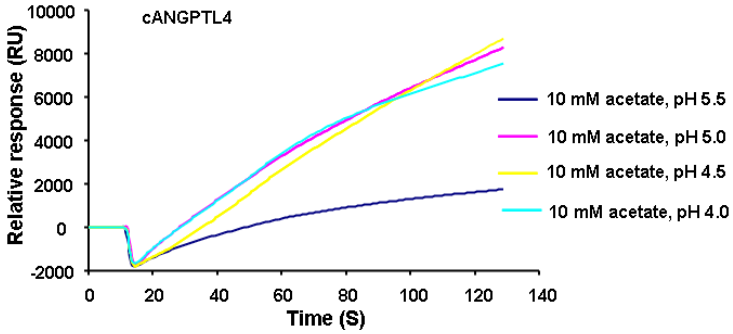

B.

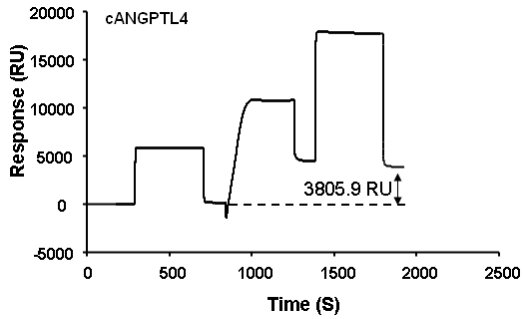

C.

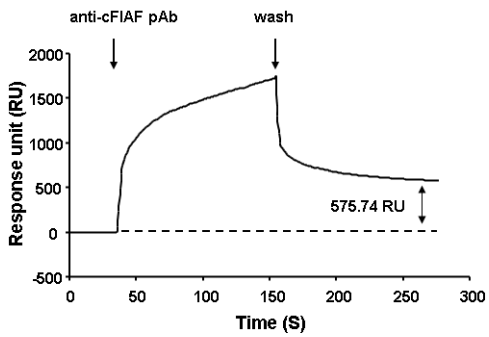

Figure 1.8 Immobilization and verification of cANGPTL4 proteins. (A) Immobilization pH scouting of cANGPTL4 protein on CM5 sensor chip. **(B)** Schematic sensorgram of the immobilization of cANGPTL4 (40 ng/µl) on CM5 sensor surface by amine coupling. The surface coverage calculated between the signals before surface activation and after inactivation was 3805.9 RU, injection time 7 mins, flow 10 µl/min. **(C)** Sensorgram showing binding of pAb cANGPTL4 (60 ng/µl) to cANGPTL4 immobilized CM5 sensor surface chip and subsequent washing in HEPES buffer (0.01 M HEPES pH 7.4, 0.15 M NaCl, 3 mM EDTA, 0.005 % v/v surfactant P20).

1.4.2.4 ANGPTL4 interacts with matrix proteins

The wound matrix contains exposed collagen fibrils, which is the most abundant components of ECM, as well as vitronectin (VN), fibronectin (FN) and fibrinogen (Midwood et al., 2004). Prompted by our earlier observation that ANGPTL4 was detected in the wound bed (see Fig. 1.3B & 1.4B), we hypothesized that plasma exudates or acute wound fluid may harbor ANGPTL4-interacting proteins using recombinant cANGPTL4 and wound plasma exudates as the bait and lysate, respectively. We have employed SPR biosensor (BIAcore) analysis as a method for the determination of both the kinetic and equilibrium binding constants. In this system, the binding of a ligand to a receptor immobilized on a dextran/gold surface can be visualized in real time by surface plasmon resonance detection, and the resulting binding curves can be used to derive the kinetic parameters of the interaction (O'Shannessy DJ et al., 1993). We identified ECM proteins, VN and FN, as ANGPTL4-binding partners (Fig. 1.9A & Table 1.3). The interaction between VN and cANGPTL4 can be blocked by pre-injection of anti-cANGPTL4 antibodies, indicating specific interaction between them (Fig. 1.9B).

The above experimental evidence suggests that ECM proteins are specific binding partners of ANGPTL4. To investigate whether ANGPTL4 exhibits selectivity over the different types of ECM proteins, we examined interactions between four major ECM proteins such as VN, FN, collagen-1 (COL-1) and laminin-5 (LN-5) with ANGPTL4. To this end, we immobilized four ECM proteins separately on CM5 sensor chip using amine coupling chemistry.

In the first instance, we determined the optimal pH for the immobilization of the four ECM proteins such as VN (Fig. 1.10A), FN (Fig. 1.10C), COL-1 (Fig. 1.10E) and

A.

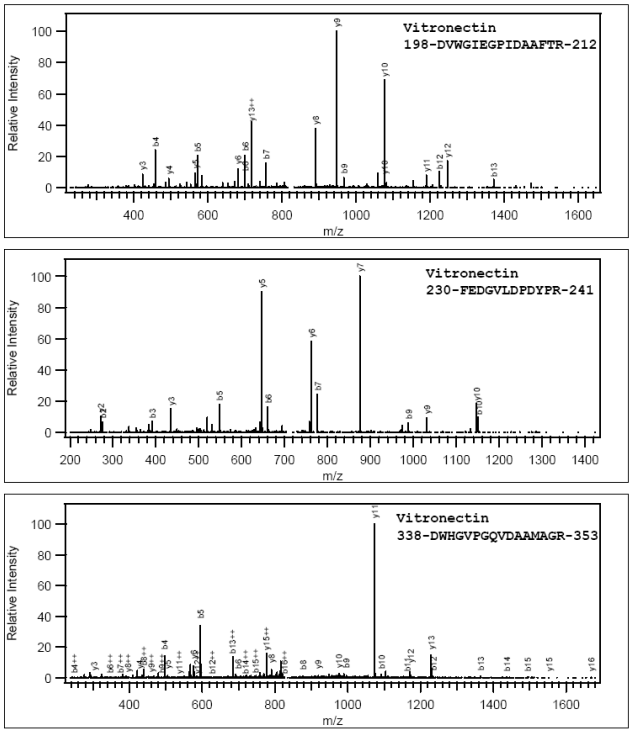

B.

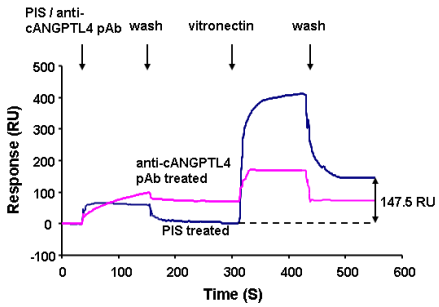

Figure 1.9 Interaction specificity of ANGPTL4 with matrix proteins. (A) MS/MS spectra showing peptide sequences of trypsin-digested cANGPTL4-binding protein. The digested cANGPTL4-binding proteins from SPR-MS were analyzed with a FPLC system coupled to an LTQ-Orbitrap mass spectrometer equipped with a nano-spray source. MS/MS spectra were extracted from the raw data file by extract_msn packaged with Biowork 3.3 (TheromoFinnigan). Protein identification was achieved by searching the combined data against the IPI human protein database (downloaded on March 02, 2007, 67665 entries, 28462007 residues) via an in-house MASCOT server (version 2.2.1). Three representatives MS/MS spectra of tryptic peptides eluted from FPLC were identified as vitronectin. **(B)** Binding study of VN to immobilized cANGPTL4 after pretreatment with pre-immune IgG (PIS) as control and anti-cANGPTL4 pAb, showing antibody blocked the binding of VN with immobilized cANGPTL4.

Table 1.3 Proteins identified using SPR-MS as potential cANGPTL4-interacting proteins

Accession number	Protein Name	Mascot Score
IPI00022418[a]	Isoform 1 of fibronectin precursor	10112
IPI00745872	Isoform 1 of serum albumin precursor	2094
IPI00298971	Vitronectin precursor	1459
IPI00021885	Isoform 1 of fibrinogen alpha chain precursor	159
IPI00298497	Fibrinogen beta chain precursor	50

LN-5 (Fig. 1.10G). The interaction of ECM proteins to the dextran surface increases as conditions become more acidic. Our results showed that an immobilization pH of 4.0 was optimal for all four ECM proteins. The amount of different ECM proteins immobilized as indicated in Fig. 1.10B, D, F and H for VN, FN, COL-1 and LN-5, respectively.

Next, purified recombinant ANGPTL4 proteins were perfused over the immobilized ECM surface, and the interaction was analyzed by SPR. The administration of ANGPTL4 (1.15, 1.45, 1.82, 2.18, 2.55, 2.91 µM) and cANGPTL4 (0.16, 0.32, 0.63, 1.25, 2.5, 5.0 µM) onto the immobilized VN (Fig. 1.11A) and FN (Fig. 1.11B) produced clear concentration dependent response curves, having binding affinity in the micromolar range (Table 1.4), whereas no binding response was obtained for COL-1 (Fig. 1.11C) and LN-5 (Fig. 1.11D) up to 5.0 µM concentration. It was also noted that there was no interaction of nANGPTL4 with all above mentioned ECM proteins (Fig. 1.11A-D, middle panels). From these analyses, the K_D value for their binding was calculated as shown in Table 1.4. When different concentrations of ANGPTL4 and cANGPTL4 were ran over the immobilized VN and FN surface, the association and dissociation phases of the curves were analysed using a single site fit binding model. It was likely that the

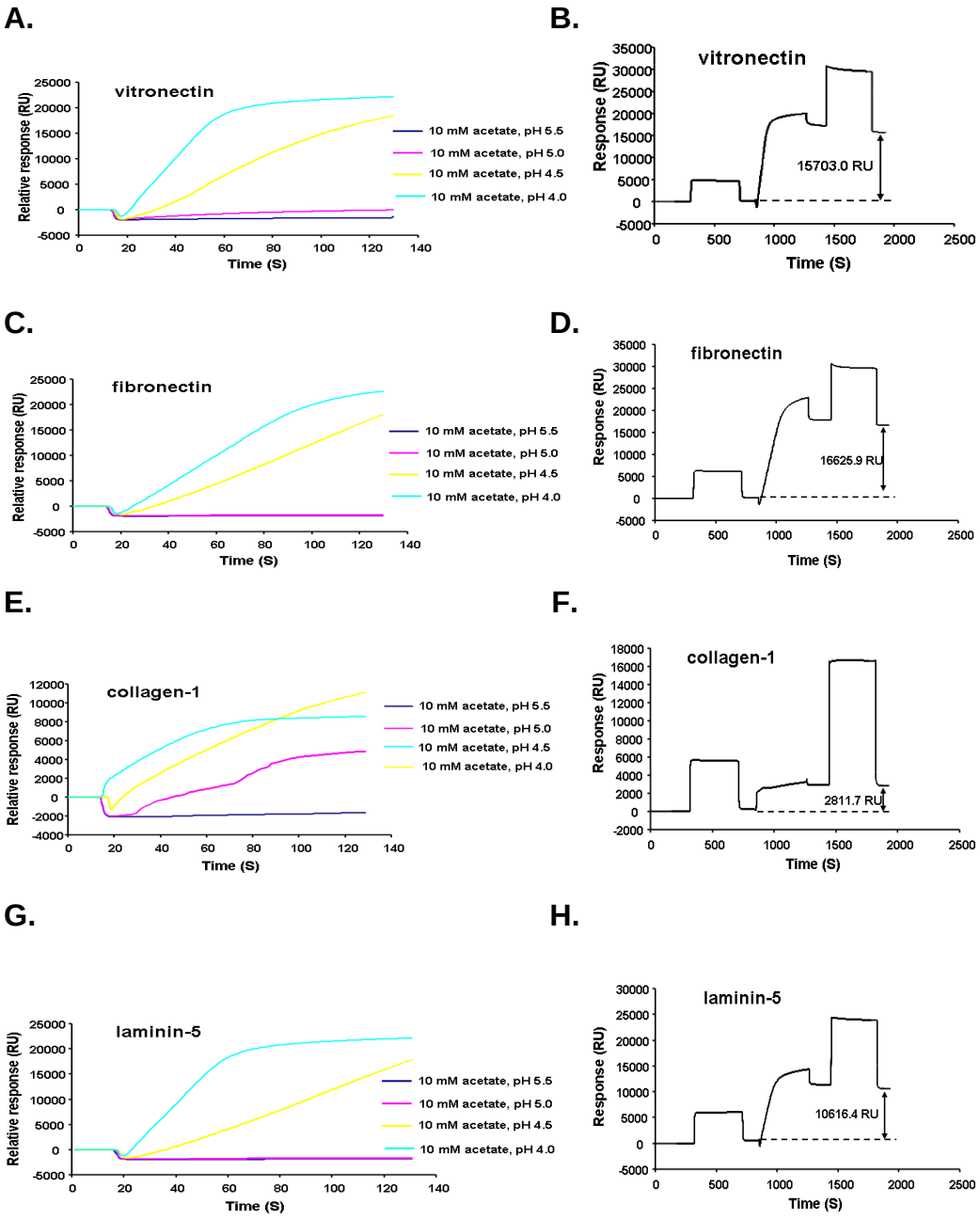

Figure 1.10 Immobilization of different extracellular matrix on CM5 sensor chip. Immobilization pH scouting and immobilization of different ECM proteins **(A, B)** vitronectin, **(C, D)** fibronectin, **(E, F)** collagen-1 and **(G, H)** laminin-5. For immobilization, protein was injected in sodium acetate buffer from pH 4.0- 5.5, as indicated on the sensorgram. The protein was attracted to the dextran matrix at a greater rate as the pH decreased, indicated by an increase in response units (RU). The amount of ligand binding is determined by the difference in the RU value as indicated with double headed arrows in the sensorgram.

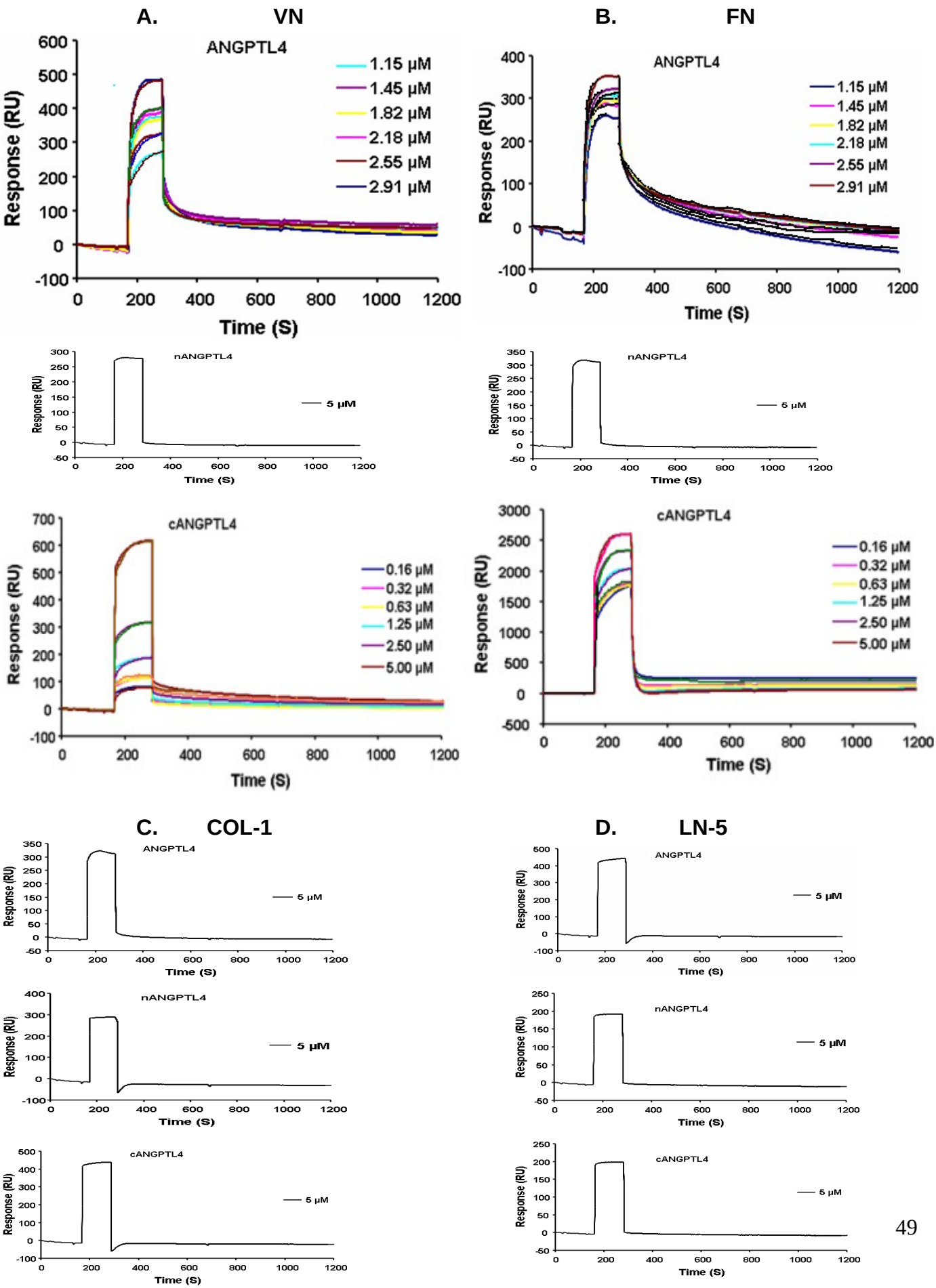

Figure 1.11 Analysis of different forms of ANGPTL4 binding affinity to immobilized extracellular matrix surface using BIAcore system. Sensorgram showing the association and dissociation of ANGPTL4, nANGPTL4 and cANGPTL4 from previously immobilized **(A)** Vitronectin (VN); **(B)** Fibronectin (FN); **(C)** Collagen-1 (COL-1) and **(D)** Laminin-5 (LN-5) ligands on CM5 sensor chip as described in materials and methods. The association rate constant (K_{on}) and dissociation rate constant (K_{off}) were determined separately from individual association and dissociation phases, respectively. The overall equilibrium dissociation constant (K_D) was derived from K_{off}/K_{on} using BIAevaluation software, version 3.1. The global fitting model was not used because of bulk refractive index changes in different sample and running buffer. Sensor chip surfaces were subsequently exposed with different concentrations of purified ANGPTL4 and SPR was performed as described before. Mean value of the equilibrium dissociation constants are summarized in Table 1.4. The following conditions and concentrations were used (bottom to top sensorgrams of each panel, respectively): ANGPTL4 at 1.15, 1.45, 1.82, 2.18, 2.55, 2.91µm; nANGPTL4 at 5.00 µm and cANGPTL4 at 0.16, 0.32, 0.63, 1.25, 2.50, 5.00 µm on VN and FN immobilized sensor chip and 5.00 µm concentration of all different forms of ANGPTL4 on COL-1 and LN-5 immobilized sensor chip. ANGPTL4 were injected at flow rate 10 µl/min. RU, response units.

Table 1.4 Equilibrium dissociation constants (K_D) of different forms of ANGPTL4 for matrix proteins as determined by SPR binding analysis

	ANGPTL4	nANGPTL4	cANGPTL4
Vitronectin	K_{on}=1.95 x10^4 (1/Ms) K_{off}=5.92 x10^{-3}(1/s) K_D=(3.04±1.33) x10^{-7} M[a]	NI[b]	K_{on}=3.38 x10^3 (1/Ms) K_{off}=2.01 x10^{-3}(1/s) K_D=(5.94±1.79) x 10^{-7} M
Fibronectin	K_{on}=7.08 x10^4 (1/Ms) K_{off}=2.7 x10^{-2}(1/s) K_D=(3.80±1.74) x 10^{-7} M	NI	K_{on}=2.9 x10^3 (1/Ms) K_{off}=1.02 x10^{-3}(1/s) K_D=(3.52±1.41) x 10^{-7} M
Collagen-1	NI	NI	NI
Laminin-5	NI	NI	NI

[a] Values are means ± SEM of 5 independent experiment (n=5) [b] NI denotes no detectable interaction. The association rate constant (K_{on}) and dissociation rate constant (K_{off}) were determined independently from the association and dissociation phases, respectively, with six different concentrations of analytes onto the specified ligand immobilized sensor chip. Apparent equilibrium dissociation constant (K_D) corresponds to the K_{off}/K_{on} ratio.

association occurs primarily to the single binding site in the complex. The kinetic parameters were independent of using different concentrations and an increased flow rate (20 to 50 µl/min), yielded comparable response curves, indicating that the kinetics were not influenced by mass transport limitations.

SPR analysis revealed that ANGPTL4 interacts with VN and FN yielding equilibrium dissociation constant (K_D) of ~10^{-7} M range (see Table 1.4). cANGPTL4 exhibited selective interaction with specific ECM proteins.

1.4.2.5 ANGPTL4 co-immunoprecipitates with vitronectin/fibronectin

To further strengthen our findings obtained from SPR, we performed *in vitro* co-immunoprecipitation assay using His-affinity Ni-NTA resins followed by immunobloting. The purified matrix proteins were incubated with immobilized different forms of purified recombinant His-tagged ANGPTL4 on the Ni-NTA resins. Western blot analysis of pull-down with a panel of antibodies against known matrix proteins revealed that VN and FN forms complex with ANGPTL4 or cANGPTL4, but not with nANGPTL4, whereas no physical interaction of laminin with all different forms of ANGPTL4 (Fig. 1.12). Negative control with Ni-NTA resin in the absence of purified recombinant His-tagged ANGPTL4, confirmed the specificity of the interaction.

1.4.2.6 Co-expression of ANGPTL4 and vitronectin/fibronectin in wound bed

ANGPTL4 and VN/FN are expressed concurrently in the skin, and since both proteins can bind to each other, it was of interest to know whether they are presented at the same

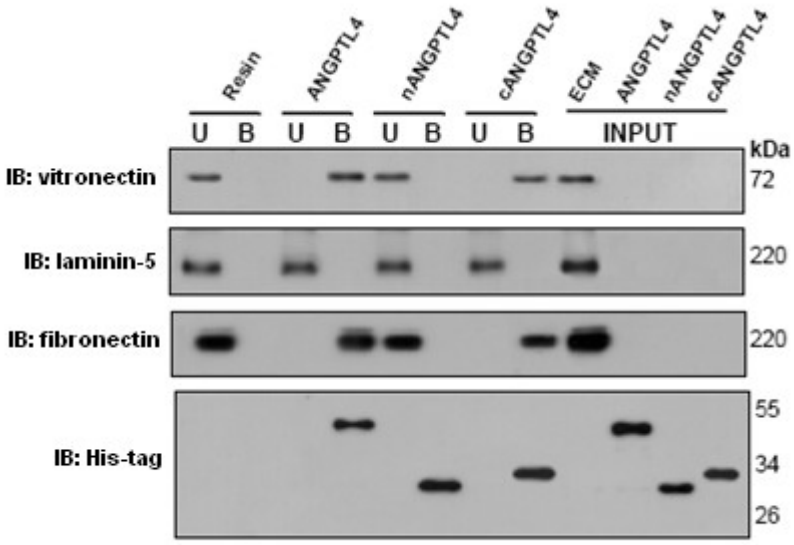

Figure 1.12 ANGPTL4 interacts directly with vitronectin and fibronectin. Co-immunoprecipitation assays were carried out by using different forms of His-tagged ANGPTL4 proteins immobilized on nickel-Sepharose and incubated with indicated purified ECM molecules. Matrix proteins and ANGPTL4 were detected by immunoblot using corresponding antibodies and revealed by chemiluminescence. U and B denote the unbound/washed and bound fractions from the resin.

site for interaction. To study this, we examine whether ANGPTL4 colocalize with VN/FN in the skin wound tissue. Dual immunofluorescence study revealed the co-localization of ANGPTL4 with VN/FN at the basal layer of the skin (Fig. 1.13), providing a strong evidence for VN and FN as interacting partners of ANGPTL4. Our findings showed that ANGPTL4 may play an important role in the progression of wound healing process via its interaction with specific ECM proteins.

1.4.2.7 ANGPTL4 interacts with integrin β_1 and integrin β_5

It was recently identified that ANGPTL3 is the first member of the angiopoietin-like family of secreted factors binding to integrin $\alpha_v\beta_3$ and suggest a possible role in the regulation of angiogenesis (Camenisch et al., 2002). The high degree of structural similarity between ANGPTL3 and ANGPTL4, suggesting integrins as potential candidate receptors. Our above results indicated that VN and FN are high affinity extracellular interacting partners of ANGPTL4, raising the question how ANGPTL4 may affect the interaction between the matrix protein and its cognate integrin receptors. We first examined if ANGPTL4 can independently interact with integrin receptors. Integrin $\alpha_v\beta_3$ is known to bind to VN and FN, $\alpha_v\beta_5$ recognizes only VN, whereas $\alpha_5\beta_1$ and $\alpha_v\beta_1$ associates only with FN (Retta et al., 2001).

Integrins are transmembrane proteins and their conformation can be altered depending on the extraction procedure. Thus, we sought a suitable membrane protein extraction protocol compatible with SPR. Despite the various procedures, membrane proteins were isolated based on two principles, either by detergent-based separation (Calbiochem kit) or via their hydrophobicity (such as Pierce kit). Following the

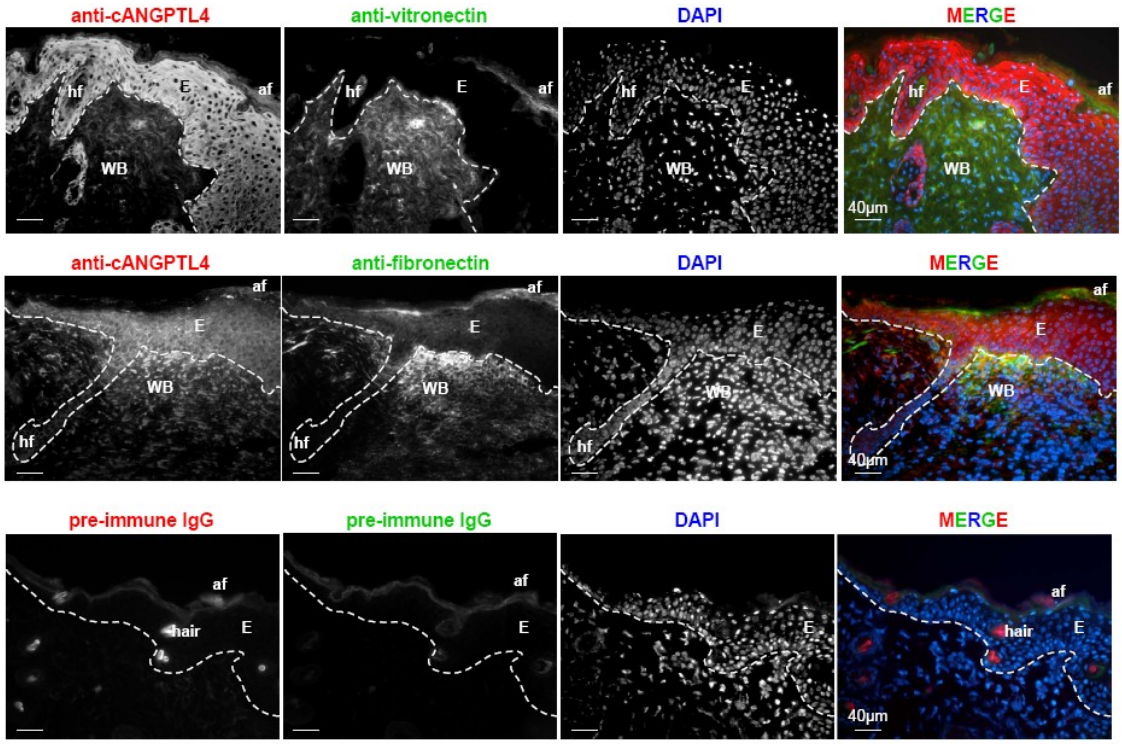

Figure 1.13 ANGPTL4 colocalizes with vitronectin and fibronectin. Double immunofluorescence staining of Day 5 mouse wound biopsies with anti-cANGPTL4 (red) and anti-vitronectin (green) or anti-fibronectin (green) antibodies. The sections were counterstained with DAPI (blue). Dotted white line represents epidermal-dermal junction. Representative pictures from wound epithelia and the adjacent wound bed were shown. E: epidermis; WB: wound bed; hf; hair follicle; af: auto-fluorescence. Scale bars 40 μm.

manufacturers' recommendations, the total protein extract from human keratinocytes were separated into the membrane and cytosolic fractions. To examine the purity of the various fractions, we performed a western blot analysis using antibodies against specific protein in the two fractions. A membrane receptor, epidermal growth factor receptor (EGFR) and a cytosolic protein, ERK-1 were used (Fig. 1.14A). The result showed some contaminations of cytosolic proteins in membrane fraction of human keratinocytes; however the purity was sufficient for subsequent analysis. Importantly, the result using anti-EGFR antibody showed that a highly enriched membrane protein fraction was obtained using the detergent-based method 1 (Fig. 1.14B).

We next examined if the purified membrane proteins were directly suitable for SPR. To this end, we studied the interaction between anti-EGFR antibody and its cognate receptor. Anti-EGFR antibody was immobilized onto a CM5 chip by amine coupling. Our results showed the optimum pH was 4.5 for anti-EGFR antibody protein binding onto the CM5 chip surface, as suggested by the highest 8775.1 response unit (RU) (Fig. 1.14C). As shown in Fig. 1.14D, a resonance response of 771.5 was obtained which indicates the binding of 4.4 μg of the antibody onto the chip surface. Injection of membrane protein and cytosolic fractions using method 1 showed 214 and 0.5 RU respectively at 40 ng/μl concentrations (Fig. 1.14E). Taken together, the results suggested that membrane protein purified using method 1 was suitable for SPR, and that a buffer exchange might be necessary for optimal interaction and maximum sensitivity.

Next, membrane protein fractions containing either β_1, β_3 and β_5 transfected 293T cells were extracted using method 1 as mentioned earlier and verified by western blot (Fig. 1.15A). We studied the binding interaction between immobilized cANGPTL4 with

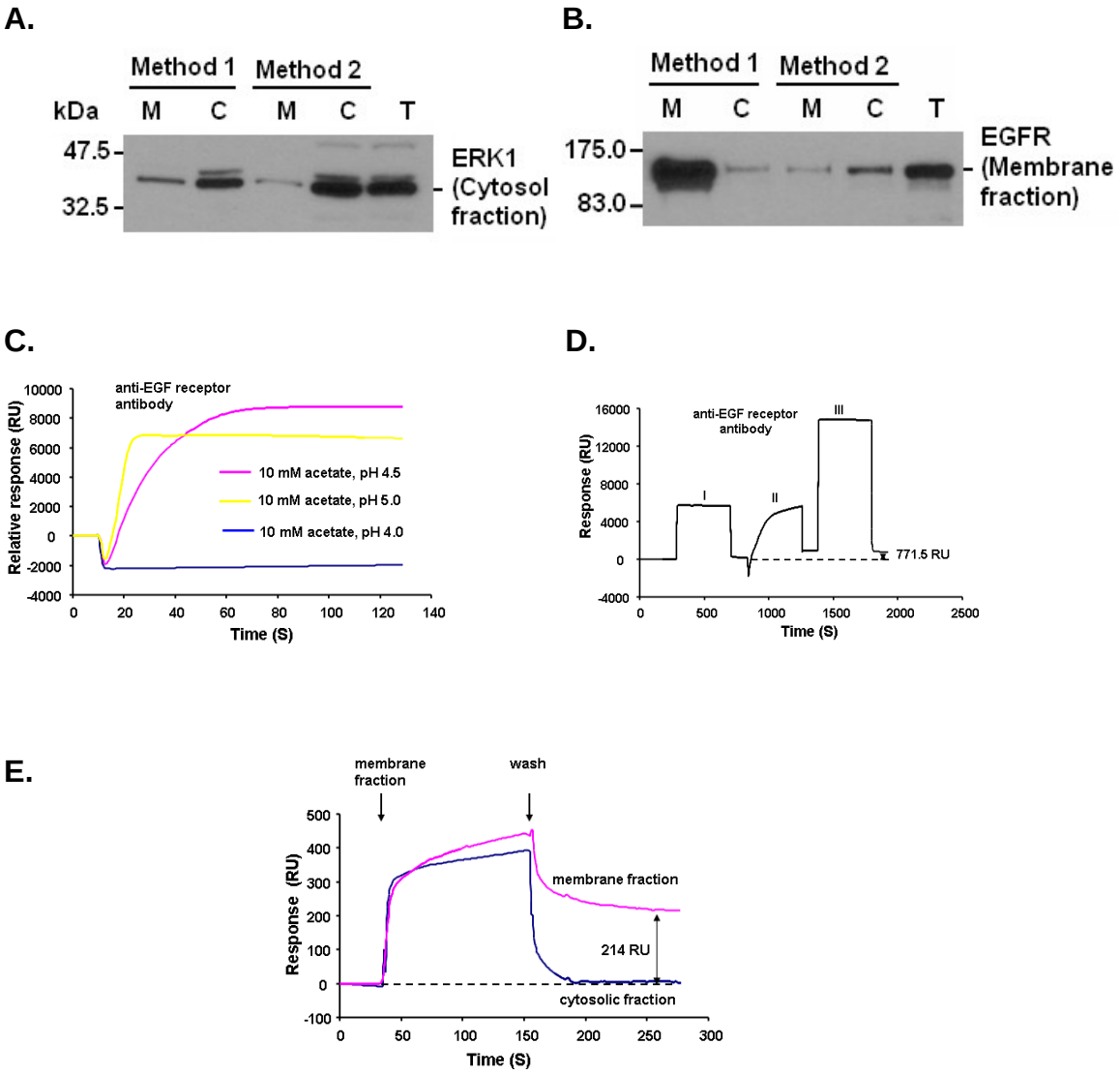

Figure 1.14 Optimization of different conditions in SPR for efficient interaction study of cANGPTL4 with membrane and cytosolic proteins extracted from human keratinocytes using two different methods. Immunoblot analysis of membrane and cytosolic protein fractions using **(A)** anti-ERK-1 polyclonal antibody and **(B)** anti-EGFR polyclonal antibody (M = Membrane fraction, C = Cytosolic fraction, T = Total protein in lysis buffer of HaCaT cell). **(C)** Immobilization pH scouting of anti-EGFR antibody on CM5 sensor chip. **(D)** Typical sensorgram of the immobilization of anti-EGFR antibody on CM5 sensor chip. (I) Surface activation with EDC and NHS, (II) Immobilization of anti-EGFR antibody (40 ng/µl) and (III) inactivation of the sensor surface with ethanolamine. The surface coverage calculated between the signals before surface activation and after inactivation was 771.5 RU, injection time 7 mins, flow 10 µl/min. **(E)** The sensorgram shows the interaction of membrane fractions of human keratinocytes on anti-EGFR antibody immbolized sensor chip at 40 ng/µl concentration whereas no interaction with cytosolic fractions.

integrins β_1, β_3 and β_5 using SPR. As shown in Fig. 1.15B, integrin β_1 and β_5 (at 80 ng/µl) showed interaction with cANGPTL4 protein as indicated by 67.3 and 97.5 RU respectively but not with integrin β_3 compared to untransfected membrane fraction of 293T cells where 1000 RU corresponds to the binding of 1 ng/mm^2 proteins (He et al., 1997). Binding study of integrin β_5 with immobilized cANGPTL4 after treatment with affinity purified and dialysed pre-immune IgG as control or anti-cANGPTL4 pAb, showing antibody blocked the binding of integrin β_5 with immobilized cANGPTL4 (Fig. 1.15C) which indicated the specific interaction between these two proteins. We also performed binding studies using injection of neutralizing anti-integrin $\alpha_v\beta_5$ mAb preincubation with integrin β_5 on cANGPTL4 (Fig. 1.15D) and VN (Fig. 1.15E) immobilized sensor chips, showing there was no binding response whereas integrin β_5 alone showing interaction of 105.6 and 501.4 RU respectively (Fig. 1.15D and E). This result revealed that the interaction of integrin β_5 with cANGPTL4 and VN was specifically blocked by neutralizing anti-integrin $\alpha_v\beta_5$ mAb, demonstrating the specificity of interaction. Taken together, our results indicated that integrin β_1 and β_5 are the interacting partners of cANGPTL4. Since integrin β_5 exhibited maximum binding capacity to cANGPTL4, it was selected for further characterization. To prove the dynamic properties of integrin β_5 with cANGPTL4 complex more thoroughly, we performed a detailed kinectic analysis using different extracellular integrin β_5 domains with cANGPTL4.

As a circulating protein, ANGPTL4 is likely to interact with the extracellular domains of integrins. We expressed and purified different domains of integrin β_5, namely the PSI (plexin semaphoring integrin), PSI-ILD (plexin semaphoring integrin-I-like

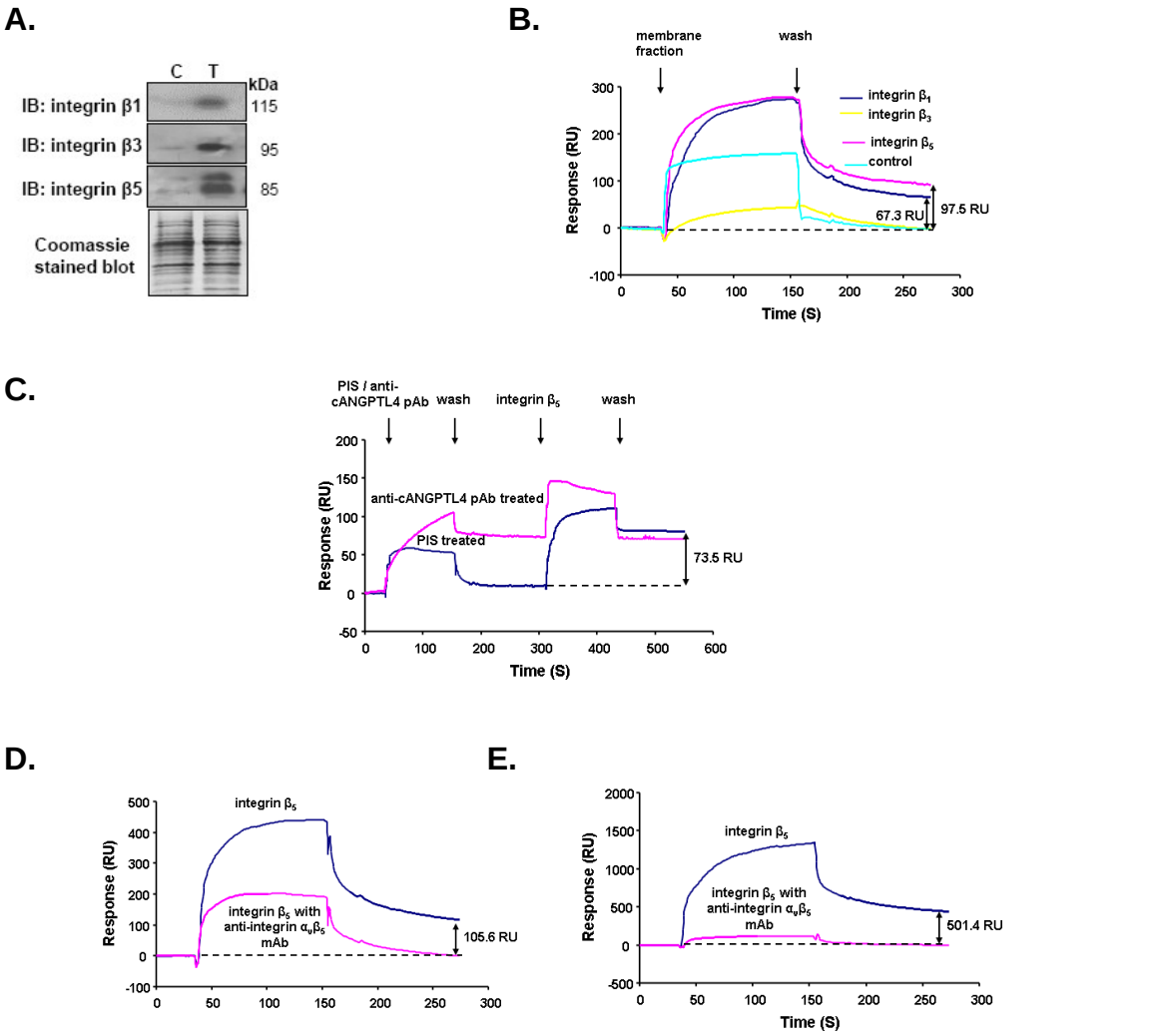

Figure 1.15 Specific binding of PSI-ILD of integrin β_5 with cANGPTL4. **(A)** Immunoblot analysis of membrane protein extracted from HEK 293T cells transfected with either empty expression vector or vector encoding for either integrin β_1, β_3 or β_5 (T). **(B)** Sensorgram showed binding profiles between membrane fractions of HEK 293T cells overexpressing integrin β_1, β_3 or β_5 with cANGPTL4 immbolized CM5 sensor chip. Specificity of ligand binding to immobilized cANGPTL4 measured by SPR. **(C)** Binding study of integrin β_5 to immobilized cANGPTL4 after pretreatment with pre-immune IgG (PIS) as control and anti-cANGPTL4 pAb, showing antibody blocked the binding of integrin β_5 with immobilized cANGPTL4. Integrin β_5 (1.15 µM) was injected for 2 min (30-150 s) and subsequent washing (151-270 s) with running buffer over the immobilized **(D)** cANGPTL4 and **(E)** VN surface with or without pre-incubation of anti-$\alpha_v\beta_5$ mAb for 30 min. Pretreatment with antibody injected at the concentration of 60 ng/ml for 2 min (30-150 s) inhibited binding to the basal level, indicating the specific interaction of integrin β_5 with both cANGPTL4 and VN. Sensor chips were regenerated at the end of each experiment with 10 mM glycine HCl, pH 3.0. RU, response units.

domain) and I-EGF (integrin-epidermal growth factor) domains. In integrin β_5, ILD was identified as a major binding region for matrix protein and its proper folding was largely supported by association of PSI domain (Mould et al., 2005; Takagi et al., 2002; Luo and Springer, 2006). Therefore, we used PSI-ILD for interaction studies instead of individual ILD.

In agreement with the above findings, our direct binding studies clearly demonstrated that the PSI-ILD of integrin β_5 interacted with ANGPTL4. The association rate constant (K_{on}) and dissociation rate constant (K_{off}) were determined separately from individual association and dissociation phases, respectively. The overall equilibrium dissociation constant (K_D) was derived from K_{off}/K_{on} using BIAevaluation software, version 3.1. The K_D value of this interaction exhibited a high affinity (7.27 nM) using cANGPTL4 immobilized CM5 sensor chip (Fig. 1.16B). In contrast, there was no binding of PSI and I-EGF domain with immobilized recombinant cANGPTL4 at 5 µM concentrations as shown in Fig. 1.16A and C, respectively. Therefore, the binding of PSI-ILD of integrin β_5 with ANGPTL4 observed under the conditions of the SPR experiments is highly specific and was subsequently confirmed by *in vitro* co-immunoprecipitation assay (Fig. 1.16D). This specific interaction can be an important parameter in determining the strength of downstream signaling in a complex mammalian system, and support previous reports showing quantitative relationships between the strength of an interaction between two signaling proteins and downstream responses (Block et al., 1996; Marles et al., 2004).

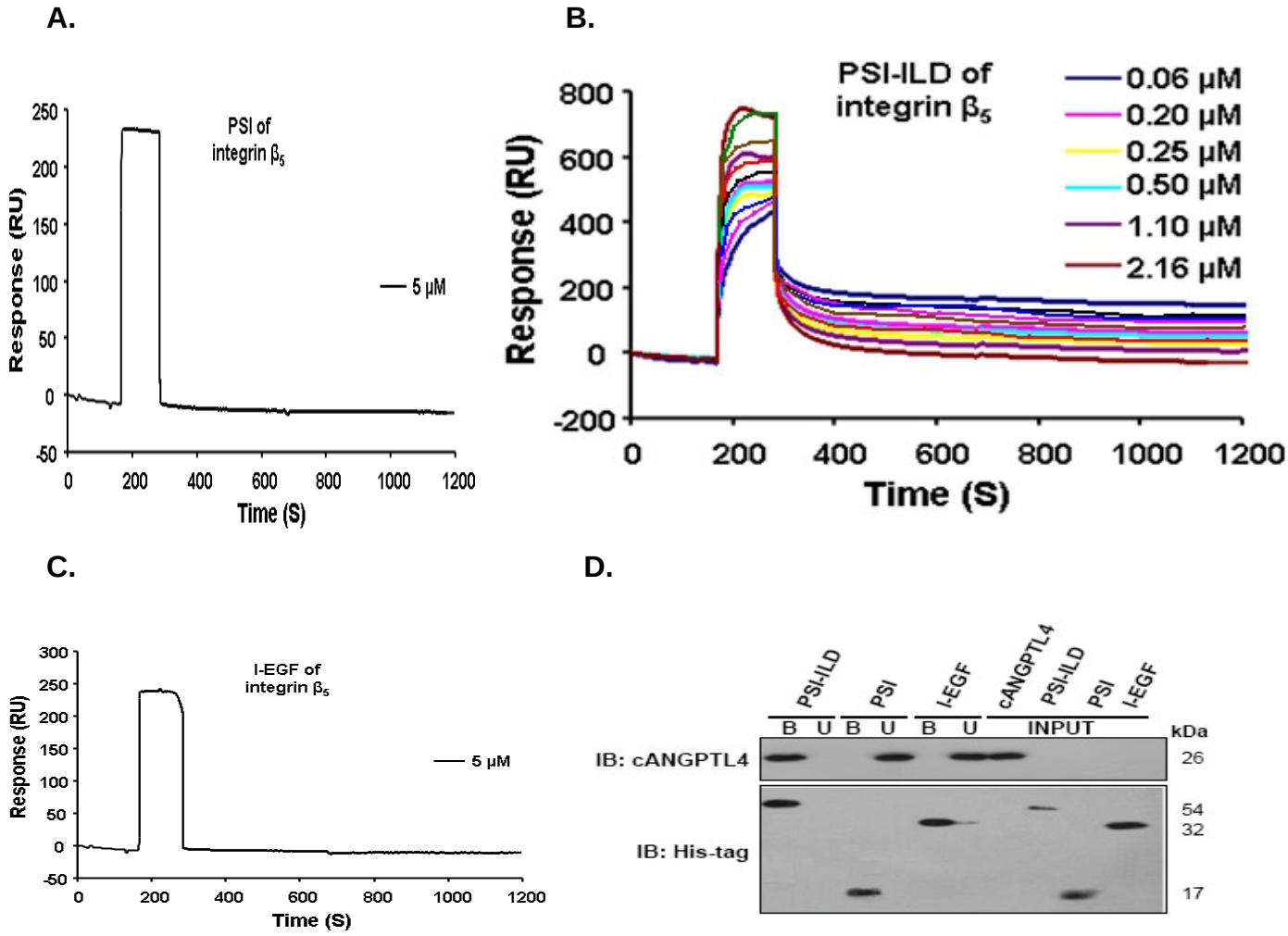

Figure 1.16 PSI-ILD of integrin β_5 interacts with cANGPTL4. Representative sensorgrams obtained from injections of **(A)** PSI domain at concentration of 5 μM; **(B)** PSI-ILD at concentration of 0.06, 0.20, 0.25, 0.50, 1.10, 2.16 μM and **(C)** I-EGF domain at concentration of 5 μM; over cANGPTL4 immobilized CM5 sensor chip. RU, response uints. The association rate constant (K_{on}) and dissociation rate constant (K_{off}) were determined separately from individual association and dissociation phases, respectively. The overall equilibrium dissociation constant (K_D) was derived from K_{off}/K_{on} using BIAevaluation software, version 3.1. Sensorgrams confirm cANGPTL4 binds to PSI-ILD of integrin β5 with binding affinity 7.27 nM**,** but not with PSI and I-EGF domain in the experimental conditions. **(D)** Co-immunoprecipitation assays were carried out using different domains of His-tagged integrin β_5 protein immobilized on nickel-sepharose and incubated with purified cANGPTL4 whose His-tag was removed by enterokinase digestion. His-tagged integrin β_5 domains and cANGPTL4 were detected by immunoblot using corresponding antibodies and revealed by chemiluminescence. U and B denote the unbound/washed and bound fractions from the resin.

1.4.2.8 ANGPTL4 and integrin β_5 are co-expressed in the same skin area

To examine the expression pattern of ANGPTL4 and integrin β_5, we performed immunofluorescence (IF) staining on OTC and human skin wound biopsies. Integrins β_5 was predominantly expressed in the epithelial basal cell layers of OTC (Fig. 1.17A), consistent with earlier studies (Pasqualini et al., 1993). Similarly, high level of ANGPTL4 was also detected in the basal layer of the wound epithelium (Fig. 1.17B, upper and middle panels). Pre-immune IgG did not show any detectable signal (Fig. 1.17B, lower panel). Taken together, our results revealed that ANGPTL4 and integrinβ_5 have overlapping expression pattern and is consistent with our earlier results that integrin β_5 is an interacting partner of cANGPTL4 protein.

1.4.2.9 Ternary complex of ANGPTL4, integrin β_5 and matrix protein

Our above results showed that the high affinity extracellular interacting partners of ANGPTL4 are VN/FN (see Fig. 1.12 & Table 1.4) and integrin β_5 (see Fig. 1.15B). Obviously, it raises the question if ANGPTL4 can still associate with integrins and its cognate matrix proteins when present together. To test this hypothesis, we performed sucrose gradient sedimentation assay as well as SPR analysis.

We allowed cANGPTL4, PSI-ILD of integrin β_5 and VN to interact in solution followed by sedimentation using sucrose gradient ultracentrifugation. Sucrose gradient ultra-centrifugation separates proteins/complexes according to their native molecular weight, with the larger protein/complex sedimenting at higher sucrose density. Consistent with our above results, immunoblot analysis after sucrose gradient ultracentrifugation showed that cANGPTL4 associated independently with VN and PSI-ILD of integrin β_5,

A.

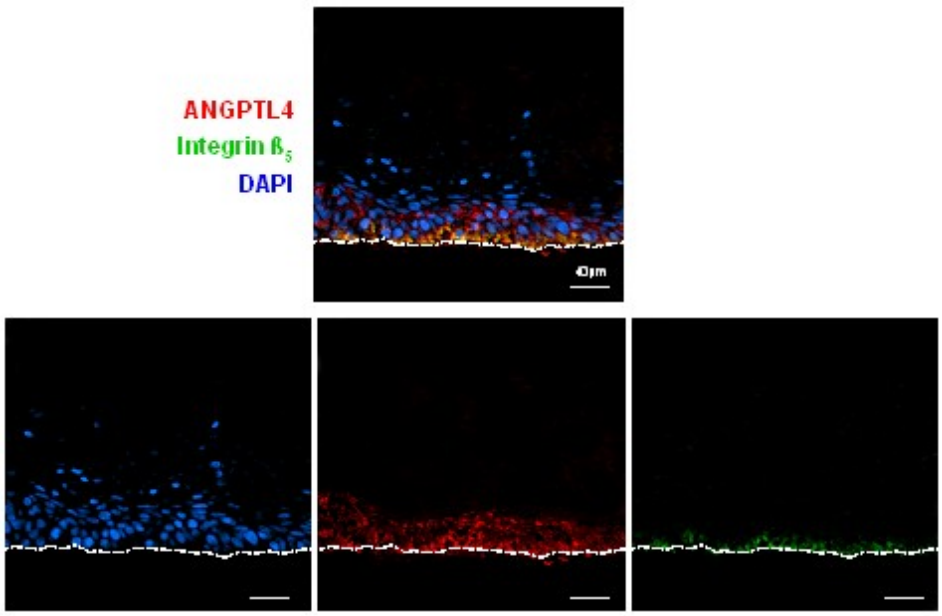

B.

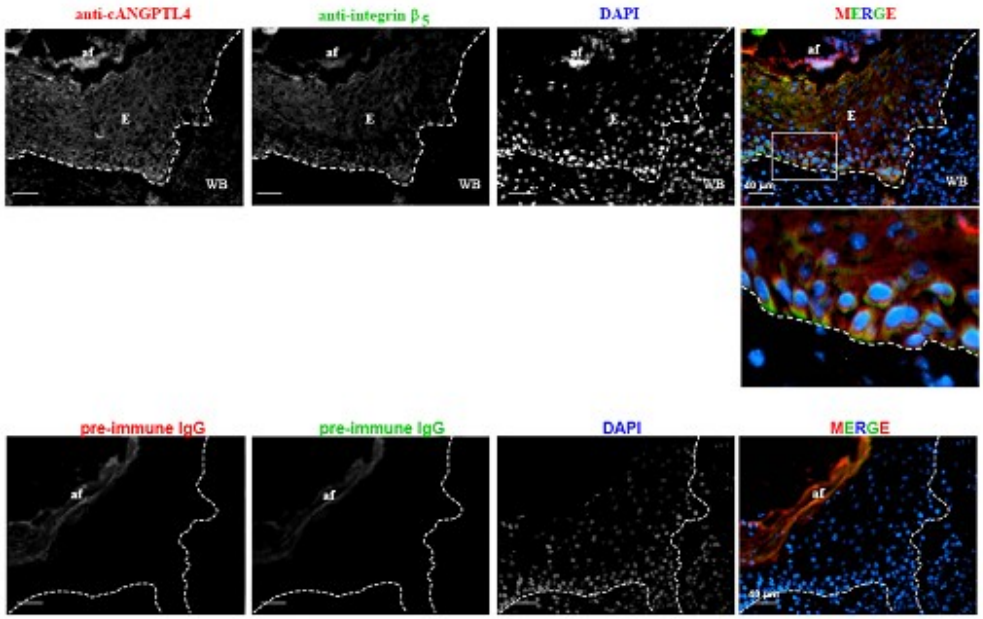

Figure 1.17 ANGPTL4 colocalizes with integrin β_5. Double immunofluorescence staining of **(A)** organotypic human skin culture and **(B)** Day 5 mouse wound biopsies with anti-cANGPTL4 (red) and anti-integrin β_5 (green) antibodies. The sections were counterstained with DAPI (blue). Dotted white line represents epidermal-dermal junction. Representative pictures from wound epithelia and the adjacent wound bed were shown. E: epidermis; WB: wound bed; af: auto-fluorescence. Scale bars 40 μm.

which were detected at higher density fractions as compared to individual protein. When the three proteins were present together, all the three proteins were detected at higher sucrose density, suggesting the formation of a ternary complex of cANGPTL4, PSI-ILD of integrin β_5 and VN (Fig. 1.18A).

We further confirmed the ternary complex using SPR technology. Firstly, we determined the concentration of cANGPTL4, VN and integrin β_5 membrane fraction required to saturate the immobilized cANGPTL4 or VN on CM5 sensor chips. Superimposed sensorgrams showed that the saturated concentrations of integrin β_5 and VN on cANGPTL4 immobilized CM5 sensor chip were 1.15 and 3.75 µM respectively (Fig. 1.18B). Conversely, the saturated concentrations of integrin β_5 and cANGPTL4 on VN immobilized CM5 sensor chip were determined to be 4.00 and 5.75 µM respectively (Fig. 1.18C). As shown in Fig. 1.18D, either integrin β_5 or cANGPTL4 were injected in sequential order at saturable concentration evidenced by a plateau binding curve on immobilized VN. Further injection of these proteins at saturable concentration did not cause an increase in the RU value. Subsequent injections of the third component of the ternary complex showed significant association, regardless of the sequence of injection. Similarly, sequential injections of integrin β_5 and VN over cANGPTL4 immobilized CM5 sensor chip indicated the formation of a ternary complex (Fig. 1.18E).

Taken together, our results indicated that ANGPTL4 can form a ternary complex when integrin β_5 and its cognate matrix protein are present together.

A.

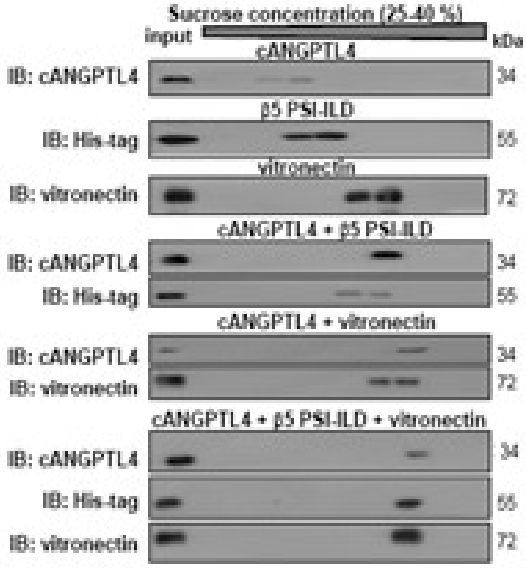

B.

C.

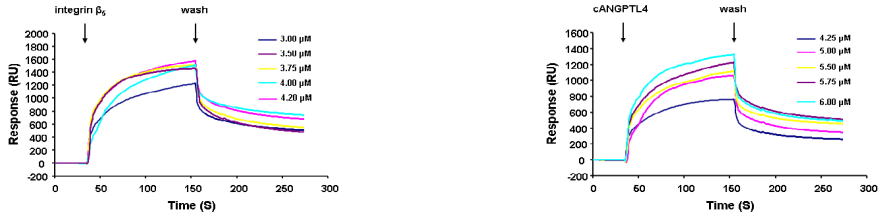

D.

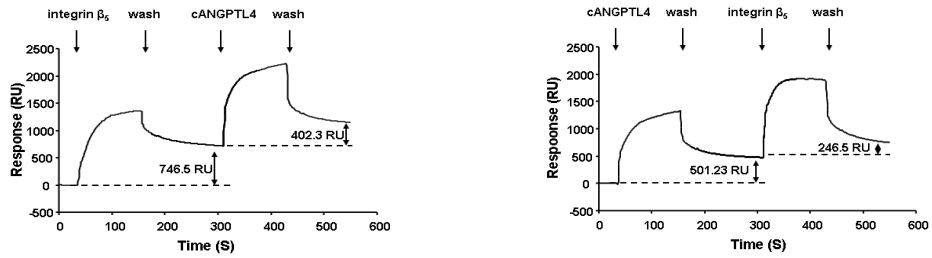

E.

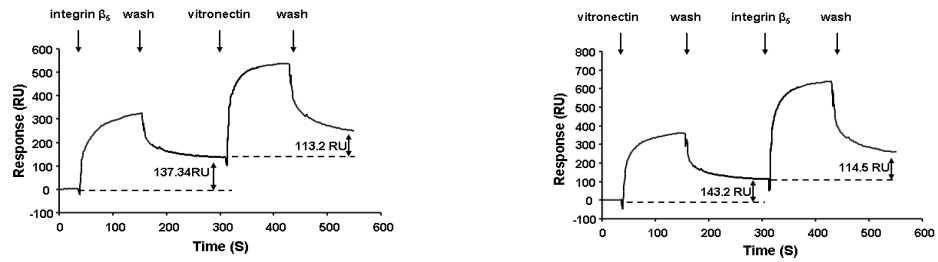

Figure 1.18 Ternary Complex of ANGPTL4, integrin β_5 and vitronectin. **(A)** Immunoblot of cANGPTL4, His-tagged PSI-ILD of integrin β_5 and VN of sucrose gradient fractions. The proteins were allowed to interact in the indicated combinations prior separation by sucrose gradient sedimentation ultracentrifugation. Blots showed increasing sucrose density from left to right. Superimposed sensorgrams obtained at different concentrations of **(B, left panel)** integrin β_5 and **(B, right panel)** VN on cANGPTL4 immobilized sensor chip showing 1.15 and 3.75 µM were saturable concentrations respectively; and that of **(C, left panel)** integrin β_5 and **(C, right panel)** cANGPTL4 on VN immobilized sensor chip showing 4.00 and 5.75 µM were saturable concentrations respectively. These saturable concentrations of individual proteins were used for this trinary complex binding study using SPR system. The protein sample was injected during association phase (30-150 s) followed by dissociation phase (151-270 s) **(D)** Sensorgram showing binding of integrin β_5 (4.00 µM) to VN immobilized CM5 sensor chip (30-150 s) and subsequent washing (151-270 s) in Tris buffer (50 mM Tris pH 8.0, 100 mM NaCl) followed by another injection of cANGPTL4 (5.75 µM) (310-430 s) and subsequent washing (431-550 s) with running buffer on **(left panel)** immobilized surface and **(right panel)** reciprocal experiment, showing binding interaction as mentioned in the curves. **(E)** Sensorgram showing binding (30-150 s) of integrin β_5 (1.15 µM) to cANGPTL4 immobilized CM5 sensor chip and subsequent washing (151-270 s) in Tris buffer (50 mM Tris pH 8.0, 100 mM NaCl) followed by another injection of VN (3.75 µM) (310-430 s) and subsequent washing (431-550 s) with running buffer on **(left panel)** immobilized surface and **(right panel)** reciprocal experiment, showing specific interaction as mentioned in the figures. Flow rate throughout the experiment was 20 µl/min. The surface was regenerated by injection of 10 mM glylcine HCl pH 3.0.

1.4.3 Biological function of ANGPTL4 on skin

Cell migration over the provisional wound bed is essential for efficient re-epithelialization of injured tissues. We observed an increase expression of ANGPTL4 corresponding to the re-epithelialization. We further showed that ANGPTL4 can interact independently with matrix protein or integrin, and formed a ternary complex when

present together. Thus we question whether the deficiency in ANGPTL4 affects keratinocyte migration.

1.4.3.1 Role of ANGPTL4 in keratinocyte migration

In the first instance, we suppressed endogenous ANGPTL4 expression by RNA interference in primary human keratinocytes. Using a lentivirus-mediated siRNA, keratinocytes were transduced with either a control or ANGPTL4 siRNA. We obtained ~90 % reduction in the ANGPTL4 mRNA and protein expression levels in keratinocytes transduced with ANGPTL4 siRNA ($K_{ANGPTL4}$) when compared to keratinocytes transduced with control siRNA (K_{CTRL}) (Fig. 1.19). The expression level of ANGPTL3, a closely related gene to ANGPTL4, remains unchanged which confirmed the specificity of ANGPTL4 knockdown (see Fig. 1.19).

To determine if ANGPTL4 is important for keratinocyte migration during wound closure, we performed *in vitro* scratch wound assay. Our results showed that K_{CTRL} closed the *in vitro* wound by 6 h while $K_{ANGPTL4}$ migration was significantly delayed and only closed after 18 h (Fig. 1.20A, movies M1-2). We also reasoned that anti-cANGPTL4 antibody may interfere with the action of ANGPTL4 and thus recapitulate the observation of $K_{ANGPLT4.}$ Indeed, the presence of anti-cANGPTL4 retarded the migration rate of K_{CTRL} by 48.8 % when compared to pre-immune IgG (13.3 ± 1.67 vs 6.8 ± 1.73) treatment (Fig. 1.20B & C, movies M3-4 & Table 1.5).

In vitro wound closure involves cell proliferation and migration. To better define the role of ANGPTL4 in cell migration, we performed similar wound scraping experiment in the presence of mitomycin C (mit C), a potent inhibitor of cellular prolifer-

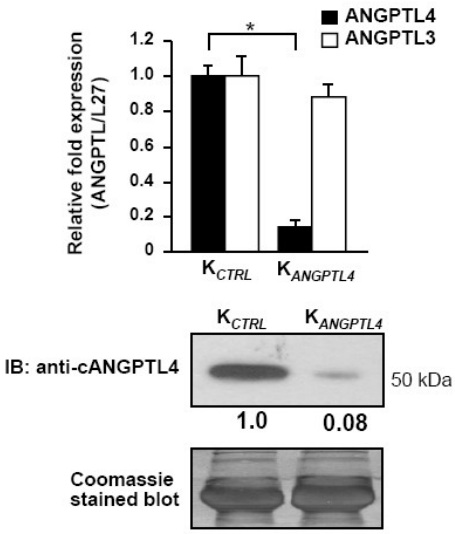

Figure 1.19 Verification of ANGPTL4-knockdown efficiency in human keratinocytes. Expression of ANGPTL4 and ANGPTL3 in keratinocytes transduced with either control (K_{CTRL}) or ANGPTL4 siRNA ($K_{ANGPTL4}$). Ribosomal protein Rpl27 was used as a normalizing housekeeping gene. Values below each band represent the mean fold differences in protein expression level with respect to control from five independent experiments (n=5). Coomassie-stained blot showed equal loading and transfer.

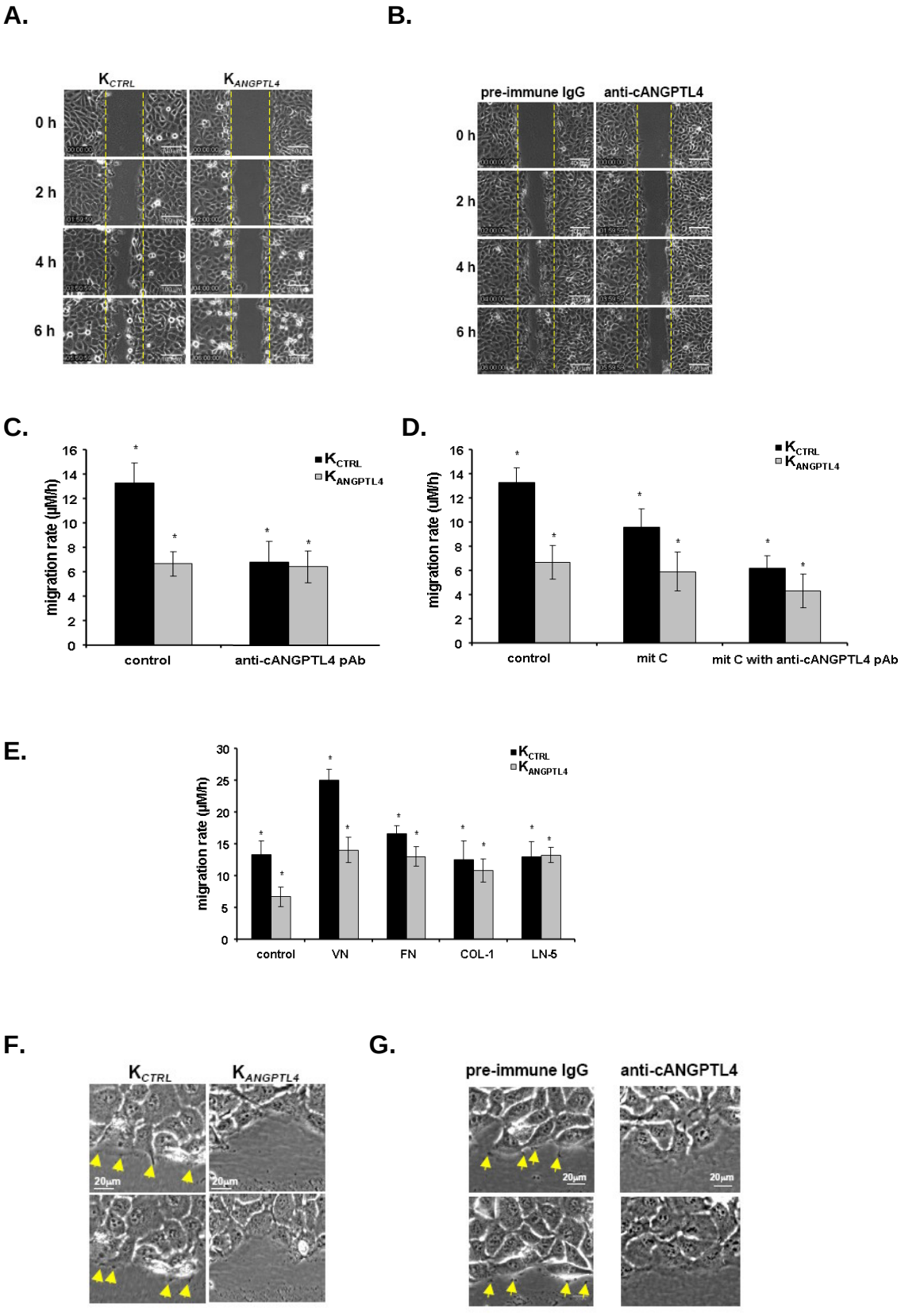

Figure 1.20 Effect of ANGPTL4 in keratinocyte migration and lamellipodia extension. (A) Time-lapsed images of wounded cultures of K_{CTRL} and $K_{ANGPTL4}$. Yellow dotted lines represent the scratch gap at the time of wounding. Scale bar 100 µm. See movies M1-4 for videos. **(B)** Time-lapsed images of wounded cultures of K_{CTRL} treated with 2 µg/ml of either pre-immune IgG or anti-cANGPTL4 antibody. Yellow dotted lines represent the scratch gap at the time of wounding. Scale bar 100 µm. See movies M3-4 for videos. **(C)** Wounded keratinocytes monolayer was incubated under anti-cANGPTL4 pAb treatment. Wound closure was significantly ($p<0.001$) inhibited by 48.8 % and 3.7 % in K_{CTRL} and $K_{ANGPTL4}$ cells respectively compared to pre-immune serum control treatment. **(D)** Keratinocytes monolayer was pre-incubated for 30 mins with anti-cANGPTL4 pAb in presence or absence of mit C after wounding as described. Time lapsed image analysis indicated a marked inhibition of cell migration rate in both K_{CTRL} and $K_{ANGPTL4}$ cell types (27.8 % and 11.3 % respectively) compared to their respective control treatment in presence of proliferation inhibitor, mitomycin C (mit C) alone, suggesting that *in vitro* wound closure depends on cell proliferation. In presence of anti-cANGPTL4 pAb and mit C, cell migration rate was lesser than mit C treatment alone, indicating wound closure depends on both event such as cell proliferation as well as cell migration. **(E)** Wound scratch assay using K_{CTRL} and $K_{ANGPTL4}$ cells was performed on dishes pre-coated with ECM proteins VN, FN, COL-1 and LN-5. Images are representative of the migration in both cell types of three separate experiments in duplicate. Data showing VN coated keratinocyte migration rate of K_{CTRL} was around 2 fold higher than $K_{ANGPTL4}$, whereas other ECM coated keratinocyte migration rate was not too much difference between two cell types but the migration rate was higher than that of control treatment, indicating that ANGPTL4 induced cell migration is VN specific. Error bars represent standard deviations. **(F)** Still images from video microscopy showing migration front of K_{CTRL} and $K_{ANGPTL4}$. Arrows indicate focal adhesion points in lamellipodia during migration. Scale bar 20 µm. See movies M5-6 for videos. **(G)** Still images from video microscopy showing migration front of pre-immune IgG and anti-cANGPTL4 antibody treated K_{CTRL}. Arrows indicate the focal adhesion points in lamellipodia during migration. Scale bar 20 µm. See movies M7-8 for videos.

Table 1.5 Keratinocyte migration rate as determined by *in vitro* wound scratch assay

Treatment	**Migration rate over 6 h time period (µm/h)**	
	K_{CTRL}	**$K_{ANGPTL4}$**
Pre-immune serum (Control)	13.3 ± 1.673*	6.65± 1.000*
Anti-cANGPTL4 pAb	6.8 ± 1.732*	6.4 ± 1.306*
Mitomycin C	9.6 ± 1.500**	5.9 ± 1.619**
Mitomycin C with anti-cANGPTL4 pAb	6.2 ± 1.000**	4.3 ± 1.415**
Vitronectin coated	25.0 ± 1.734**	14.0 ± 2.000**
Fibronectin coated	16.6 ± 1.234**	13.0 ± 1.514**
Collagen-1 coated	12.5± 3.143**	10.8 ± 1.826**
Laminin-5 coated	13.0 ± 2.356**	12.7 ± 1.217**

Statistical analysis was determined using two-tailed Mann-Whitney test, * denotes $p<0.005$ and ** denotes $p<0.001$. Values are means ± SEM of 3 independent experiments (n=3).

ation. At 5 µg/ml concentration of mit C, keratinocytes migration rate (µm/h) was significantly ($p<0.001$) reduced by 27.8 % (13.3 ± 1.67 vs 9.6 ± 1.50) and 11.3 % (6.65 ± 1.00 vs 5.9 ± 1.61), whereas in presence of anti-cANGPTL4 antibody (2 µg/ml) with mit C (5 µg/ml), wound closure was further inhibited by 53.38 % (13.3 ± 1.67 vs 6.2 ± 1.00) and 35.3 % (6.65 ± 1.00 vs 4.3 ± 1.41) (see Fig. 1.20D, Table 1.5) compared to pre-immune serum (control) treatment in K_{CTRL} and $K_{ANGPTL4}$ cell types respectively. Overall, these findings suggest that cellular proliferation is crucial event for cANGPTL4-induced wound closure.

Since, ANGPTL4 interacts with specific matrix proteins; we next examined its deficiency in cell migration on surface pre-coated with different ECM proteins (VN, FN, COL-1, LN-5). We found that cell migration rate of K_{CTRL} was maximal on VN (more than 44 %), moderate on FN (more than 22 %) and very little on COL-1 or LN-5 (less than 15 %) compared to $K_{ANGPTL4}$ (see Fig. 1.20E, Table 1.5). Overall, this result revealed the stimulatory role of cANGPTL4 protein in the migratory behavior of these cells.

Careful live-imaging observation further revealed that $K_{ANGPTL4}$ or K_{CTRL} treated with anti-cANGPTL4 exhibited rigid cell morphology and did not display any pronounced lamellipodia formation at the leading edge of migrating cells (see Fig. 1.20F & G, movies M5-8).

The formation of lamellipodia is a pre-requisite for cell migration. The members of the Rho small GTPases family are pivotal intracellular mediators for the formation of lamelliopdia, cytoskeleton network and cell migration. To gain insight into the mechanism of action, we examined the activation of Rho-GTPases, specifically cdc42, Rac1 and RhoA in K_{CRTL} and $K_{ANGPTL4}$ cells stimulated with serum. K_{CTRL} responded with a sustained activation of cdc42, Rac1 and RhoA (Fig. 1.21A). In contrast, $K_{ANGPTL4}$ showed minimal activation of cdc42 and Rac1 with a reduced and transient activation of RhoA. These observations clearly indicated that ANGPTL4 expression is crucial for active lamellipodial actin network formation and stability. More importantly, it also provides insight into the possible action of ANGPTL4 via integrin and the focal adhesion kinase (FAK), which is indispensible for the regulation of lamellipodial persistence, adhesion turnover and cell motility (Parsons et al., 2000).

1.4.3.2 ANGPTL4 modulates integrin-mediated FAK dependent signaling pathways

Integrins are the main cellular receptors involved in epithelial migration, and they function as sensors and integrators between matrix proteins and the cytoskeleton. Upon clustering and activation by their cognate ECM, integrins initiate FAK-dependent and independent signaling cascades to modulate cellular behavior, such as migration, growth and differentiation (Parsons et al., 2000). To examine if the interactions among ANGPTL4, matrix proteins and integrins modulate these cell-matrix triggered signaling events, we performed immunoblot analysis on K_{CTRL} and $K_{ANGPTL4}$ cytoplasmic proteins. We detected a reduced phosphorylated FAK, consistent with the notion of decreased integrin ligation and clustering. Phosphorylation of FAK is important for the recruitment of SH2-containing proteins, including phosphotidylinositol 3-kinase (PI3K) which is an important cell survival mechanism (Parsons et al., 2000). Further analysis also showed a reduced activation of the downstream mediators of the PI3K cascade, such as PDK-1 and GSK-3β (Fig. 1.21B).

Together with our earlier observations that ANGPTL4-deficient cells lack lamellipodia formation and persistence associated with diminished Rho GTPases activation, we envisaged that this interaction potentially modulates the intracellular signal transduction from integrins via FAK.

1.4.3.3 ANGPTL4 retards extracellular matrix degradation

During re-epithelialization, the migration of wound keratinocytes over the provisional wound bed requires the controlled turnover of matrix proteins by proteases (Page-McCaw et al., 2007). To determine if ANGPTL4 can affect the turnover rate of matrix proteins,

A.

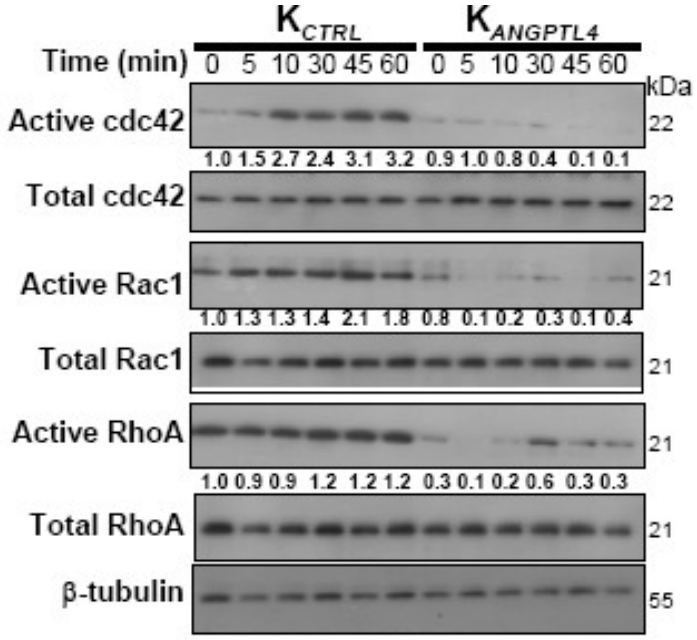

B.

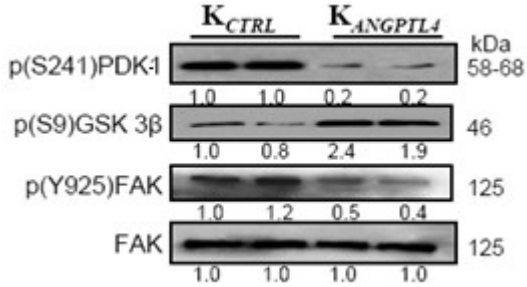

Figure 1.21 ANGPTL4 modulates FAK-dependent signaling to influence cell migration. (A) Immunoblotting analysis of active cdc42, Rac1 and RhoA in K_{CTRL} and $K_{ANGPTL4}$ keratinocytes exposed for the indicated time periods (min) with serum. Numbers below the blots represented the changes in active relative to basal cdc42, Rac1 and RhoA from 3 independent experiments. **(B)** Immunoblot analysis of cytoplasmic proteins from K_{CTRL} and $K_{ANGPTL4}$ keratinocytes. Numbers below each band represented the fold differences in protein expression levels with respect to control K_{CTRL}, which was assigned the value one. FAK: focal adhesion kinase; GSK-3: glycogen synthase kinase-3; PDK-1: 3-phosphoinositide-dependent kinase-1.

we examined the matrix protein degradation in the presence or absence of recombinant ANGPTL4 proteins. We pre-incubated purified VN, FN or laminin-5 with various recombinant ANGPTL4 proteins before subjecting the mixture to serum-free conditioned medium from $K_{ANGPTL4}$ to eliminate possible contribution from endogenous ANGPTL4.

The serum-free conditioned medium (CM) was obtained from $K_{ANGPTL4}$ exposed to either tumor necrosis factor-alpha (TNF-α) or IL-1 to mimic *in vivo* wounding. Strikingly, our results revealed that the degradation of VN and FN was slower in dose-dependent fashion in the presence of full-length ANGPTL4 and cANGPTL4 when compared to either vehicle control or in the presence of nANGPTL4 (Fig. 1.22A & B). Altogether, our findings showed that cANGPTL4 interacts with VN and FN to retard their degradation by proteases produced by wound keratinocytes.

1.4.3.4 Neutralization of ANGPTL4 by anti-cANGPTL4 antibodies delays re-epithelialization

Deficiency in ANGPTL4 impaired integrin-mediated signaling pathways and cell migration, thus we questioned whether there was an impact of this scarcity on wound healing process, which relies on integrin-mediated cell migration. Thus, we examined the effect of topically administered anti-cANGPTL4 antibody on the re-epithelialization of full-thickness excisional skin wounds. Histomorphometric analysis of the Day 7 post-injury wound biopsies showed a delayed re-epithelialization of wound treated with anti-cANGPTL4 when compared to pre-immune IgG-treated wound (Fig. 1.23). A delay in re-epithelialization was also observed on anti-cANGPTL4 treated incisional wounds (data not shown). Altogether, we showed that the interaction between the fibrinogen-like

A.

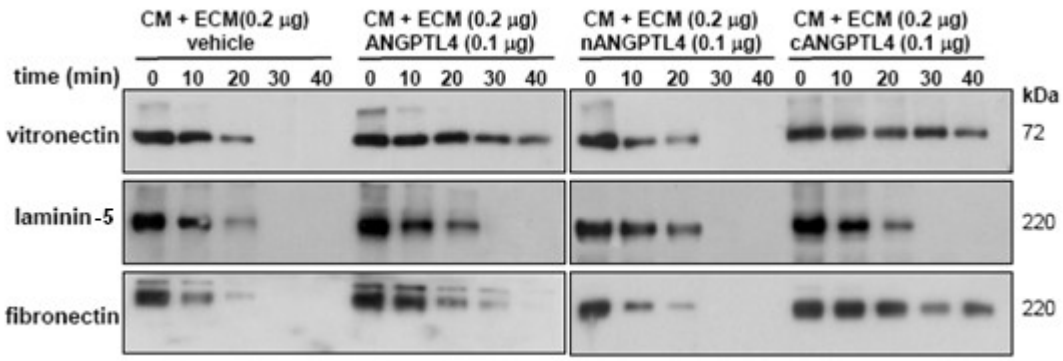

B.

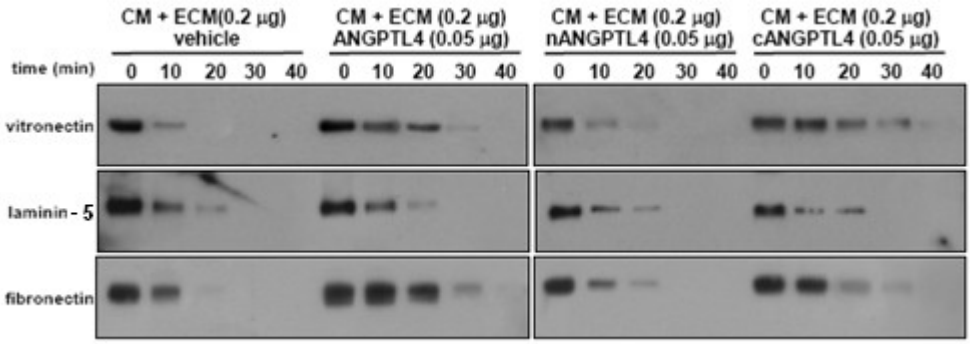

Figure 1.22 ANGPTL4 interacts with vitronectin and fibronectin to retard their degradation by proteases. Matrix protein degradation assays. Purified matrix proteins (200 ng) were first allowed to interact with **(A)** 100 ng and **(B)** 50 ng of recombinant N-terminal histidine tagged ANGPTL4 proteins, prior incubation at 37 ^{o}C with conditioned medium from $K_{ANGPTL4}$ culture. At indicated time, aliquots of the reaction were ceased by SDS-loading dye. Immunoblot of the matrix protein were performed using corresponding antibodies and revealed by chemiluminescence. Representative immunoblots are shown**.** Result showed ANGPTL4 bound to vitronectin and fibronectin to retard their degradation.

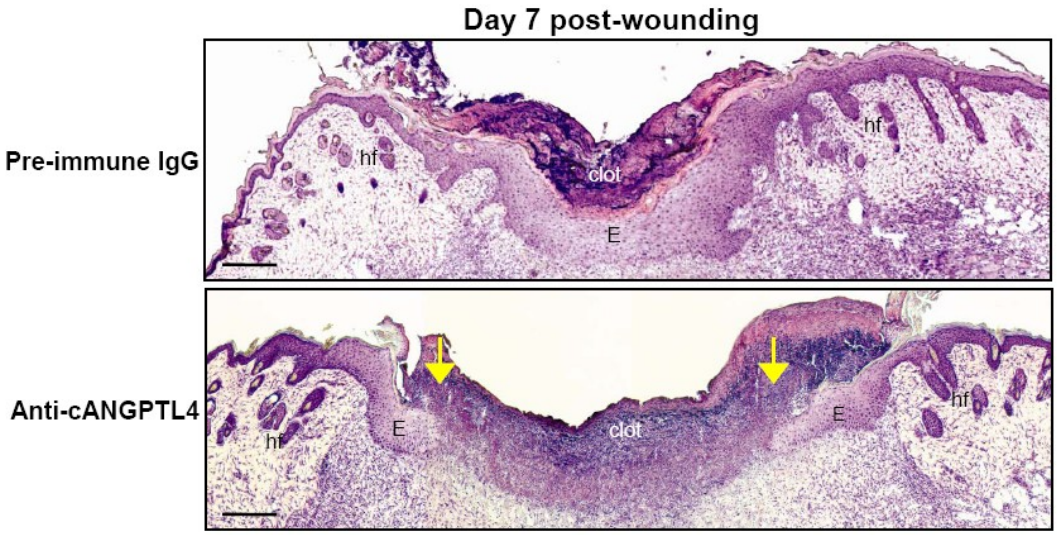

Figure 1.23 Histomorphometric analysis of Day 7 post-injury mice skin wound biopsies treated with either pre-immune IgG or anti-cANGPTL4. Wounding was performed as previously described. Wounds were topically treated daily with 50 µg of either pre-immune IgG or anti-cANGPTL4 antibodies. Treatments were rotated to avoid site bias. At Day 7 post-wounding, wounds were excised for analysis. Representative H&E (haematoxylin and eosin) stained pictures from wound edges were shown. Yellow arrows indicate the epithelial front. E: epidermis, hf: hair follicle. Scale bar 200 µm.

domain of ANGPTL4 with specific integrins and ECM proteins modulates the intracellular signal transduction from integrins, and thus influences keratinocyte migration.

1.5 DISCUSSION

Cell migration is a central process in development and many physiological as well as disease states. It is a fundamental cellular process indispensable for efficient re-epithelialization. Re-epithelialization of epithelial tissue occurs with the migration and proliferation of epithelial cells from the periphery of the wound over a denuded surface to form a primary barrier between the wound and the environment. Upon complete re-epithelialization, the newly formed epithelial cells begin the process of stratification which involves the differentiation of keratinocytes. This restores the water proof property of the skin. Extracellular stimuli that control cell migration are transduced into intracellular signals through the interaction of transmembrane integrins that bind to extracellular matrix proteins and secreted factors. Herein, we show that angiopoietin-like 4 (ANGPTL4) modulates cell-matrix communication which is essential for cell migration. We reveal that the expression of ANGPTL4 is elevated in wound epithelium and the wound bed, where it forms high affinity complexes with extracellular matrix proteins, VN and FN, as well as integrin receptors to enhance integrin-mediated FAK, Rho GTPases and 14-3-3σ-mediated signaling pathways. Keratinocytes deficient in ANGPTL4 or whose activity is neutralized by anti-ANGPTL4 antibodies displayed minimal cell migration associated with impaired extended lamellipodia formation *in vitro* and delay wound closure *in vivo*.

Numerous secreted factors, like growth factors and extracellular matrix proteins, necessary for wound repair have been characterized in detail (Werner and Grose, 2003). In contrast, much less is known about the matricellular proteins, a group of extracellular proteins that differ structurally and functionally from the ECM proteins in that they do

not contribute directly to the formation of structural elements in cells, yet modulate cell functions, such as cell behavior, including differentiation and migration (Bornstein and Sage, 2002; Midwood et al., 2004). We showed that ANGPTL4 functions as a novel matricellular protein, which is essential for re-epithelialization and the subsequent formation and differentiation of the neoepidermis. Except for a defect in the partitioning of postnatal intestinal lymphatic and blood vessels, ANGPTL4-null mice akin other matricellular proteins knockout mice, exhibited no apparent aberrant skin phenotype (Backhed et al., 2007). The expression of ANGPTL4, while only weakly detectable in normal intact skin is markedly elevated in the early phase of the skin injury and remains elevated until wound closure. Moreover, the suppression or neutralization of ANGPTL4 using RNA interference or anti-cANGPTL4 antibodies respectively, delayed both *in vitro* and *in vivo* wound closure. In addition, epidermis derived from ANGPTL4-deficient keratinocytes also displayed an altered epidermal architecture with impaired differentiation. Indeed, a distinguishing feature of matricellular proteins is that their expressions are increased in response to injuries, hence mice null for matricellular proteins like SPARC (secreted protein acidic and rich in cysteine) and thrombospondin 1 produce superficially mild phenotypes that are exacerbated only upon injury (Bornstein, 2001; Bradshaw et al., 2002).

Depending on the organs that were examined, different proteolytically cleaved forms of ANGPTL4 can be detected. The native ANGPTL4 and a truncated ANGPTL4 corresponding to nANGPTL4 were detected in the liver, whereas only the latter was found in the plasma and white adipose tissue (Mandard et al., 2004). Similarly, we only detected the native ANGPTL4 and cANGPTL4 in the skin wound biopsies. The

mechanism underlying these observations remains unknown. The N-terminal coiled-coil domain of ANGPTL4 binds to LPL and converts the enzyme from catalytically active dimers to inactive monomers (Sukonina et al., 2006). We showed that the C-terminal fibrinogen-like domain of ANGPTL4 interacts with matrix proteins and modulates integrin-mediated signaling in tissue repair. It is tempting to speculate that the processing of native ANGPTL4 aims to dissociate these two distinct functions. Interestingly, a metabolic role of matricellular proteins have also been described, for example SPARC was implicated in adipose tissue hyperplasia and adipogenesis (Bradshaw and Sage, 2001). Our findings underscore that besides the expression level of native ANGPTL4 protein, the expression level of different post-translationally cleaved forms of ANGPTL4 may govern or influence the eventual biological outcome of the cells and tissues. This raises interesting questions on the context- and tissue-dependent effect of ANGPTL4 and clearly additional studies are required.

Several hypotheses have been proposed that ANGPTL4 exerts its biological functions, at least with respect to angiogenesis which involves cell migration, via binding to ECM or to integrins (Cazes et al., 2006). As a secreted protein, ANGPTL4 is likely to mediate its action via interaction with specific extracellular protein partners. The identification of extracellular matrix proteins and integrin receptors as ANGPTL4 interacting partners revealed crucial insight into its molecular mechanism and has underscored the importance of ANGPTL4 in the regulation of cell migration and differentiation. ANGPTL4 associates with matrix proteins vitronectin and fibronectin via its C-terminal fibrinogen-like domain and retards their degradation, as well as forms a complex with integrin and matrix protein. Immunofluorescence also revealed that the

expression patterns of ANGPTL4, integrin β_5 and its cognate ligand vitronectin have extensive overlap in skin wound biopsies. Typically ligands interacting with integrins exhibit a RGD motif, which is absent in cANGPTL4. This suggests that there are differences in how β_5 integrin interacts with cANGPTL4 and vitronectin. Furthermore, the specificity of cANGPTL4 for β_5, rather than β_3 integrin, is also worth-noting. Many proteins without RGD-motif have been shown to interact with integrins (Rodgers and Weiss, 2004). Of particular interest, angiopoietin-like protein 3 (ANGPTL3) which display high homology to ANGPTL4 was reported to interact with β_3 integrins and to stimulate endothelial cell adhesion and migration (Camenisch et al., 2002). This observation may be analogous to nuclear localization signal (NLS) motifs found in primary sequences of proteins that serve as "signature" for nuclear targeting. There are many nuclear proteins that do not harbor a recognizable NLS. Recent work now revealed that similar NLS motif could be recognized only at the protein's tertiary structure. This NLS motif, whose three-dimensional configuration aligns strikingly well with a "classical" NLS, is functional (Sessler and Noy, 2005).

The ternary complex of ANGPTL4, integrin and matrix protein can modulate cell-matrix communication via integrin-initiated FAK-, Rho GTPases and 14-3-3σ-dependent signaling cascades to modulate a diverse array of cellular processes, including cell migration, proliferation and differentiation (Porter et al., 2006; Schlaepfer and Mitra, 2004). Indeed, the deficiency in ANGPTL4 has a dramatic impact on cell migration. In concordance with its effect on integrin-matrix interaction, many key intracellular signaling pathways involved in actin polymerisation and integrin recycling that are necessary for the establishment of a leading lamellipodia in migrating cells were also

impaired. First, ANGPTL4-deficient keratinocytes displayed impaired lamellipodia formation associated with attenuated active GTP-bound cdc42, Rac1 and RhoA profiles. Rac1 plays a role in the protrusion of lamellipodia and in forward movements; whereas cdc42 maintains cell polarity, including lamellipodia activity at the leading wound edge (Parsons et al., 2000). Second, keratinocytes adhered faster on surface coated with vitronectin and fibronectin, both interacting proteins of ANGPTL4. In additional support, it was observed that control keratinocytes migrate significantly faster on vitronectin and fibronectin, but not collagen and laminin 5, when compared to ANGPTL4-deficient keratinocytes. Finally, consistent with our *in vitro* findings, the neutralization of wound ANGPTL4 by topical application of anti-ANGPTL4 antibodies delays wound closure. A delayed wound closure was similarly observed in mice deficient in PPAR$_{\delta}$, which directly regulate ANGPTL4 expression in keratinocytes (Tan et al, 2001). Altogether, ANGPTL4 modulates cell-matrix communications through its interactions and effects on matrix proteins and integrins. Importantly, it provides a novel means by which migrating wound keratinocytes can better scrutinize the changes in the wound ECM and fine-tune their cells behaviour.

Angiopoietins are secreted factors that regulate angiogenesis by binding to the endothelial cell specific tyrosine kinase receptor Tie2 via their fibrinogen-like domain. The coiled-coil domain present in the family of secreted ligands was found to be necessary for ligand oligomerization. Similar to the angiopoietins, ANGPTL3 and ANGPTL4 are secreted glycoproteins, each consisting of an N-terminal signal peptide, followed by a coiled-coil domain and a C-terminal fibrinogen-like domain. It was observed that ANGPTL3 binds to integrin $\alpha_v\beta_3$ through the fibrinogen-like domain (fisch

et al., 2002). We determined that fibrinogen-like domain of ANGPTL4 binds to PSI-ILD of integrin β_5. However, unlike angiopoietin 1 which binds to Tie2 receptor to initiate phosphatidylinositol 3-kinase (PI3K)/Akt survival mechanism, ANGPTL4 does not bind to either Tie1 or Tie2 receptors (Kim et al., 2000). ANGPTL4 confers an anti-apoptotic property to keratinocytes through the activation of integrin-mediated FAK- and 14-3-3σ-mediated signaling pathways (Goh et al., in submission). The phosphorylation of FAK recruits SH2-containing proteins, including PI3K. We detected a reduced phosphorylation i.e activation of downstream mediators of PI3K cascade, such as PDK-1 and GSK-3 β, in ANGPTL4-deficient keratinocytes. The expression of 14-3-3σ, a key keratinocyte differentiation marker and shuttle protein that stimulates the Raf-dependent MEK-ERK MAPK survival pathway, was also reduced in ANGPTL4-deficient keratinocytes. Notably, the down-regulation of FAK can also lead to a reduced activation of the Raf-MEK-ERK signaling pathway (Porter et al., 2006). An elevated 14-3-3σ expression is required to sequester pro-apoptotic proteins like Bax from the mitochondria, which inhibits cytochrome C release and thus prevents apoptosis (Samuel et al., 2001; Tsuruta et al., 2004). Recent reports have shown that 14-3-3σ associates with protein kinase C (PKC) to regulate epidermal differentiation (Porter et al., 2006). The dysregulation of 14-3-3 σ and its effector PKC would have a direct influence on keratinocyte differentiation. Besides a reduced 14-3-3σ expression, we also showed that the expression of its effectors, PKC and RACK1 proteins, in ANGPTL4-deficient keratinocytes was decreased, indicating an attenuated PKC-mediated signal transduction (Schechtman and Mochly-Rosen, 2001).

After an injury, multiple signaling pathways become activated, and often they have opposing effects. How these various signaling cascades culminate to an appropriate cellular response remains a central question in signal transduction studies. Our lab previously showed that nuclear receptor PPAR$_{\beta/\delta}$ is highly upregulated during wound repair process. This receptor plays an important role in keratinocyte response to inflammation signals produced immediately after a skin injury (Tan et al., 2004). In Chapter 1, we further showed that PPARβ/δ target gene ANGPTL4 plays an important role in wound re-epithelialization phase. Although numerous cytokines have been shown to be involved in wound healing, TGF-β1 exerts the broadest effect. Our previous studies have found a dual role of TGF-β1 as a chemoattractant of inflammatory cells and also attenuated inflammation-induced PPARβ/δ expression (Tan et al., 2005). Using exogenous TGF-β1 application as well as Smad3 and PPARβ/δ single-and double-knock-out mice, it revealed a novel *in vivo* cross-talk between TGF-β1 and PPARβ/δ signaling (Tan et al., 2005). In addition to the TGF-β1-activated canonical Smad signaling pathway, TGF-β1 also activates the TGF-β1 activated kinase (TAK1) signaling pathway. TAK1 belongs to the MAPK kinase kinase family which is the key intermediate in inflammatory cytokines TNF-α, IL-1 and TGF-β1 mediated signaling pathways. Studies of keratinocyte-specific TAK1 knock-out mice confirmed the role of TAK1 in skin inflammation (Omori et al., 2006). Although the role of TAK1 in inflammatory response is well established, its mechanism of action in keratinocyte proliferation and migration remain unknown. Therefore, we were interested to find out the molecular mechanism of TAK1 in wound healing process as described in Chapter 2.

Cancer metastasis and wound repair share numerous characteristics during cell migration, thus it was not surprising that ANGPTL4 has been implicated in cancer metastasis (Steeg, 2006). Particularly, *ANGPTL4* was identified as one of the most predictive genes associated with breast cancer metastasis to lung (Minn et al., 2005). However, the role of ANGPTL4 in cancer metastasis remains debatable since there is evidence that ANGPTL4 may potentiate or attenuate tumor cell invasiveness associated with the disparate effects in vascular integrity (Galaup et al., 2006; Padua et al., 2008). The reason for this discrepancy is unclear. In addition, the autocrine role of ANGPTL4 on tumor cell behavior was not examined in those studies. Although this question is not directly addressed in this study, our data clearly suggest that ANGPTL4 may be crucial for tumor cell migration and tumor-derived ANGPTL4 may also affect vascular permeability via integrin-mediated signaling. In support, ANGPTL3, a member of the angiopoetin-like family, was shown to modulate vascular barrier properties and angiogenesis through a possible signaling pathway involving integrin $\alpha V\beta 3$, PI3K/PKB and FAK (Li et al., 2008). Altogether, our findings that specific matrix proteins and integrins are 'receptors' of ANGPTL4, which together can assemble into a ternary complex underscored the important role of ANGPTL4 as a novel matricellular protein to modulate integrin-mediate signaling and added a new facet to the cell-matrix interactions and signaling during wound repair and cancer metastasis.

1.6 FUTURE STUDIES

Previous studies have revealed that ANGPTL4, a secreted glycoprotein that functions in the oxidative stress and hypoxia responses, regulates lipid catabolism and angiogenesis. The evidence presented here suggests that adipokine ANGPTL4 modulates cell-matrix communication which is necessary for keratinocyte migration and survival during epidermal wound repair. These processes require the integration of signals elicited by chemotactic and mechanotactic stimuli. In turn, this is associated with the activation of intracellular pathways that converge on cytoskeleton remodeling. This includes the pathways involving activation of small Rho GTPases family, FAK, phosphorylated FAK and some other growth factors. Firstly, a critical question for future studies will be to determine how these pathways interact and how their timing is adjusted in the cell to generate appropriate cell migration. Recent studies reported that ANGPTL4 is highly expressed in several types of tumors that have a principle role in mediating tumor-host interactions. This concept and advance hypothesis on how gene expression on the primary tumors and the microenvironment can favor the spread of the metastasis seeds and how this knowledge can provide tools to secondary prevention is crucially important. Secondly, future studies should also attempt to elucidate the role of ANGPTL4 on molecular mechanism of detachment-induced apoptosis, also known as anoikis seems to be of particular importance for cancer research. We learned that disturbance of cell-anchorage frequently lead to the immediate initiation of a suicide program–apoptosis within the cell. Therefore, anoikis provides a useful system to study many aspects of the complex balance between survival and death signals which eventually determine the fate of a cell. Studying anoikis enables us to understand which components of the

environment are critical for cell survival and how these components mediate survival on a molecular level. In addition, more work is needed to better characterize vascular proliferation in response to ANGPTL4, the mechanism of action remains unknown in cancer as well as diabetic chronic wound repairing process. Thirdly, the structure determination of ANGPTL4 is another challenge because so far, no structural information of the angiopoietin-like family is available. However, the crystal structure of Angiopoietin-like protein 1 (Ang1), closely related to ANGPTL4, has been elucidated with its receptor Tie-2. Via computer modeling, we can derive the structure of ANGPTL4, which will enables us to design peptides that recognize VN/FN and integrin. This peptide may inhibit the complex formation of ANGPTL4 with integrin receptors and extracellular matrix proteins, VN/FN, mimic the function of ANGPTL4. This will provide important interaction about the structure function relationship of ANGPTL4. Previous studies have indicated that ANGPTL4 is a oligomer formed by intermolecular disulfide bonds and undergoes regulated proteolytic processing upon secretion. Depending on the organ examined, different proteolytically cleaved fragments were observed (Yin et al., 2009). The mechanism underlying this observation remains unclear, but earlier studies suggested that the mechanism of cleavage is serum-dependent (Mandard et al., 2004). Clearly, differentiated expression of protolytic enzyme may be responsible, although their identity is unclear. This warrants further investigation on the mechanism and site of cleavage of full-length human ANGPTL4.

1.7 REFERENCES

Backhed F, Crawford PA, O'Donnell D, Gordon J (2007) Postnatal lymphatic partitioning from the blood vasculature in the small intestine requires fasting-induced adipose factor. *Proc Natl Acad Sci U S A* **104:** 606-611

Backhed F, Ding H, Wang T, Hooper LV, Koh GY, Nagy A, Semenkovich CF, Gordon JI (2004) The gut microbiota as an environmental factor that regulates fat storage *Proc Natl Acad Sci U S A* **101:**15718-23

Block C, Janknecht R, Herrmann C, Nassar N, Wittinghofer A (1996) Quantitative structure–activity analysis correlating Ras/ Raf interaction *in vitro* to Raf activation *in vivo*. *Nat Struct Biol* **3:** 244–251

Bornstein P (2001) Thrombospondins as matricellular modulators of cell function. *J Clin Invest* **107:** 929-934

Bornstein P, Sage EH (2002) Matricellular proteins: extracellular modulators of cell function. *Curr Opin Cell Biol* **14:** 608-616

Bradshaw AD, Sage EH (2001) SPARC, a matricellular protein that functions in cellular differentiation and tissue response to injury. *J Clin Invest* **107:** 1049-1054

Bradshaw AD, Reed MJ, Sage EH (2002) SPARC-null mice exhibit accelerated cutaneous wound closure. *J Histochem Cytochem* **50:** 1-10

Brigham PA, McLoughlin E (1996) Burn incidence and medical care use in the United States: estimate, trends, and data sources. *J Burn Care Rehabil* **17:** 95–107

Brooks PC, Montgomery AM, Rosenfeld M, Reisfeld RA, Hu T, Klier G, Cheresh DA (1994) Integrin $\alpha_v\beta_3$ antagonists promote tumor regression by inducing apoptosis of angiogenic blood vessels. *Cell* **79:** 1157-64

Camenisch G, Pisabarro MT, Sherman D, Kowalski J, Nagel M, Hass P, Xie MH, Gurney A, Bodary S, Liang XH, Clark K, Beresini M, Ferrara N, Gerber HP (2002) ANGPTL3 Stimulates Endothelial Cell Adhesion and Migration via Integrin alpha vbeta3 and Induces Blood Vessel Formation *in Vivo*. *J Biol Chem* **277:** 17281-90

Cazes A, Galaup A, Chomel C, Bignon M, Brechot N, Le Jan S, Weber H, Corvol P, Muller L, Germain S, Monnot C (2006) Extracellular matrix-bound angiopoietin-like 4 inhibits endothelial cell adhesion, migration and sprouting and alters actin cytoskeleton. *Circ Res* **99:** 1207-15

Chomel C, Cazes A, Faye C, Bignon M, Gomez E, Ardidie-Robouant C, Barret A, Ricard-Blum S, Muller L, Germain S, Monnot C (2009) Interaction of the coiled-

coil domain with glycosaminoglycans protects angiopoietin-like 4 from proteolysis and regulates its antiangiogenic activity. *FASEB J* **23:** 940-9

Chong HC, Tan MJ, Philippe V, Tan SH, Tan CK, Ku CW, Goh YY, Wahli W, Michalik L, Tan NS (2009) Regulation of epithelial-mesenchymal IL-1 signaling by PPARbeta/delta is essential for skin homeostasis and wound healing. *J Cell Biol* **184:** 817-31

Clark EA, King WG, Brugge JS, Symons M, Hynes RO (1998) Integrin mediated signals regulated by members of the Rho family of GTPases**.** *J Cell Biol* **142**: 1-14

Deuel TF (1989) Polypeptide growth factors: roles in normal and abnormal cell growth. *Annu Rev Cell Biol* **3:** 443–492

Donaldson DJ, Mahan JT (1983) Fibrinogen and fibronectin as substrates for epidermal cell migration during wound closure. *J Cell Sci* **62:**117–127

Felsenfeld DP, Schwartzberg PL, Venegas A, Tse R, Sheetz MP (1999) Selective regulation of integrin-cytoskeleton interactions by the tyrosine kinase Src. *Nat Cell Biol* **1:** 200–206

Frank S, Stallmeyer B, Kämpfer H, Kolb N, Pfeilschifter J (2000) Leptin enhances wound re-epithelialization and constitutes a direct function of leptin in skin repair. *J Clin Invest* **106:** 501–509

Galaup A, Cazes A, Le Jan S, Philippe J, Connault E, Le Coz E, Mekid H, Mir LM, Opolon P, Corvol P, Monnot C, Germain S (2006) Angiopoietin-like 4 prevents metastasis through inhibition of vascular permeability and tumor cell motility and invasiveness. *Proc Natl Acad Sci* **103:** 18721-6

Ge H, Yang G, Huang L, Motola DL, Pourbahrami T, Li C (2004) Oligomerization and regulated proteolytic processing of angiopoietin-like protein 4**.** *J Biol Chem* **279:** 2038-2045

Gladson CL, Seegmiller JE, Smith JW, Klier J, Cheresh DA (1990) Glioblastoma cells synthesize and secrete the adhesive protein vitronectin. *J Exp Neurol* **49:** 339-345

Goh YY, Pal M, Punugu L, Chong HC, Zhu P, Tan MJ, Tan CK, Sze SK, Tan SM, Tang MBY, Ding JL, Kersten S, Tan NS. Regulation of cell-matrix communication by Angiopoietin-like 4 in wound healing (Manuscript in submission)

Grinnell F (1992) Wound repair, keratinocyte activation and integrin modulation. *J Cell Sci* **101:** 1–5

Herard AL, Zahm JM, Pierrot D, Hinnrasky J, Fuchey C, Puchelle E (1996) Epithelial barrier integrity during in vitro wound repair of the airway epithelium. *Am J Respir Cell Mol Biol* **15:** 624–632

He X, Ye J, Esmon CT and Rezaie AR (1997) Influence of Arginines 93, 97, and 101 of thrombin to its functional specificity. *Biochemistry* **36:** 8969-8976

Hotamisligil GS, Shargill NS, Spiegelman BM (1993) Adipose expression of tumor necrosis factor-alpha: direct role in obesity-linked insulin resistance. *Science* **259:** 87-91

Hynes RO (2002) Integrins: bidirectional, allosteric signaling machines. *Cell* **110:** 673-687

Irvine CA (1997) US Markets for Wound Management Products. *Medical Data International*

Kersten S, Desvergne B, Wahli W (2000) Roles of PPARs in health and disease. *Nature* **405:** 421–424

Kim I, Kim HG, Kim H, Kim HH, Park SK, Uhm CS, Lee ZH, Koh GY (2000) Hepatic expression, synthesis and secretion of a novel fibrinogen/angiopoietin-related protein that prevents endothelial cell apoptosis. *Biochem J* **346:** 603-10

Kirfel G and Herzog V (2004) Migration of epidermal keratinocytes: mechanisms, regulation, and biological significance. (Review article) *Protoplasma* **223:** 67–78

Li Y, Sun L, Xu H, Fang Z, Yao W, Guo W, Rao J, Zha X (2008) Angiopoietin-like protein 3 modulates barrier properties of human glomerular endothelial cells through a possible signaling pathway involving phosphatidylinositol-3 kinase/protein kinase B and integrin alphaVbeta3. *Acta Biochim Biophys Sin (Shanghai)* **40:** 459-65

Luo BH, Springer TA (2006) Integrin structures and conformational signaling. *Curr Opin Cell Biol* **18:** 579-86

Mackay DJG, Hall A (1998) Rho GTPases**.** *J Biol Chem* **273:** 20685-20688

Maas-Szabowski N, Shimotoyodome A, Fusenig NE (1999) Keratinocyte growth regulation in fibroblast cocultures via a double paracrine mechanism. *J Cell Sci* **112:** 1843–1853

Mandard S , Zandbergen F, Tan NS, Escher P, Patsouris D, Koenig W, Kleemann R, Bakker A, Veenman F, Wahli W, Muller M, Kersten S (2004) The Direct Peroxisome Proliferator-activated Receptor Target Fasting-induced Adipose Factor (FIAF/PGAR/ANGPTL4) Is Present in Blood Plasma as a Truncated

Protein That Is Increased by Fenofibrate Treatment. *J Biol Chem* **279:** 34411-34420

Mandard S , Zandbergen F, Van Straten E, Wahli W, Kuipers F, Muller M, Kersten S (2006) The fasting-induced adipose factor/angiopoietin-like protein 4 is physically associated with lipoproteins and governs plasma lipid levels and adiposity. *J Biol Chem* **281:** 934-944

Marles JA, Dahesh S, Haynes J, Andrews BJ, Davidson AR (2004) Protein–protein interaction affinity plays a crucial role in controlling the sho1p-mediated signal transduction pathway in yeast. *Mol Cell* **14:** 813–823

Michalik L, Desvergne B, Tan NS, Basu-Modak S, Escher P, Rieusset J, Peters JM, Kaya G, Gonzalez FJ, Zakany J (2001) Impaired skin wound healing in peroxisome proliferator-activated receptor (PPAR)alpha and PPARbeta mutant mice. *J Cell Biol* **154:** 799-814

Midwood KS, Williams LV, Schwarzbauer JE (2004) Tissue repair and the dynamics of the extracellular matrix. *Int J Biochem Cell Biol* **36:** 1031-1037

Minn AJ, Gupta GP, Siegel PM, Bos PD, Shu W, Giri DD, Viale A, Olshen AB, Gerald WL, Massague J (2005) Genes that mediate breast cancer metastasis to lung. *Nature* **436:** 518-524

Mould AP, Travis MA, Barton SJ, Hamilton JA, Askari JA, Craig SE, Macdonald PR, Kammerer RA, Buckley PA, Humphries MJ (2005) Evidence that monoclonal antibodies directed against the integrin beta subunit plexin/semaphorin/integrin domain stimulate function by inducing receptor extension. *J Biol Chem* **280:** 4238-46

Murad A, Nath AK, Cha ST, Demir E, Flores-Riveros J, Sierra-Honigmann MR (2003) Leptin is an autocrine/paracrine regulator of wound healing. *FASEB J* **13:**1895-7

Nickoloff BJ, Mitra RS, Riser BL, Dixit VM, Varani J (1988) Modulation of keratinocyte motility: correlation with production of extracellular matrix molecules in response to growth promoting and antiproliferative factors. *Am J Pathol* **132:** 543–551

Omori E, Matsumoto K, Sanjo H, Sato S, Akira S, Smart RC, Ninomiya-Tsuji J (2006) TAK1 is a master regulator of epidermal homeostasis involving skin inflammation and apoptosis. *J Biol Chem* **281:** 19610-7

O'Shannessy DJ, Brigham-Burke M, Soneson KK, Hensley P, Brooks I (1993) Determination of rate and equilibrium binding constants for macromolecular interactions using surface plasmon resonance: use of nonlinear least squares analysis methods. *Anal biochem* **212:** 457-468

Padua D, Zhang XH, Wang Q, Nadal C, Gerald WL, Gomis RR, Massagué J (2008) TGFbeta primes breast tumors for lung metastasis seeding through angiopoietin-like 4. *Cell* **133:** 66-77

Page-McCaw A, Ewald AJ, Werb Z (2007) Matrix metalloproteinases and the regulation of tissue remodelling. *Nat Rev Mol Cell Biol* **8:** 221-233

Parsons JT, Martin KH, Slack JK, Taylor JM, Weed SA (2000) Focal adhesion kinase: a regulator of focal adhesion dynamics and cell movement. *Oncogene* **19:** 5606-5613

Pasqualini R, Bodorova J, Ye S, Hemler ME (1993) A study of the structure, function and distribution of beta 5 integrins using novel anti-beta 5 monoclonal antibodies. *J Cell Sci* **105:** 101-11

Porter GW, Khuri FR, Fu H (2006) Dynamic 14-3-3/client protein interactions integrate survival and apoptotic pathways. *Semin Cancer Biol* **16:** 193-202

Preissner KT (1991) Structure and biological role of vitronectin. *Annu Rev Cell Biol* **7:** 275-310

Prud'homme GJ (2007) Pathobiology of transforming growth factor β in cancer, fibrosis and immunologic disease, and therapeutic considerations. *Laboratory Investigation* **87:** 1077–1091

Retta SF, Cassarà G, D'Amato M, Alessandro R, Pellegrino M, Degani S, De Leo G, Silengo L, Tarone G (2001) Cross talk between beta(1) and alpha(V) integrins: beta(1) affects beta(3) mRNA stability. *Mol Biol Cell* **12:** 3126-38

Righetti PG, Wenisch E, Jungbauer A, Katinger H, Faupel M (1990) Preparative purification of human monoclonal antibody isoforms in a multicompartment electrolyzer with Immobiline membranes. *J Chromatogr* **500:** 681-696

Rodgers UR, Weiss AS (2004) Integrin alpha v beta 3 binds a unique non-RGD site near the C-terminus of human tropoelastin. *Biochimie* **86:** 173-8

Samuel T, Weber HO, Rauch P, Verdoodt B, Eppel JT, McShea A, Hermeking H, Funk JO (2001) The G2/M regulator 14-3-3sigma prevents apoptosis through sequestration of Bax. *J Biol Chem* **276:** 45201-45206

Schechtman D, Mochly-Rosen D (2001) Adaptor proteins in protein kinase C-mediated signal transduction. *Oncogene* **20:** 6339-6347

Schlaepfer DD, Mitra SK (2004) Multiple connections link FAK to cell motility and invasion. *Curr Opin Genet Dev* **14:** 92-101

Schuck P (1996) Kinetics of ligand binding to receptor immobilized in a polymer matrix, as detected with an evanescent wave biosensor. I. A computer simulation of the influence of mass transport. *Biophys J* **70:** 1230–1249

Sessler RJ, Noy N (2005) A ligand-activated nuclear localization signal in cellular retinoic acid binding protein-II. *Mol Cell* **18:** 343-53

Shimomura I, Funahashi T, Takahashi M, Maeda K, Kotani K, Nakamura T, Yamashita S, Miura M, Fukuda Y, Takemura K, Tokunaga K, Matsuzawa Y (1996) Enhanced expression of PAI-1 in visceral fat: possible contributor to vascular disease in obesity. *Nat Med* **2:** 800-3

Singer AJ, Thode HC Jr, Hollander JE (2002) National epidemiology of lacerations. *Ann Emerg Med* **40:** S41

Stallmeyer B, KaÈmpfer H, Podda M, Kaufmann R, Pfeilschifter J, Frank S (2001) A Novel Keratinocyte Mitogen: Regulation of Leptin and its Functional Receptor in Skin Repair. *J Invest Dermatol* **117:** 98-105

Steeg PS (2006) Tumor metastasis: mechanistic insights and clinical challenges. *Nat Med* **12:** 895-904

Sukonina V, Lookene A, Olivecrona T, Olivecrona G (2006) Angiopoietin-like protein 4 converts lipoprotein lipase to inactive monomers and modulates lipase activity in adipose tissue. *Proc Natl Acad Sci U. S. A.* **103:** 17450-17455

Takagi J, DeBottis DP, Erickson HP, Springer TA (2002) The role of the specificity-determining loop of the integrin beta subunit I-like domain in autonomous expression, association with the alpha subunit, and ligand binding. *Biochemistry* **41:** 4339-47

Takashima A, Billingham RE, Grinnell F (1986) Activation of rabbit keratinocyte fibronectin receptor function in vivo during wound healing. *J Invest Dermatol* **86:** 585–590

Tan NS, Ho Bow, Ding JL (2002) Engineering a novel secretion signal for cross-host recombinant protein expression. *Protein Engineering* **15:** 337-345

Tan NS, Michalik L, Desvergne B, Wahli W (2004) Peroxisome proliferator-activated receptor-β as a target for wound healing drugs. *Expert Opinion on Therapeutic Targets* **8:** 39-48

Tan NS, Michalik L, Desvergne B, Wahli W (2005) Genetic- or transforming growth factor-beta 1-induced changes in epidermal peroxisome proliferator-activated receptor beta/delta expression dictate wound repair kinetics. *J Biol Chem* **280:** 18163-70

Tan NS, Michalik L, Noy N, Yasmin R, Pacot C, Heim M, Fluhmann B, Desvergne B, Wahli W (2001) Critical roles of PPAR beta/delta in keratinocyte response to inflammation. *Genes Dev* **15:** 3263-3277

Tartaglia LA, Dembski M, Weng X, Deng N, Culpepper J, Devos R, Richards GJ, Campfield LA, Clark FT, Deeds J, Muir C, Sanker S, Moriarty A, Moore KJ, Smutko JS, Mays GG, Wool EA, Monroe CA, Tepper RI (1995) Identification and expression cloning of a leptin receptor, OB-R. *Cell* **83:** 1263-71

Tsuruta F, Sunayama J, Mori Y, Hattori S, Shimizu S, Tsujimoto Y, Yoshioka K, Masuyama N, Gotoh Y (2004) JNK promotes Bax translocation to mitochondria through phosphorylation of 14-3-3 proteins. *EMBO J* **23:** 1889-1899

Tustin CA (2001) US Markets for Current Emerging Wound Closure Technologies *MedTech Insight*, August 2002

Werner S, Grose R (2003) Regulation of wound healing by growth factors and cytokines**.** *Physiol Rev* **83:** 835–870

Werner S, Krieg T, Smola H (2007) Keratinocyte–Fibroblast Interactions in Wound Healing. *J Invest Dermatol* **127:** 998–1008

Wessel D, Flugge UI (1984) A method for the quantitative recovery of protein in dilute solution in the presence of detergents and lipids. *Anal Biochem* **138:** 141-143

www.wikipedia.org/wiki/Skin

Xu A, Lam MC, Chan KW, Wang Y, Zhang J, Hoo RLC, Xu JY, Chen B, Chow WS, Tso AWK, Lam KS (2005) Angiopoietin-like protein 4 decreases blood glucose and improves glucose tolerance but induces hyperlipidemia and hepatic steatosis in mice. *Proc Natl Acad Sci U S A* **102:** 6086-6091

Yamada KM (1991) Fibronectin and other cell interactive glycoproteins. In: Hay ED, ed. Cell Biology of Extracellular Matrix. San Diego: Academic Press, pp111–146

Yang YH, Wang Y, Lam KS, Yau MH, Cheng KK, Zhang J, Zhu W, Wu D, Xu A (2008) Suppression of the Raf/MEK/ERK signaling cascade and inhibition of angiogenesis by the carboxyl terminus of angiopoietin-like protein 4. *Arterioscler Thromb Vasc Biol* **28:** 835-40

Yin W, Romeo S, Chang S, Grishin NV, Hobbs HH, Cohen JC (2009) Genetic Variation in ANGPTL4 Provides Insights into Protein Processing and Function. *J Biol Chem* **284:** 13213–13222

Zhang Y, Proenca R, Maffei M, Barone M, Leopold L, Friedman JM (1994) Positional cloning of the mouse obese gene and its human homologue. *Nature* **372:** 425-432.

CHAPTER 2

TAK1 DEFICIENCY ENHANCES INTEGRIN-MEDIATED KERATINOCYTES MIGRATION DURING WOUND REPAIR

Publication: Tan SH*, **PAL M***, Tan MJ*****, Wong MH, TAM FU, Teo JW, Chong HC, Tan CK, Goh YY, Tang MB, Cheung PC, Tan NS (2009) Regulation of cell proliferation and migration by TAK1 is via transcriptional control of von Hippel-Lindau tumor suppressor. *J Biol Chem* **284:** 18047-18058 (* Authors contributed equally).

2.1 ABSTRACT

Skin maintenance and healing after wounding requires complex epithelial-mesenchymal interactions purportedly mediated by growth factors and cytokines. Recent studies have shown that TAK1 is essential in the regulation of keratinocytes growth, survival and differentiation. However, the molecular mechanism underlying the promotion of wound healing is less understood. In order to delineate the underlying mechanism, we examined the signaling events activated in normal keratinocytes compared with TAK1 deficient keratinocytes. We showed here that TAK1 deficiency in keratinocytes enhances cell migration. TAK1-deficient keratinocytes displayed lamellipodia formation with distinct microspikes protrusion, associated with an elevated expression of integrin β_1, β_5, and sustained activation of cdc42, Rac1 and RhoA. Taken together, our data suggest that TAK1 is central in regulating wound repair. Our findings provide evidence for a novel homeostatic control of keratinocyte migration mediated via TAK1 regulation of integrin β_1, β_5 and small Rho GTPases. Dysfunctional regulation of TAK1 may contribute to the pathology of chronic inflammatory wound and psoriasis.

2.2 INTRODUCTION

Cell migration is important in a variety of biological and pathological processes, including embryonic development, wound healing, angiogenesis, inflammation, tumor invasion and metastasis (Ridley et al., 2003). In humans, problems with wound healing can manifest as either delayed wound healing (which occurs with diabetes or radiation exposure) or excessive healing (as occurs with hypertrophic and keloid scars), characterized by improper deposition of large amounts of extracellular matrix (ECM) and by alterations in local vascularization and cell proliferation. Therefore, the tissue integrity and homeostatic mechanism of the skin is very important in the context of wound repairing process. In order for locomotion of cells to occur, a defined sequence of changes in cellular morphology must take place: extension of the cellular membrane, attachment to the substratum, translocation of the cytosol, and detachment and retraction of the lagging edge into the cell body. As such, each of these processes involves an extensive network of signaling events in order to coordinate and sustain cell motility. In multicellular organism, cells do not exist in isolation. Instead, they associate with the neighboring cells and the extracellular environment. The ECM is a part of this environment and provides the physical support on which the cells adhere. The ECM also provides a cell with information regarding its context within a tissue or organ, information required for proliferation, migration, differentiation and survival. Perhaps the most fundamental component of these processes is adhesion to the ECM, which the cell achieves through the activation of several adhesion receptors and signaling molecules.

One of the most important signaling molecules for most cell-ECM interaction is integrin (Fig. 2.1). It is also clear that several integrins with distinct subunit composition

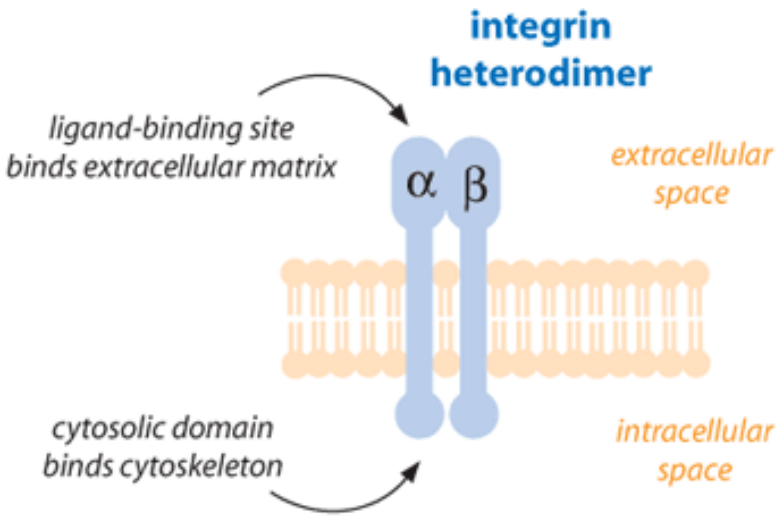

Figure 2.1 The basic structure of the integrin, a cell surface protein receptor (Eslami, 2005)

recognize the same ligand. For example, α2, α3, α6 when coupled to β1 subunit have demonstrated laminin recognition capability (Languino et al., 1989). Different forms of integrin α subunit can also give rise to multiple receptors for collagen (Wayner and Carter, 1987), fibronectin (Wayner et al., 1989) and fibrinogen (Smith et al., 1990a, b). These integrin receptors are expressed in human epidermal cells that mediate cellular responses to various ECM, involved in wound repairing process (Larjava et al., 1996). During wound healing, migrating epithelial cells on the basement membrane (Fig. 2.2), temporarily express some integrins which are redistributed in the cell membrane, and thereby change epithelial cell behavior (Larjava et al., 1993). The mechanisms propagated from integrins to culminate the cell migration are of intense research.

The transmembrane integrin receptors play key roles in two-way signaling across the membrane. The diverse cytoplasmic domain sequences within the various integrin α

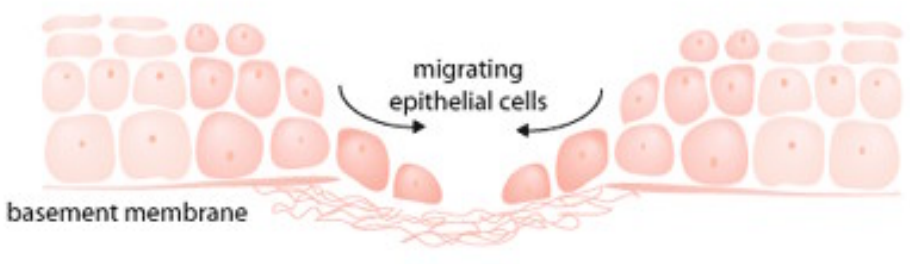

Figure 2.2 Integrins enable epithelial cells to migrate during wound closure (Eslami, 2005)

and β subunits are particularly important in this regard. In response to cytoplasmic signals, integrin conformation can be changed, resulting in modulation of their ligand-binding affinity, which is termed inside-out signaling (Schwartz, 1993). Conversely, external ligand binding may cause changes in cytoplasmic domains (outside-in signaling) associated with a diversity of post-ligand binding events, such as cell spreading, migration, differentiation and gene induction (Chan et al., 1992). Signaling mediated through integrin clustering and ligation with ECM-derived ligands has been termed ouside-in signaling. Integrins achieve signaling by interacting with intracellular effectors that couple integrins and growth-factor receptors to downstream components such as focal-adhesion kinase (FAK) and integrin-linked kinase (ILK) (Dedhar, 1999).

Initially, integrins were thought to act simply as cell adhesion receptors, but it has become clear that they also play crucial roles in the communication of cellular signal transduction pathways leading to adhesion and rearrangement of the actin cytoskeleton (Ridley et al., 2003). Cell migration not only requires a coordinated assembly and disassembly of focal adhesions to move the cell body on the ECM, it also needs active actin polymerization along the plasma membrane to contact the cell cortex. The Rho family of small GTPases, via the recruitment and stimulation of FAK and Src, is a key

regulator of the actin cytoskeleton (Fig. 2.3). Twenty-two mammalian genes encoding Rho GTPases have been described, in particular cdc42, Rac1 and RhoA, are the most well characterized in the context of cell migration.

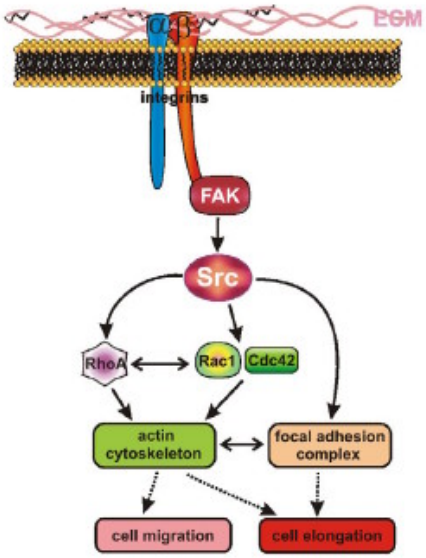

Figure 2.3 Schematic overview of the integrin signaling. **Signaling pathways downstream of FAK and Src controlling actin cytoskeletal rearrangement and focal adhesions**. Integrin activation induces recruitment and stimulation of FAK and Src, which target RhoA or Rac1 and Cdc42 GTPases, thereby controlling cell migration and elongation via regulation of the actin cytoskeleton. The elongated cell morphology might also be caused by deregulated focal adhesions (Schneider et al., 2008).

This regulatory Rho GTPases act as molecular switches cycling between an active GTP bound state and an inactive GDP-bound state. This activity is controlled by (a) guanine nucleotide exchange factors (GEFs) that catalyze the exchange of GDP for GTP to activate the switch (Schmidt & Hall 2002); (b) GTPase-activating proteins (GAPs) that stimulate the intrinsic GTPase activity to inactivate the switch (Bernards 2003); and (c) guanine nucleotide dissociation inhibitors (GDIs), whose role appears to be the blocking

of spontaneous activation (Olofsson 1999) (Fig. 2.4). The dynamic reorganization of the actin cytoskeleton provides the driving force, directing protrusion at the front and retraction at the rear of the cells (Webb et al., 2002). The activation of cdc42, Rac1 and

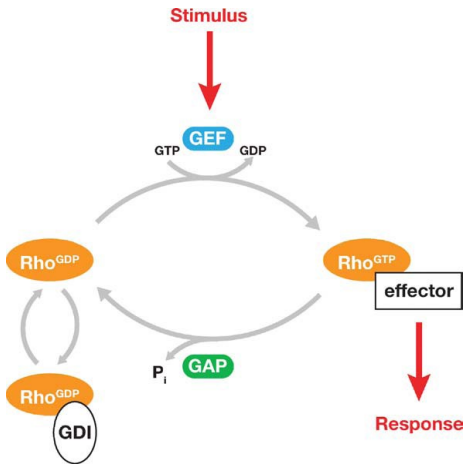

Figure 2.4 Rho GTPases cycle between an inactive GDP-bound form and an active GTP-bound form. In mammalian cells, their activity is regulated by a large family of 85 GEFs, an equally large family of 80 GAPs, and 3 GDIs. Active GTPases interact with effector proteins to mediate a response (Jaffe and Hall, 2005).

RhoA leads to the assembly of protrusive actin-rich filopodia (thin, cylindrical, needle-like projection), lamellipodia (highly compact meshwork of actin filament) and contractile actin:myosin filaments, respectively (Etienne-Manneville & Hall 2002). The elongated filaments generate stiffness that is required for efficient pushing of the plasma membrane and hence facilitate cell migration. Activated Rho GTPases also promote the assembly of small focal adhesion complexes at the periphery of the cells. The assembly of these complexes involves Rho specific protein kinases such as focal adhesion kinase (FAK), protein kinases Cα (PKCα) and structural proteins like talin, vinculin and α-actinin (Burridge et al., 1988; Jaken et al., 1989). Through the focal adhesion complex,

the actin filaments link to integrins at the inner surface of plasma membrane. Therefore, the system requires an optimal level of active Rho GTPase.

Rho GTPases mediate their effect via numerous downstream effectors. One of the well-studied downstream effectors which have been widely used for the study of cdc42 and Rac1 activity is p21-activated kinase (PAK). PAK is a ubiquitous serine/threonine protein kinase and it has six mammalian isoforms, PAK 1 to 6 (Bagrodia and Cerione, 1999). The structure of PAK involves N-terminal regulatory domain, C-terminal catalytic domain, homodimerization domain, cdc42 and Rac interactive binding (CRIB) motif (Burbelo et al., 1995), p21-binding domain (PBD) and autoinhibitory switch domain (Bokoch, 2003). It is reported that PBD contributes to the overall binding affinity of PAK to GTP-bound cdc42 and Rac1 (Manser et al., 1994). PAK is involved in the regulation of cytoskeletal dynamics, cell polarity and motility, cell growth signaling and transformation, cell death and survival signaling (Bokoch, 2003). The other downstream effector protein that has been widely used to study Rho activity is serine/threonine kinase, Rhotekin (RTKN) which contains Rho binding motif for the binding of RhoA (Reid et al., 1996). These regulators also affect on gene transcription through different signal transduction pathways, including the mitogen activated protein kinase (MAPK) cascade, which itself has cell context dependent pleiotropic roles (Coso et al., 1995; Minden et al., 1995).

MAPK signal transduction pathways are evolutionarily conserved among eukaryotes and have been implicated to play key roles in a number of biological processes, including cell growth, differentiation, apoptosis, inflammation and responses to environmental stresses (Sayama et al., 2006). They are typically organized in a three-

tiered architecture consisting of a MAPK, a MAPK activator (MAPK kinase) and a MAPKK activator (MAPKK kinase). MAPK pathway can be regulated at multiple levels as well as via multiple mechanisms, of which the regulation of mitogen-activated protein kinase kinase kinase (MAPKKK) has been proved to be the most challenging due to the great diversity and versatility between different modules at this level. The transduction of exogenous signals is achieved through sequential phosphorylation and activation of the components in the individual cascade leading to the activation of certain transcription factors and other kinases (Sayama et al., 2002).

Transforming growth factor-β (TGF-β) activated kinase 1 (TAK1) belongs to the MAPKKK family. This serine/threonine kinase is a key intermediate in inflammatory cytokines tumor necrosis factor-α (TNF-α) and interleukin-1 (IL-1) (Ninomiya-Tsuji et al., 1999; Sato et al., 2005) as well as TGF-β (Yamaguchi et al., 1995) mediated signaling pathways. Activated TAK1 has the capacity to stimulate its downstream MAPK and NF-κB-inducing kinase-IκB kinase cascades (Wang et al., 2001). The former activates c-Jun N-terminal kinase (JNK) and p38 MAPK while the latter activates NF-κB (Ninomiya-Tsuji et al., 1999; Takaesu et al., 2003;Yao et al., 2007). A deficiency in TAK1 results in impaired TNF-α and IL-1 stimulated JNK activity, p38 phosphorylation and IκBα degradation (Takaesu et al., 2003; Shim et al., 2005). Studies of keratinocyte-specific TAK1 knockout (TAK1-KO) mice confirmed the role of TAK1 in skin inflammation. These TAK1-KO mice died by postnatal Day 7 and developed intra-epidermal micro-abscesses (Omori et al., 2006; Sayama et al., 2006), displayed abnormal epidermis with impaired differentiation and increased cellular proliferation; however no significant difference in proliferation index was observed in *in vitro* culture of these mutant

keratinocytes. Nevertheless, the latter suggests a crucial role of the underlying dermis in mitigating some effects of epidermal TAK1. Findings from our lab showed that the expression of TAK1 was increased on the wound epithelium. Our lab has generated TAK1 knockdown keratinocytes using lentivirus mediated RNA interference (Tan et al., 2009). We provide evidence of a double paracrine mechanism that makes a pivotal contribution to the enhanced cell proliferation in TAK1-deficient epidermis. However, the role of TAK1 and its mechanism of action in keratinocyte migration remain unknown.

Herein, we found that TAK1 defficient keratinocytes expressed elevated levels of integrin β_1, integrin β_5 and small Rho GTPases. Taken together, these data highlight a novel mechanism by which TAK1 signaling through integrin β_1, integrin β_5 and small Rho GTPases influences cellular function as well as cell morphology.

2.3 MATERIALS AND METHODS

2.3.1 Reagents & Antibodies

Human keratinocytes and corresponding culture medium were purchased from Cascade Biologics. Antibodies against TAK1 for immunoblot (Cell Signaling); cdc42, Rac1 and RhoA (Cytoskeleton); goat anti-rabbit IgG HRP and goat anti-mouse IgG HRP (Santa Cruz Biotechnology). Otherwise, chemicals were from Sigma-Aldrich.

2.3.2 Immunoblots

Total protein was extracted from cells with ice-cold lysis buffer (20 mM $Na_2H_2PO_4$, 250 mM NaCl, 1 % Triton-100, 0.1 % SDS). Equal amount of protein extracts were resolved by SDS-PAGE and electrotransferred onto PVDF membranes. Membranes were processed according to standard procedure and proteins were detected by chemiluminesence. Signal intensities were quantified using Image J analysis software and were normalized with the mean intensity of the positive controls on each membrane. Silver stained membrane was used to check the expression of proteins into induced and uninduced bacterial lysate as well as bound proteins with Ni-resin.

2.3.3 GTPases activation assay for cdc42, Rac1 and RhoA

GTPases activation assays were carried out as previously described (Tan et al., 2007). Purified recombinant GST-p21 binding domain (PBD) of PAK was used to measure active cdc42 and Rac1, while GST-Rho binding domain (RBD) of rhotekin was used to measure active RhoA.

2.3.4 In vitro scratch wound assay

The cells (human keratinocytes) were cultured in culture-insert (400 μM width of cell free gap) (ibidi) until confluency. Typically, 5.0 x 10^4 cells in DMEM supplemented with 10 % FBS were seeded into the insert. The wound insert was removed on the next day to reveal the 400 μM scratch wound. Subsequently, the wounded monolayer was washed twice with serum free DMEM. The migrated distance and the rate of migration of the wounded monolayer were then determined by taking serial photomicrographs at 2 min intervals for 9 h using a microscope as mentioned in section *1.3.21*. The distances re-occupied by the migrating cells were derived using 5 measurements per microscopic field. The mean values were calculated from three independent experiments.

2.3.5 Integrin-mediated cell adhesion assay

The principle of integrin-mediated cell adhesion assay is based on immobilization of monoclonal antibodies generated against human αvβ3 integrin, αvβ5 integrin, or human β1 onto a goat anti-mouse antibody coated microculture plate. These anti-integrin antibodies capture cells expressing cognate integrins on their cell surface. A goat anti-mouse antibody coated microplate was used as a negative assay control.

This assay was performed as per the manufacturer's (Chemicon) instructions. Briefly, integrin coated and uncoated control strips of 96-well microculture plates were rehydrated with PBS for 10 min at room temperature. Wild type (K_{CTRL}) and TAK1 knockdown ($K_{TAK1\text{-}B}$) keratinocyte cells (1X10^4) were added to each well in 100 μl serum free DMEM medium. Cells were allowed to adhere at 37 °C in a CO_2 incubator for 1 hr and then the nonadherent cells were removed by gently washing the plates in PBS

containing 1 mM $CaCl_2$ and 1 mM $MgCl_2$. Adherent cells were fixed with 1 % glutaraldehyde in PBS for 15 min, stained with 0.1 % crystal violet for 30 min and eluted cells bound stain after gently rotating on shaker at room temperature for 10 min. Adhesion was quantified in triplicate by measuring the absorbance of eluted stain at 562 nm on spectrophotometer.

2.4 RESULTS

The enhancement of keratinocyte migration by TAK1 deficiency is associated with elevated expression of active cdc42, Rac1 and RhoA

Cell migration over the provisional wound bed is essential for re-epithelialization of injured tissues. As expression of TAK1 was increased during re-epithelialization of the wound, we questioned whether TAK1 deficiency affects keratinocyte migration. We used human keratinocytes whose endogenous TAK1 expression was suppressed by lentivirus-mediated RNA interference (Tan et al., 2009).

We investigated the effect of TAK1 deficiency in keratinocyte migration using *in-vitro* scratch wound assay. Interestingly, our live-imaging results showed that TAK1 deficient keratinocytes ($K_{TAK1\text{-}B}$) closed the *in vitro* wound 3 to 4 h ahead of wild type keratinocytes (K_{CTRL}) (Fig. 2.5A, videos V1-2). Cell proliferation and migration contribute to the closure of the *in vitro* wound. To more precisely determine the contribution of cell migration towards wound closure, we performed similar experiments in the presence of mitomycin C (mit C). Consistent with the above observation; $K_{TAK1\text{-}B}$ closed the *in-vitro* wound by 10 h in the presence of mit C, a 2 h delay as compared to vehicle-treated $K_{TAK1\text{-}B}$. In contrast, K_{CTRL} failed to close the wound even by the end of the 12 h experimental period (Fig. 2.5B, videos V5-6). Close examination of the migratory front revealed that $K_{TAK1\text{-}B}$ displayed more extended lamellipodia with numerous microspike-like features when compared to K_{CTRL} (Fig. 2.5A, videos V3-4). The role of small Rho GTPases- cdc42, Rac1 and RhoA to the formation of lamellipodia and cell migration is well established.

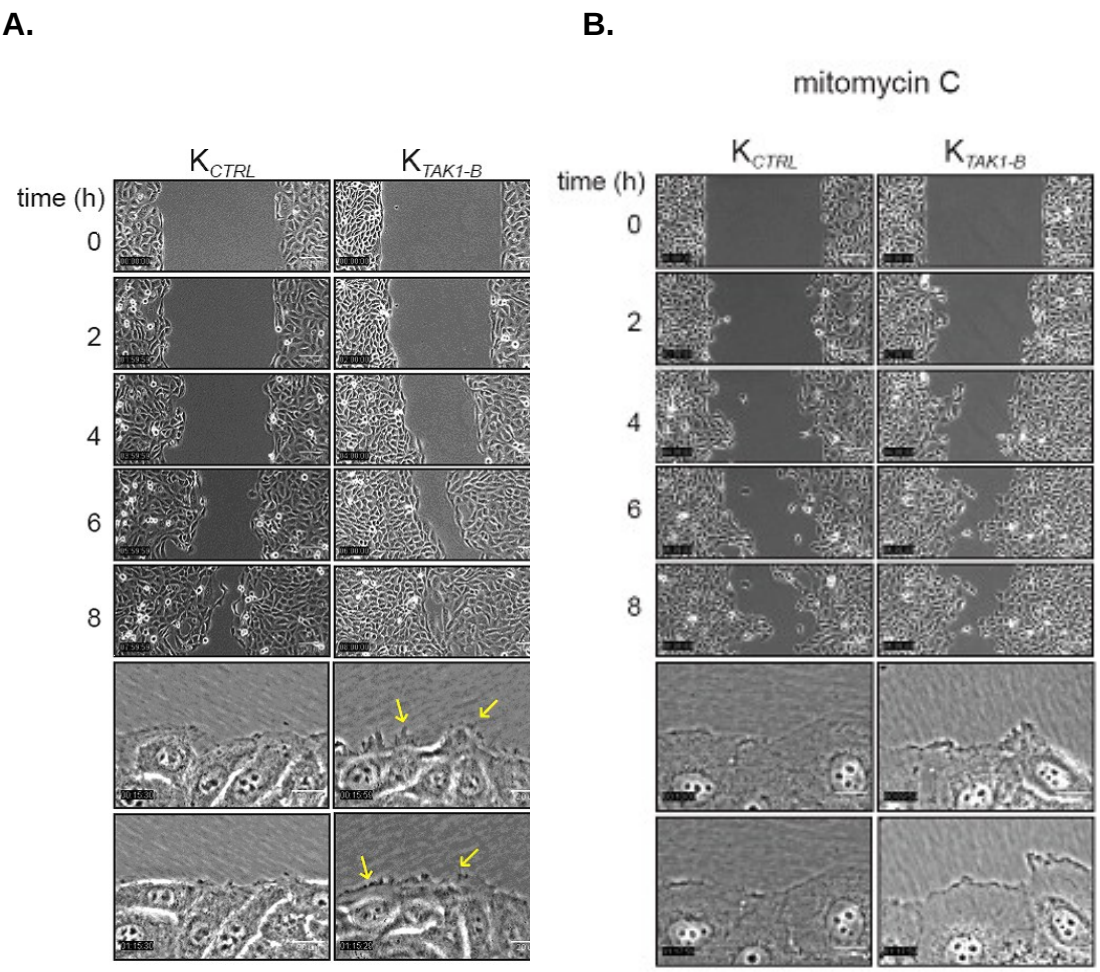

Figure 2.5 TAK1 deficiency enhances cell migration, independent of cell proliferation. **(A)** Time-lapsed images of wounded cultures of control (K_{CTRL}) and TAK1-knockdown (K_{TAK1-B}) (top five panels). Scale bar 100 µm. See videos V1-2. Higher magnification images from video microscopy showing migratory front of K_{CTRL} and K_{TAK1-B} (bottom two panels). Arrows indicate the focal adhesion points and microspike-like extensions in lamellipodia during migration. Scale bar 20 µm. Also see videos V3-4. **(B)** Time-lapsed images of wounded cultures of control (K_{CTRL}) and TAK1-knockdown (K_{TAK1-B}) treated with mitomycin C (2 µg/ml). Yellow dotted lines represent the scratch gap at the time of wounding (top 5 panels). Scale bar 100 µm. See videos V5-6. Higher magnification images from video microscopy showing migratory front of K_{CTRL} and K_{TAK1-B} (bottom two panels). Arrows indicate the focal adhesion points and microspike-like extensions in lamellipodia during migration. Scale bar 20 µm. See videos V7-8.

To gain further insight into the mechanism, we examined the activation of small Rho GTPases, specifically cdc42, Rac1 and RhoA in K_{CRTL} and $K_{TAK1\text{-}B}$ cells stimulated with serum. K_{CTRL} responded a transient activation of the three GTPases, whereas $K_{TAK1\text{-}B}$ displayed sustained activation of active cdc42, Rac1 and RhoA (Fig. 2.6B) after confirmation of specific binding of GST-PBD-PAK and GST-RBD-Rhotekin on GST beads using silver staining of PVDF membrane (Fig. 2.6A). Notably, we observed a prominent upregulation of active RhoA at 10 min after serum induction which pick at 45 min in $K_{TAK1\text{-}B}$. Following additional Rho GTPases activation assay (n=5), we were able to better show the elaborated read by representative of the relative fold change in active Rho GTPases as mean±S.D. A representative immunoblot was shown in Fig. 2.6B. We also found an elevated basal expression level of active cdc42, Rac1 and RhoA in $K_{TAK1\text{-}B}$ when compared to K_{CTRL} before serum stimulation, thus we hypothesized that TAK1 is likely to exert its action upstream of GTPases activation. Integrin ligation and clustering triggers the subsequent activation of the GTPases cdc42, Rac1 and RhoA. Immunoblot analysis revealed higher expression level of integrins β_1 and β_5, but not β_3 in $K_{TAK1\text{-}B}$ when compared to K_{CTRL} (Fig. 2.6C). Consistent with increased integrin ligation, we also detected enhanced activation i.e. phosphorylation of focal adhesion kinase (FAK) in $K_{TAK1\text{-}B}$ (Fig. 2.6C). The observation was further confirmed using integrin-mediated adhesion assay, which showed significant increase in integrins β_1 and β_5 expression in $K_{TAK1\text{-}B}$ (Fig. 2.6D). Altogether, our results showed that the deficiency in TAK1 enhances keratinocyte migration associated with an elevated expression of integrins β_1, β_5 and exacerbated activation of cdc42, Rac1 and RhoA. Overall these studies revealed that

A.

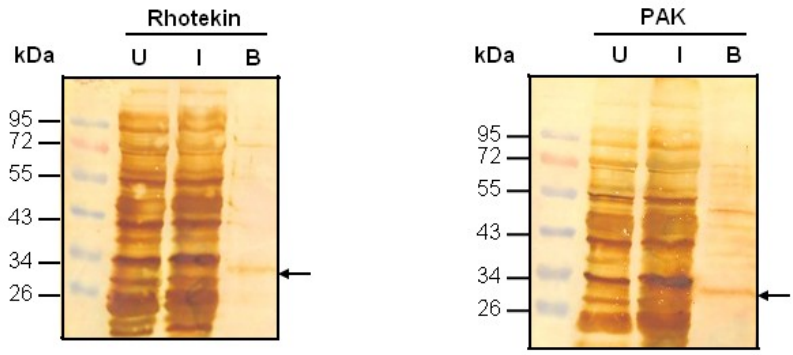

B.

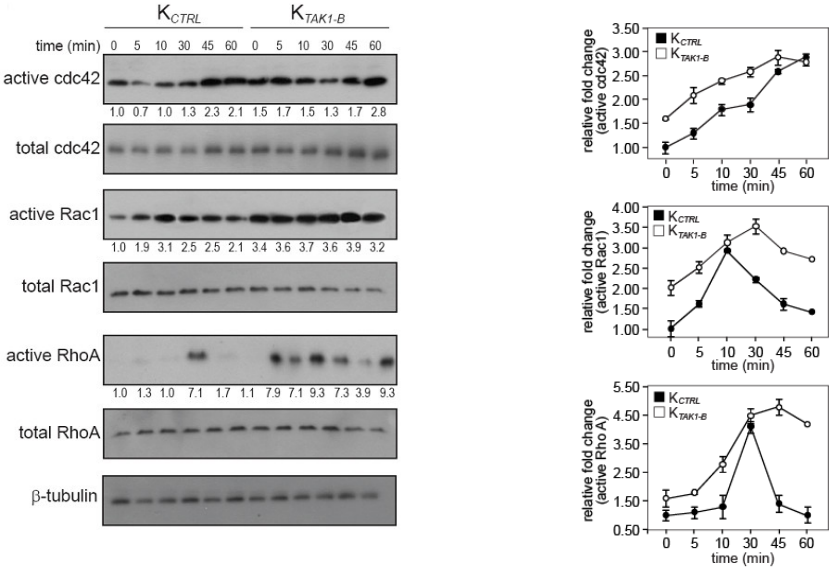

C.

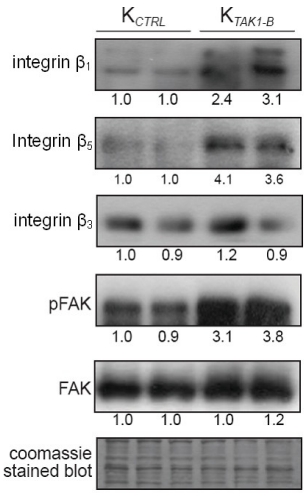

D.

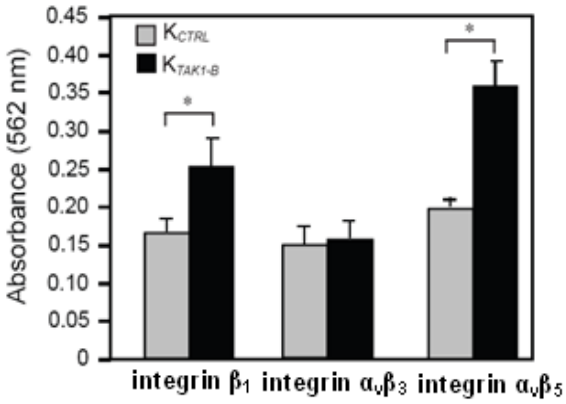

Figure 2.6 TAK1 deficiency upregulates the expression of active Rho GTPases, integrin β_1 and integrin β_5. (A) Confirmation of specific binding of GST-RBD-Rhotekin and GST-PBD-PAK on GST beads using silver staining of PVDF membrane containing total protein lysates from (U) uninduced, (I) induced with IPTG, and (B) GST-bead bound recombinant GST-RBD-Rhotekin (arrow at left panel) and GST-PBD-PAK (arrow at right panel). Molecular weights of RBD-Rhotekin and PBD-PAK are 35 kDa and 34 kDa respectively. **(B)** Immunoblot analysis of active cdc42, Rac1 and RhoA in $K_{\boldsymbol{CTRL}}$ and $K_{\boldsymbol{TAK1\text{-}B}}$ exposed for the indicated time periods (min) with serum. Numbers below the blots represent the mean fold change in active cdc42, Rac1 and RhoA relative to level at zero min of $K_{\boldsymbol{CTRL}}$. Representative pictures of immunoblot were shown. Graphs in right panel showed relative -fold change of active cdc42 (top), Rac1 (middle), and RhoA (bottom) inK_{CTRL} and $K_{TAK1\text{-}B}$ exposed for the indicated time periods (min) with serum. Values represent the mean–fold change in active cdc42, Rac1, and RhoA relative to level at zero min of K_{CTRL} (mean±S.D.; n=5). **(C)** TAK1 modulates the expression of integrins and activation of focal adhesion kinase (FAK). Immunoblot analyses of integrins β_1, β_3, β_5, total FAK and phosphorylated FAK (pFAK) in $K_{\boldsymbol{CTRL}}$ and $K_{\boldsymbol{TAK1\text{-}B}}$**.** Coomassie-stained blot showed equal loading and transfer. **(D)** Integrin-mediated cell adhesion assay showed elevated expression of integrins β_1 and $\alpha_v\beta_5$ in TAK1-deficient keratinocytes. Assay was performed accordingly to manufacturer's protocol. Statistical analysis was determined using two-tailed Mann-Whitney test, * denotes $p<0.01$.

TAK1 deficiency enhanced cell migration during re-epithelialization of the wound with increased expression of integrins β_1, β_5 and active Rho GTPases.

2.5 DISCUSSION

Following injury, the restoration of its functional integrity is of utmost importance to the survival of animals. The regeneration and maintenance of epithelium to close the wound is dictated by epithelial-mesenchymal interactions and purportedly mediated by the action of central players, such as chemokines and growth factors. This communication is crucial in preventing either insufficient or excess wound repair. Previous work has shown that mice with a keratinocyte-specific deletion of TAK1 exhibit severe skin inflammation and displayed abnormal epidermis with impaired differentiation, increased cell proliferation and apoptosis (Omori et al., 2008; Sayama et al., 2006). We revealed that the expression of TAK1 is accelerated during wound repairing process. Our *in vitro* findings showed that keratinocyte-specific TAK1 regulates epidermal proliferation via a double paracrine mechanism and showed that von Hippel-Lindau tumor suppressor (pVHL), whose expression is regulated by TAK1/NF-κB signaling, interacts and sequesters transcription factor Sp1, which is required for platelet-derived growth factor-B (PDGF-B) expression (Tan et al., 2009). In order to close the wound, keratinocytes need to proliferate, survive and migrate into wound bed. In this study, we revealed a novel homeostatic role of TAK1 in the control of keratinocyte migration.

Cell migration during re-epithelialization is crucial for efficient wound closure. The molecular mechanisms underlying the motility and directed movement of a cell involve a number of interdependent processes including extension of the leading edge in the direction of movement by protrusion of filopodia, lamellipodia, or both, the formation and breakage of adhesion sites between the cell and the substratum, and contraction of the cell to move the cell mass relative to the substratum. These processes must be

coordinated and the activities of these three proteins are linked to each other in a hierarchical fashion, such that activation of cdc42 leads to the induction of filopodia and to the activation of Rac and the formation of lamellipodia.

Recent work in our lab reveals that TAK1 regulates cell migration via the transcriptional control of pVHL, while TAK1 employs similar regulatory mechanism i.e. via pVHL to modulate integrins β_1 and β_5 expressions. In support of a role in cell migration for VHL, it was reported that highly aggressive breast cancer expressed either no VHL or low VHL level (Zia et al., 2007). High VHL expression also resulted in a decrease of tubulin turnover indicating a role for VHL in cellular processes such as migration, polarization, and cell-cell interactions (Lolkema et al., 2004).

The familial VHL disease related tumor is highly vascularized in the central nervous system, retina and kidney due to functional inactivation of pVHL tumor suppressor gene. pVHL has been shown to play a role in the destruction of transcription factor hypoxia-inducible factor-1 (HIF-α) subunits via ubiquitin-mediated proteolysis (Stickle et al., 2004). Immunomodulatory peptides, including IL-1 and TNF-α, stimulate HIF-1 dependent gene expression even in normoxic cells involve PI3K and MAPK signaling pathways (Thomas and Kim, 2005). Loss of pVHL function leads to stabilization of HIF-1 and expression under normoxic conditions of hypoxia-inducible genes including vascular endothelial growth factor (VEGF). However, pVHL has also been implicated in HIF-α independent multiple biological processes.

The formation of normal epidermal tissue requires a continuous exchange of signals with the underlying dermal fibroblasts. Previous studies have indicated that gene expression changes in the dermal fibroblasts significantly influence epithelial cell fate

(Cheng et al., 2005; Bhowmick and Moses, 2005). Keratinocyte-specific TAK1-knockout mice displayed enhanced epidermal proliferation which is not observed in monolayer culture, suggesting that dermal fibroblasts have pivotal contribution. We revealed that a double paracrine PDGF/HGF signaling plays an important role in TAK1-mediated epidermal proliferation (Fig. 2.7). We further show that NF-κB, a downstream mediator of TAK1, regulates the expression of pVHL. The pVHL protein regulates the expression of PDGF-B via binding with transcription factor Sp1 (Rafty and Khachigian, 2002). A similar mechanism was also exploited by pVHL to repress VEGF gene expression (Mukhopadhyay et al., 1997). PDGF-B was previously reported to increase HGF production in the fibroblasts to stimulate keratinocyte proliferation (Lederle et al., 2006). Indeed, PDGF-BB secreted by keratinocytes acts as a paracrine factor to induce HGF production by fibroblasts, which in return, enhance epidermal proliferation. This study underscores the fact that TAK1 in the epidermal keratinocytes fulfils a homeostatic role during epidermal formation, modulating cell proliferation via a double paracrine fashion, involving the underlying dermal fibroblasts. The paracrine mechanism described herein emphasizes the importance of epithelial-mesenchymal communication in the regulation of epidermal proliferation, which was not observed in TAK1-knock-out monolayer culture.

Our data show that TAK1 play an important role in cell migration mediated through integrins β_1, β_5, Rho GTPases and pVHL. Wound healing and cancer metastasis share numerous similar characteristics (Chang et al., 2005) including cell migration. Although the role of TAK1 in cancer metastasis remains unknown and is not directly

addressed in this study, our data suggested that the deregulation of TAK1 expression may have a significant impact on cancer cell migration and cancer metastasis.

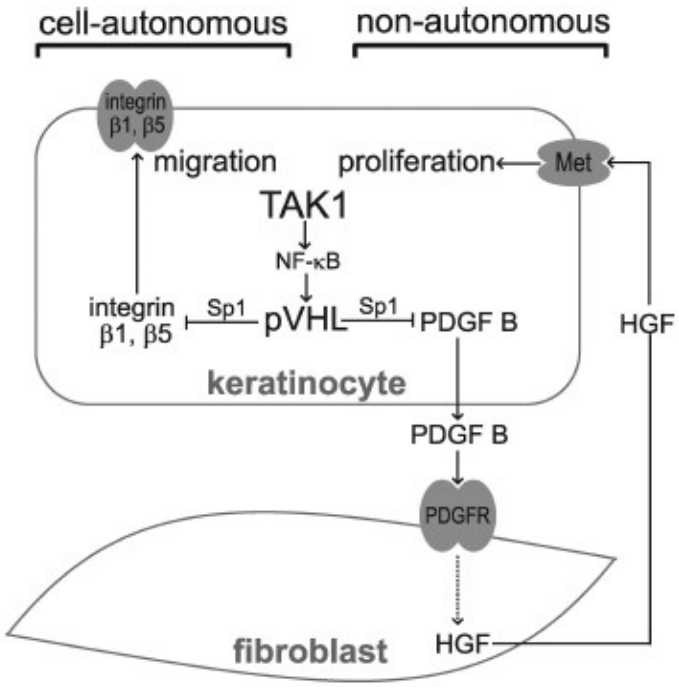

Figure 2.7 TAK1 plays a homeostatic role in regulating cell migration and proliferation. Epidermal TAK1 regulates keratinocyte proliferation by a double paracrine mechanism through release of PGDF-B, which induces HGF in the fibroblasts. TAK1 activates NF-κB to stimulate the expression of pVHL. This facilitates pVHL-Sp1 interaction and sequesters Sp1 from promoting PDGF-B expression. In response to PDGF, the fibroblasts increase the release of HGF, which acts via its receptor, Met, to stimulate keratinocytes proliferation. Via a similar mechanism, TAK1 negatively regulates the expression of integrins β_1 and β_5 in a cell-autonomous manner (Tan et al., 2009).

2.6 FUTURE STUDIES

Our data together with previous findings suggest that TAK1 may play a central role in the homeostasis process of keratinocyte migration in wound repairing process. To achieve proper tissue homeostasis during wound healing, the fine-tuned balance between complex networks of various cell subsets and numerous pro- and anti-inflammatory mediators is crucial. Given the pivotal role of TAK1 as a critical mediator of many pro-inflammatory cytokines, the dysregulation of TAK1 is likely to result in many pathological and chronic inflammatory skin diseases. Of particular interest, the role of TAK1 in the etiology of psoriasis is worth further investigation. Psoriasis is a non-contagious chronic inflammatory skin disease characterized by hyperproliferative epidermal growth, a phenotype that was similarly observed in mice with a keratinocyte-specific deletion of TAK1. Recent report suggests that TAK1 deletion causes dysregulation of reactive oxygen species (ROS) in keratinocytes, which is causally associated with skin inflammation. ROS has been associated with psoriasis. Therefore, the development of approaches to diagnosis, treatment, and drug design requires a search for critical links in the pathogenesis, i.e., candidate genes and the corresponding protein products. One classical genetic method using DNA microarrays are at the moment a highly informative tool for quantitatively assessing the gene expression of large gene groups in the research of autoimmune diseases and postgenomic technologies are applicable for detecting the biological markers and studying the etiology of psoriasis.

Our results show that TAK1 directly regulates the expression of pVHL, a tumor suppressor. In addition, we showed that this modulates the activity of transcription factor Sp1 to regulate the expression of integrin β_1 and β_5. Clearly, the pathological role of

TAK1 in cancer growth and metastasis will be an interesting research avenue. In the first instance, it will be interesting to determine TAK1 activity in the large number of cancers. Further investigation will reveal if TAK1 is a potential anti-tumor target in solid tumors. Preliminary data from our lab shows that TAK1-deficient carcinoma growth at a slower rate *in vivo* (unpublished).

2.7 REFERENCES

Bagrodia S, Cerione RA (1999) PAK to the future. *Trends Cell Biol* **9:** 350-355

Bernards A (2003) GAPs galore! A survey of putative Ras superfamily GTPase activating proteins in man and Drosophila. *Biochim Biophys Acta* **1603:** 47-82

Bhowmick NA, Moses HL (2005) Tumor-stroma interactions. *Curr Opin Genet Dev* **15:** 97-101

Bokoch GM (2003) Biology of the p21-activated kinases. *Annu Rev Biochem* **72:** 743-781

Burbelo PD, Drechsel D, Hall A (1995) A conserved binding motif defines numerous candidate target proteins for both Cdc42 and Rac GTPases. *J Biol Chem* **270:** 29071–74

Burridge K, Fath K, Kelly T, Nuckolls G, Turner C (1988) Focal adhesions: transmembrane junctions between the extracellular matrix and the cytoskeleton. *Annu Rev Cell Biol* **4:** 487-525

Chan BMC, Kassner PD, Schiro JA, Byers HR, Kupper TS, Hemler ME (1992) Distinct cellular functions mediated by different VLA integrin α subunit cytoplasmic domains. *Cell* **68:** 1051-1060

Chang HY, Nuyten DS, Sneddon JB, Hastie T, Tibshirani R, Sørlie T, Dai H, He YD, van't Veer LJ, Bartelink H, van de Rijn M, Brown PO, van de Vijver MJ (2005) Robustness, scalability, and integration of a wound-response gene expression signature in predicting breast cancer survival. *Proc Natl Acad Sci U S A* **102:** 3738-43

Cheng N, Bhowmick NA, Chytil A, Gorksa AE, Brown KA, Muraoka R, Arteaga CL, Neilson EG, Hayward SW, Moses HL (2005) Loss of TGF-beta type II receptor in fibroblasts promotes mammary carcinoma growth and invasion through upregulation of TGF-alpha-, MSP- and HGF-mediated signaling networks. *Oncogene* **24:** 5053-5068

Coso OA, Chiariello M, Yu JC, Teramoto H, Crespo P, Xu N, Miki T, Gutkind JS (1995) The small GTP-binding proteins Rac1 and cdc42 regulate the activity of the JNK/SAPK signaling pathway. *Cell* **81:** 1137–46

Dedhar S (1999) Integrins and signal transduction. *Curr Opin Hematol* **6:** 37-43

Eslami A (2005) The role of integrins in wound healing. *The science creative quarterly*, Issue 2, Sep-Nov

Etienne-Manneville S, Hall A (2002) Rho GTPases in cell biology. *Nature* **420:** 629–35

Jaken S, Leach K, Klauck T (1989) Association of type 3 protein kinase C with focal contacts in rat embryo fibroblasts. *J Cell Biol* **109:** 697-704

Jaffe AB, Hall A (2005) Rho GTPases: biochemistry and biology. *Annu Rev Cell Dev Biol* **21:** 247-69

Languino LR, Gehlsen KR, Wayner EA, Carter WG, Engvall E, E Ruoslnhti (1989) Endothelial cells use α2β1 integrin as a laminin receptor. *J Cell Biol* **109:** 2455-2462

Larjava H, Haapasalmi K, Salo T, Wiebe C, Uitto VJ (1996) Keratinocyte integrins in wound healing and chronic inflammation of the human periodontium. *Oral Dis* **2:** 77-86

Larjava H, Salo T, Haapasalmi K, Kramer RH, Heino J (1993) Expression of integrins and basement membrane components by wound keratinocytes. *J Clin Invest* **92:**1425-35

Lederle W, Stark HJ, Skobe M, Fusenig NE, Mueller MM (2006) Platelet-derived growth factor-BB controls epithelial tumor phenotype by differential growth factor regulation in stromal cells. *Am J Pathol* **169:** 1767-1783

Lolkema MP, Mehra N, Jorna AS, van BM, Giles RH, Voest EE (2004) The von Hippel-Lindau tumor suppressor protein influences microtubule dynamics at the cell periphery. *Exp Cell Res* **301:** 139-146

Manser E, Leung T, Salihuddin H, Zhao ZS, Lim L (1994) A brain serine/threonine protein kinase activated by Cdc42 and Rac1. *Nature* **367:** 40-46

Minden A, Lin A, Claret FX, Abo A, Karin M (1995) Selective activation of the JNK signaling cascade and c-Jun transcriptional activity by the small GTPases Rac and Cdc42Hs. *Cell* **81:** 1147–57

Mukhopadhyay D, Knebelmann B, Cohen HT, Ananth S, Sukhatme VP (1997) The von Hippel-Lindau tumor suppressor gene product interacts with Sp1 to repress vascular endothelial growth factor promoter activity. *Mol Cell Biol* **17:** 5629-5639

Ninomiya-Tsuji J, Kishimoto K, Hiyama A, Inoue J, Cao Z, Matsumoto K (1999) The kinase TAK1 can activate the NIK-I kappaB as well as the MAP kinase cascade in the IL-1 signalling pathway. *Nature* **398:** 252-256

Olofsson B (1999) Rho guanine dissociation inhibitors: pivotal molecules in cellular signalling. *Cell Signal* **11:** 545–54

Omori E, Matsumoto K, SanjoH, Sato S, Akira S, Smart RC, Ninomiya-Tsuji J (2006) TAK1 is a master regulator of epidermal homeostasis involving skin inflammation and apoptosis. *J Biol Chem* **281:** 19610-19617

Omori E., Morioka S, Matsumoto K, Ninomiya-Tsuji J (2008) TAK1 regulates reactive oxygen species and cell death in keratinocytes, which is essential for skin integrity. *J Biol Chem* **283:** 26161-26168

Rafty LA, Khachigian LM (2002) von Hippel-Lindau tumor suppressor protein represses platelet-derived growth factor B-chain gene expression via the Sp1 binding element in the proximal PDGF-B promoter. *J Cell Biochem* **85:** 490-495

Reid T, Furayashiki T, Ishizaki T, Watanabe G, Watanabe N, Fujisawa K, Morii N, Madaule P, Narumiya S (1996) Rhotekin, a new putative target for Rho bearing homology to a serine/threonine kinase, PKN, and rhophilin in the Rho-binding domain. *J Biol Chem* **271:** 13556-13560

Ridley AJ, Schwartz MA, Burridge K, Firtel RA, Ginsberg MH, Borisy G, Parsons JT, Horwitz AR (2003) Cell migration: integrating signals from front to back. *Science* **302:** 1704-1709

Sato S, Sanjo H, Takeda K, Ninomiya-Tsuji J, Yamamoto M, Kawai T, Matsumoto K, Takeuchi O, Akira S (2005) Essential function for the kinase TAK1 in innate and adaptive immune responses. *Nat Immunol* **6:** 1087-1095

Sayama K, Hanakawa Y, Nagai H, Shirakata Y, Dai X, Hirakawa S, Tokumaru S, Tohyama M, Yang L, Sato S, Shizuo A, Hashimoto K (2006) Transforming growth factor-beta-activated kinase 1 is essential for differentiation and the prevention of apoptosis in epidermis. *J Biol Chem* **281:** 22013-22020

Sayama K, Yamasaki K, Hanakawa Y, Shirakata Y, Tokumaru S, Ijuin T, Takenawa T, Hashimoto K (2002) Phosphatidylinositol 3-kinase is a key regulator of early phase differentiation in keratinocytes. *J Biol Chem* **277:** 40390-6

Schmidt A, Hall A (2002) Guanine nucleotide exchange factors for Rho GTPases: turning on the switch. *Genes Dev* **16:** 1587–609

Schneider S, Weydig C, Wessler S (2008) Targeting focal adhesions: Helicobacter *pylori*-host communication in cell migration. *Cell Commun Signal* **6:** 2

Schwartz MA (1993) Signaling by integrins: implication for tumorigenesis. *Cancer Res* **53:** 1503-1506

Shim JH, Xiao C, Paschal AE, Bailey ST, Rao P, Hayden MS, Lee KY, Bussey C, Steckel M, Tanaka N, Yamada G, Akira S, Matsumoto K, Ghosh S (2005) TAK1, but not TAB1 or TAB2, plays an essential role in multiple signaling pathways *in vivo*. *Genes Dev* **19:** 2668-2681

Smith JW, Ruggeri ZM, Kunicki TJ, Cheresh DA (1990b) Interaction of integrins $\alpha v\beta 3$ and glycoprotein IIb-HIa with fibrinogen. Differential peptide recognition accounts for distinct binding sites. *J Biol Chem* **265:** 12267-12271

Smith JW, Vestal DJ, Irwin SV, Burke TA,. Cheresh DA (1990a) Purification and functional characterization of integrin $\alpha v\beta 5$: an adhesion receptor for vitronectin. *J Biol Chem* **265:** 11008-11013

Stickle NH, Chung J, Klco JM, Hill RP, Kaelin WG Jr, Ohh M (2004) pVHL modification by NEDD8 is required for fibronectin matrix assembly and suppression of tumor development. *Mol Cell Biol* **24:** 3251-61

Takaesu G, Surabhi RM, Park KJ, Ninomiya-Tsuji J, Matsumoto K, Gaynor RB (2003) TAK1 is critical for IkappaB kinase-mediated activation of the NF-kappaB pathway. *J Mol Biol* **326:** 105-115

Tan NS, Icre G, Montagner A, Bordier-ten-Heggeler B, Wahli W, Michalik L (2007) The nuclear hormone receptor peroxisome proliferator-activated receptor beta/delta potentiates cell chemotactism, polarization, and migration. *Mol Cell Biol* **27:** 7161-75

Tan SH, PAL M, Tan MJ, Wong MH, TAM FU, Teo JW, Chong HC, Tan CK, Goh YY, Tang MB, Cheung PC, Tan NS (2009) Regulation of cell proliferation and migration by TAK1 is via transcriptional control of von Hippel-Lindau tumor suppressor. *J Biol Chem* in press **284**: 18047-18058

Thomas R, Kim MH (2005) Epigallocatechin gallate inhibits HIF-1alpha degradation in prostate cancer cells. *Biochem Biophys Res Commun* **334:** 543-8

Wang C, Deng L, Hong M, Akkaraju GR, Inoue J, Chen ZJ (2001) TAK1 is a ubiquitin-dependent kinase of MKK and IKK. *Nature* **412:** 346-351

Wayner EA, Garcia-Pardo A, Humphries M J, MacDonald JA, Carter WG (1989) Identification and characterization of the T lymphocyte adhesion receptor for an alternative cell attachment domain (CS-1) in plasma fibronectin. *J Cell Biol* **109:** 1321-1330

Wayner EA, Carter WG (1987) Identification of multiple cell adhesion receptors for type VI collagen and fibronectin in human fibrosarcoma cells possessing unique a and common beta subunits. *J Cell Biol* **105:** 1873-1884

Webb DJ, Parsons JT, Horwitz AF (2002) Adhesion assembly, disassembly and turnover in migrating cells--over and over again. *Nat Cell Biol* **4:** E97-100

Yamaguchi K, Shirakabe K, Shibuya H, Irie K, Oishi I, Ueno N, Taniguchi T, Nishida E, Matsumoto K (1995). Identification of a member of the MAPKKK family as a potential mediator of TGF-beta signal transduction. *Science* **270:** 2008-2011

Yao J, Kim TW, Qin J, Jiang Z, Qian Y, Xiao H, Lu Y, Qian W, Gulen MF, Sizemore N, DiDonato J, Sato S, Akira S, Su B, Li X (2007) Interleukin-1 (IL-1)-induced TAK1-dependent Versus MEKK3-dependent NFkappaB activation pathways bifurcate at IL-1 receptor-associated kinase modification. *J Biol Chem* **282:** 6075-6089

Zia MK, Rmali KA, Watkins G, Mansel RE, Jiang WG (2007) The expression of the von Hippel-Lindau gene product and its impact on invasiveness of human breast cancer cells. *Int J Mol Med* **20:** 605-611.